The Zoo of Pulsars

John Middleditch

September 26, 2007

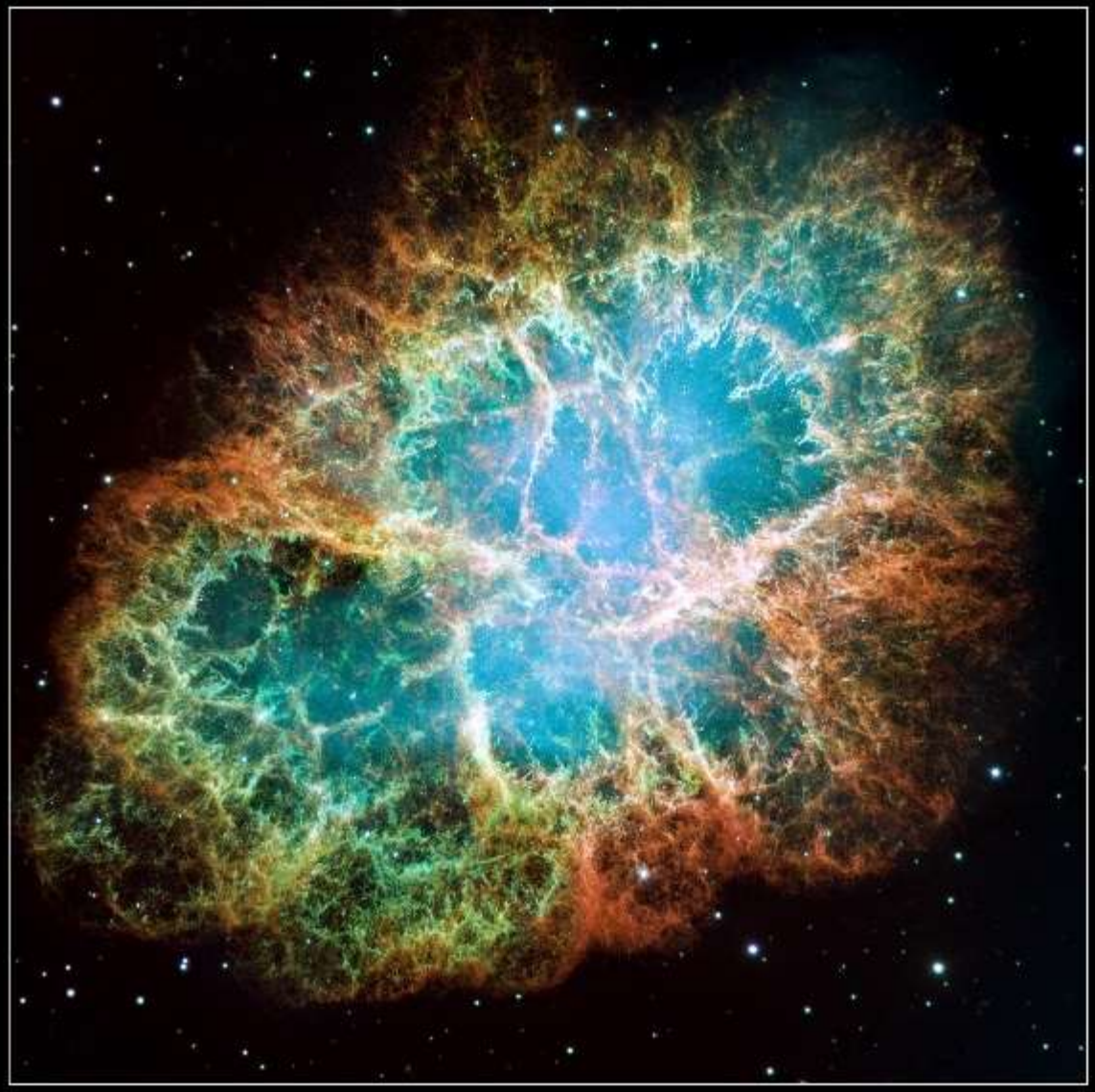

Crab Nebula • M1
Hubble Space Telescope • WFPC2

NASA, ESA, and J. Hester (Arizona State University)

STScI-PRC05-37

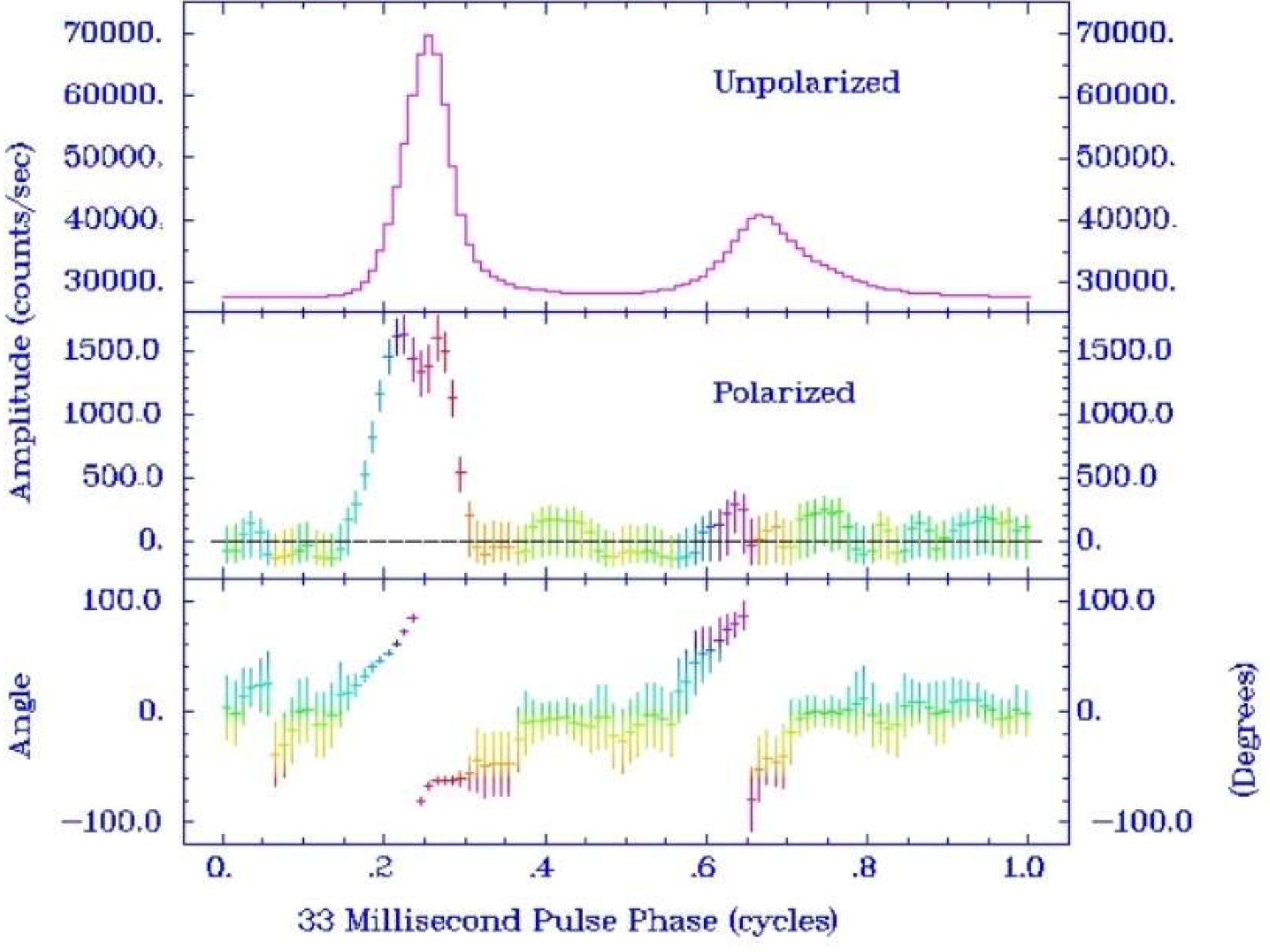
Unpolarized
Polarized
70000.
60000.
50000.
40000.
30000.
1500.0
1000.0
500.0
0.
100.0
0.
−100.0
Amplitude (counts/sec)
Angle
(Degrees)
0.
.2
.4
.6
.8
1.0
33 Millisecond Pulse Phase (cycles)

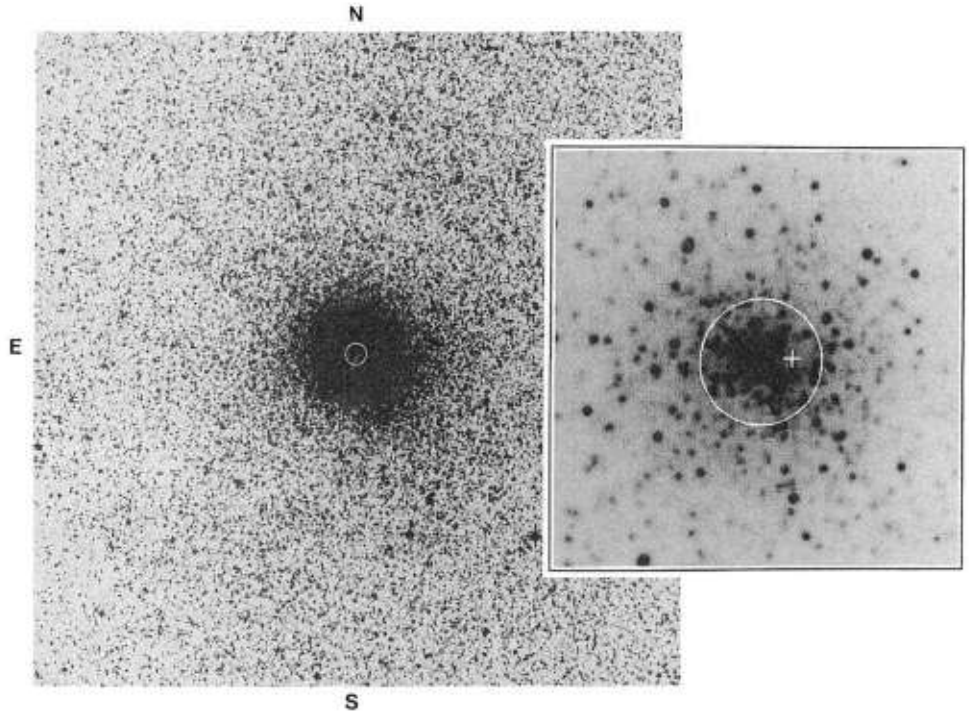

Fig. 1 The globular cluster M28 and the position of the millisecond pulsar. The main photograph shows a 21.5-arc min square centred on M28 (Royal Observatory, Edinburgh, UK Schmidt Telescope). Inset is a CCD image of the core obtained by Drs I. King and S. Djorgovski from the 1.5-m Cerro Tololo telescope with a Johnson B filter. In both diagrams, the white circle represents the extent of the core and is centred on the centroid of the cluster and has a radius of 21 arc s (ref. 11). The position of the pulsar is shown by a cross.

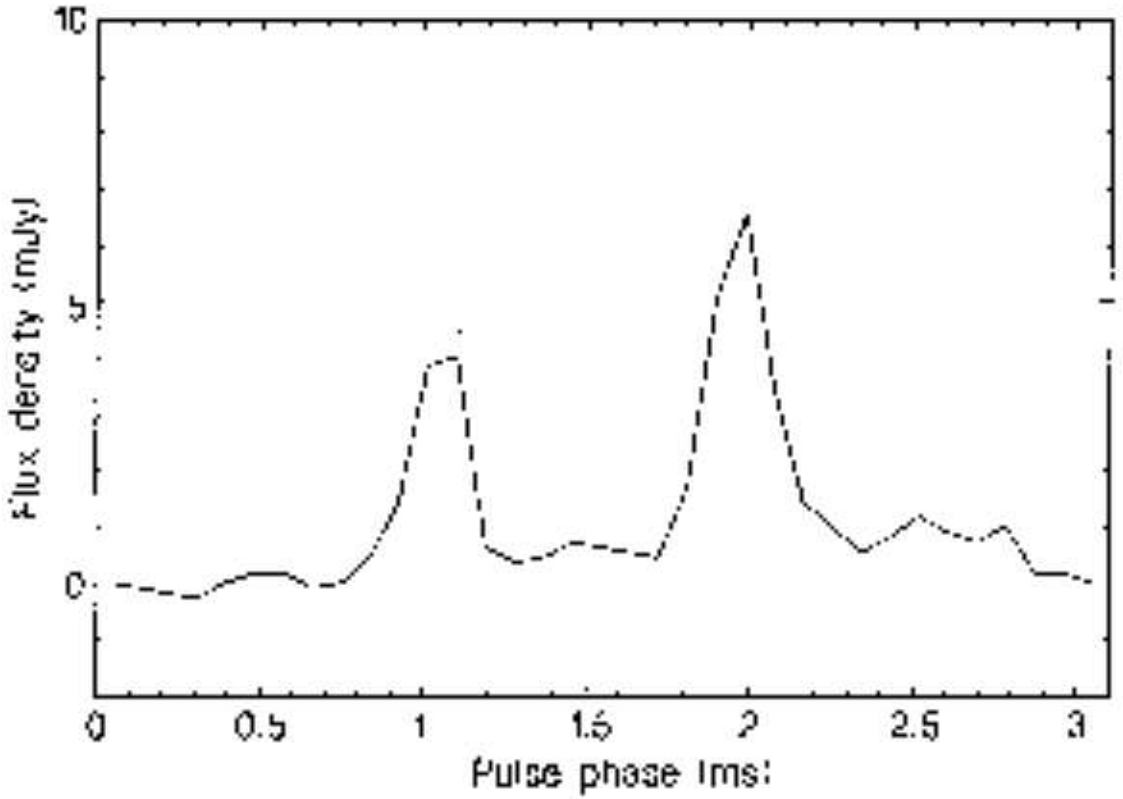

Fig. 2 The pulse profile obtained at 1,420 MHz. The total instrumental broadening amounts to about 130 μs.

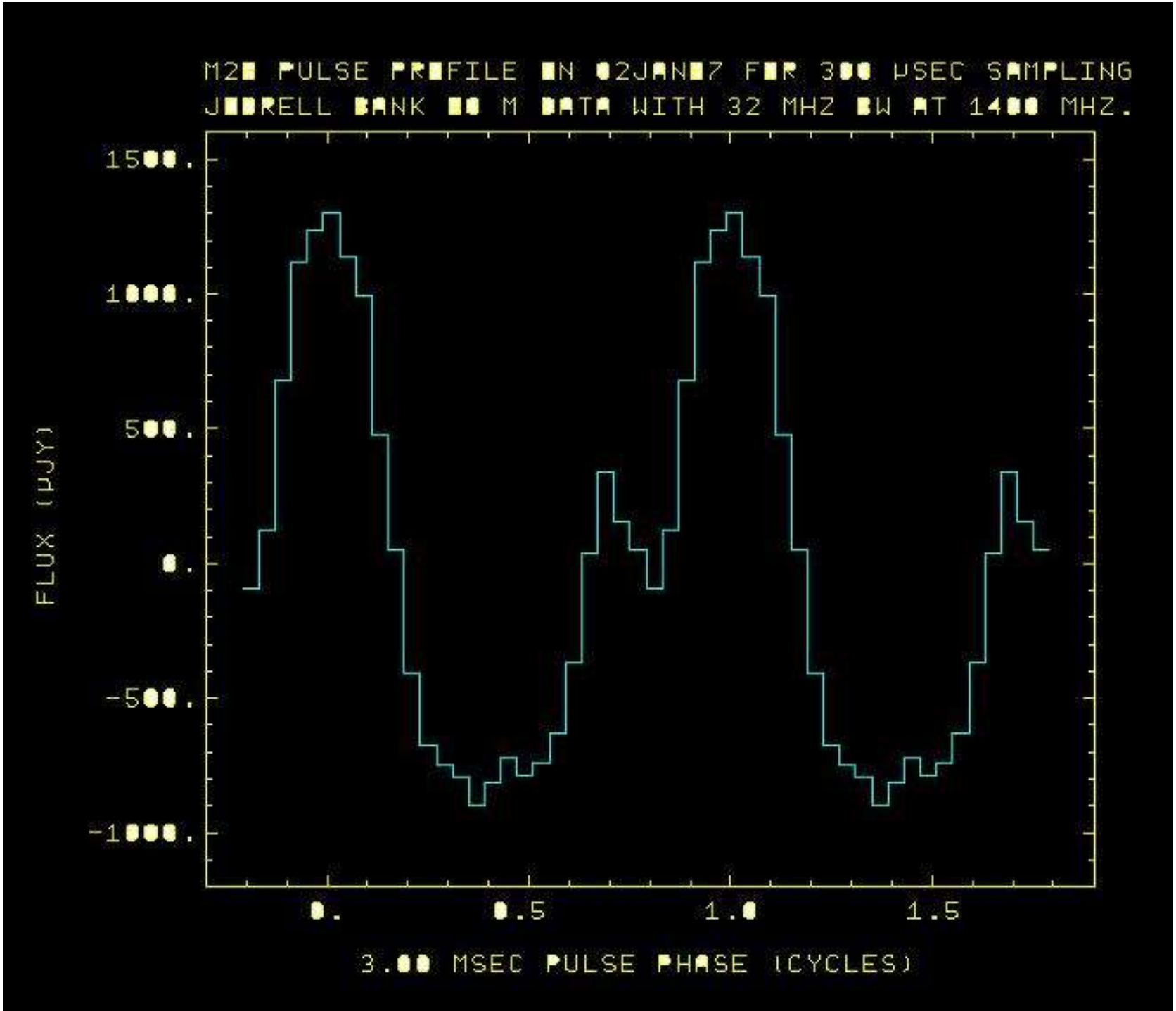
M28 PULSE PROFILE ON 02JAN87 FOR 300 USEC SAMPLING
JODRELL BANK 76 M DATA WITH 32 MHZ BW AT 1408 MHZ.
1500.
1000.
500.
0.
-500.
-1000.
FLUX (MJY)
0.
0.5
1.0
1.5
3.00 MSEC PULSE PHASE (CYCLES)

Central Portion of M15 in U+B+V

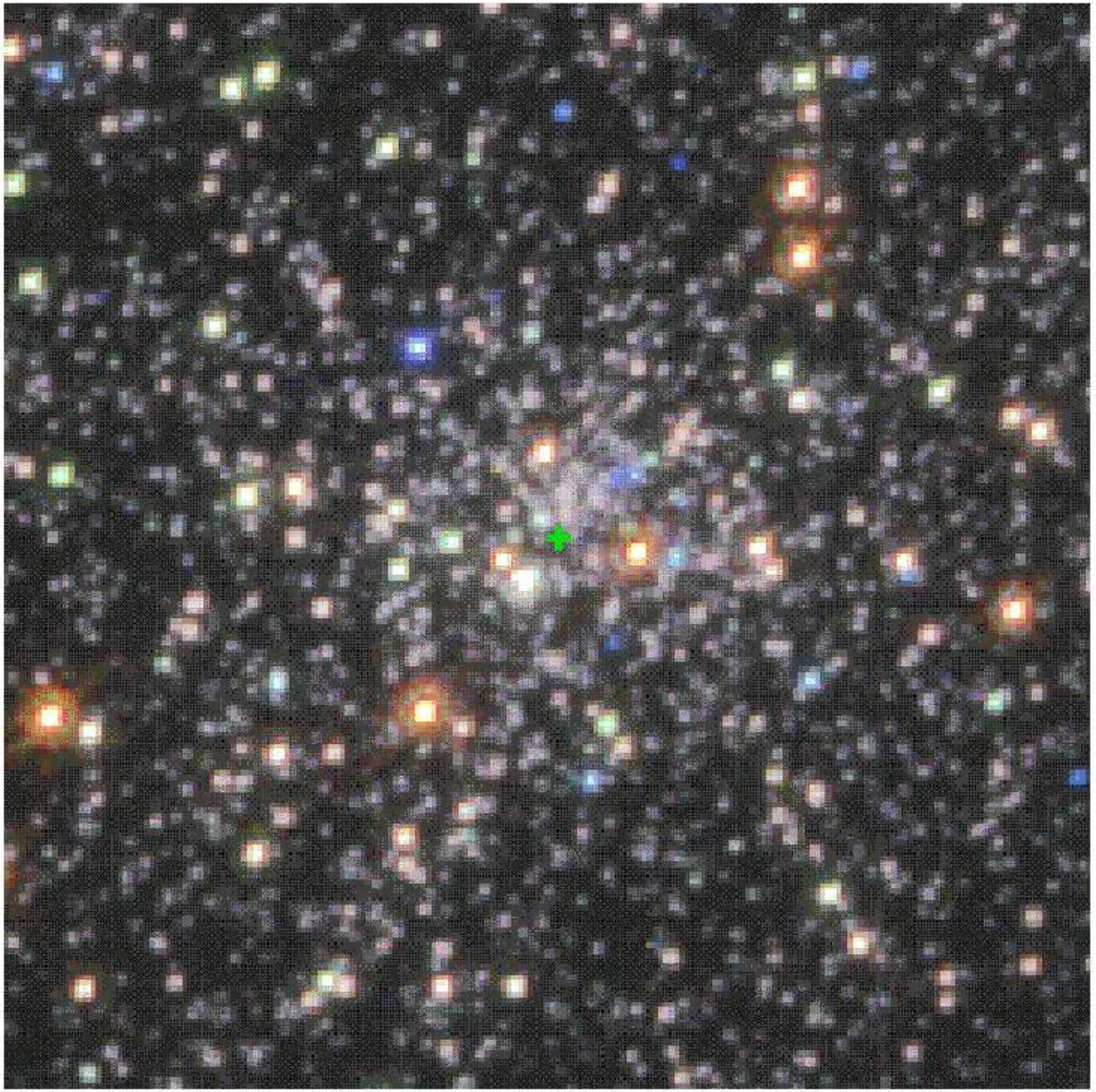

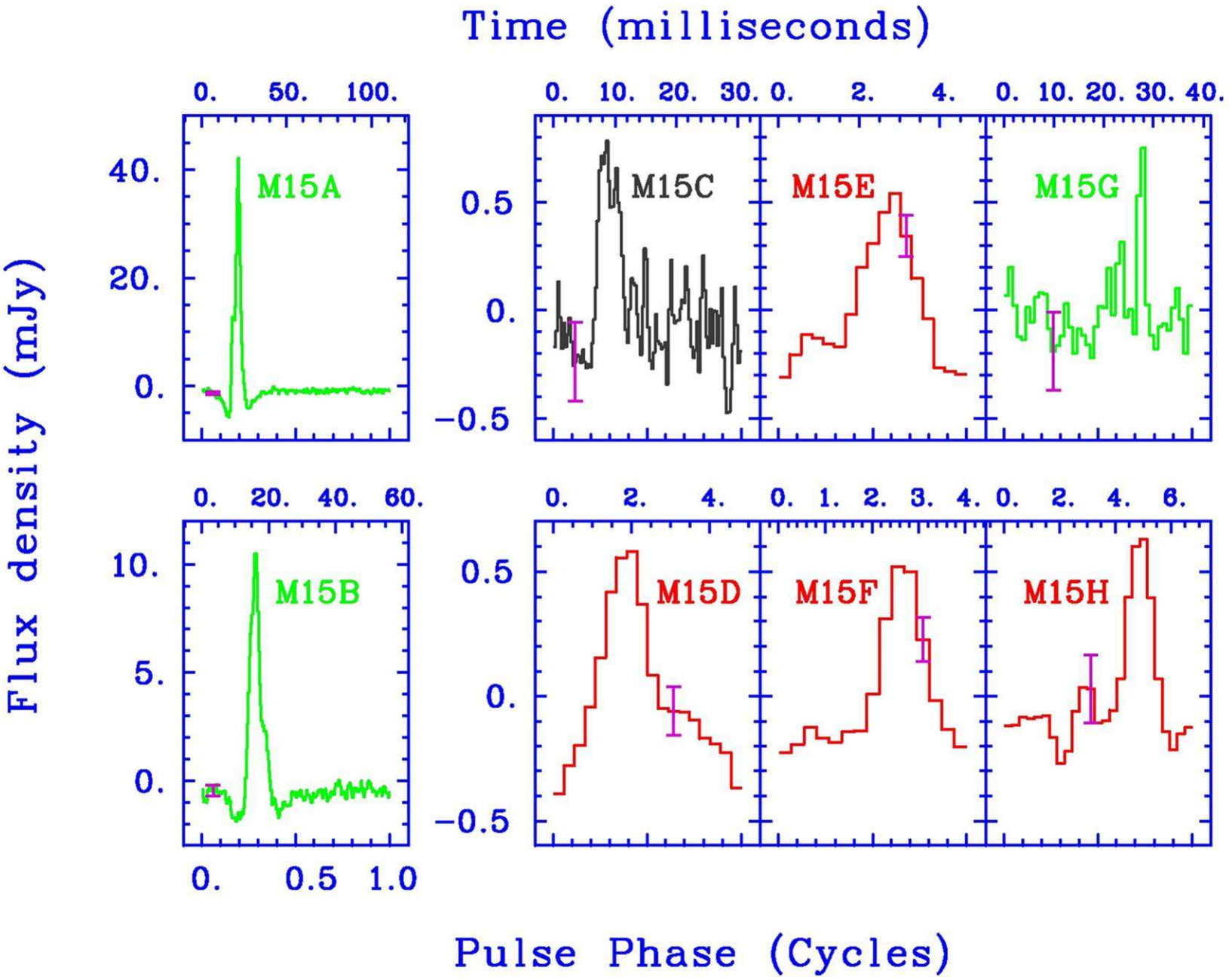
Time (milliseconds)
Flux density (mJy)
Pulse Phase (Cycles)
M15A
M15B
M15C
M15D
M15E
M15F
M15G
M15H
0. 50. 100.
40.
20.
0.
0. 20. 40. 60.
10.
5.
0.
0. 0.5 1.0
0. 10. 20. 30.
0.5
0.
−0.5
0. 2. 4.
0. 1. 2. 3. 4.
0. 10. 20. 30. 40.
0. 2. 4. 6.

Elliptical Galaxy NGC 1316

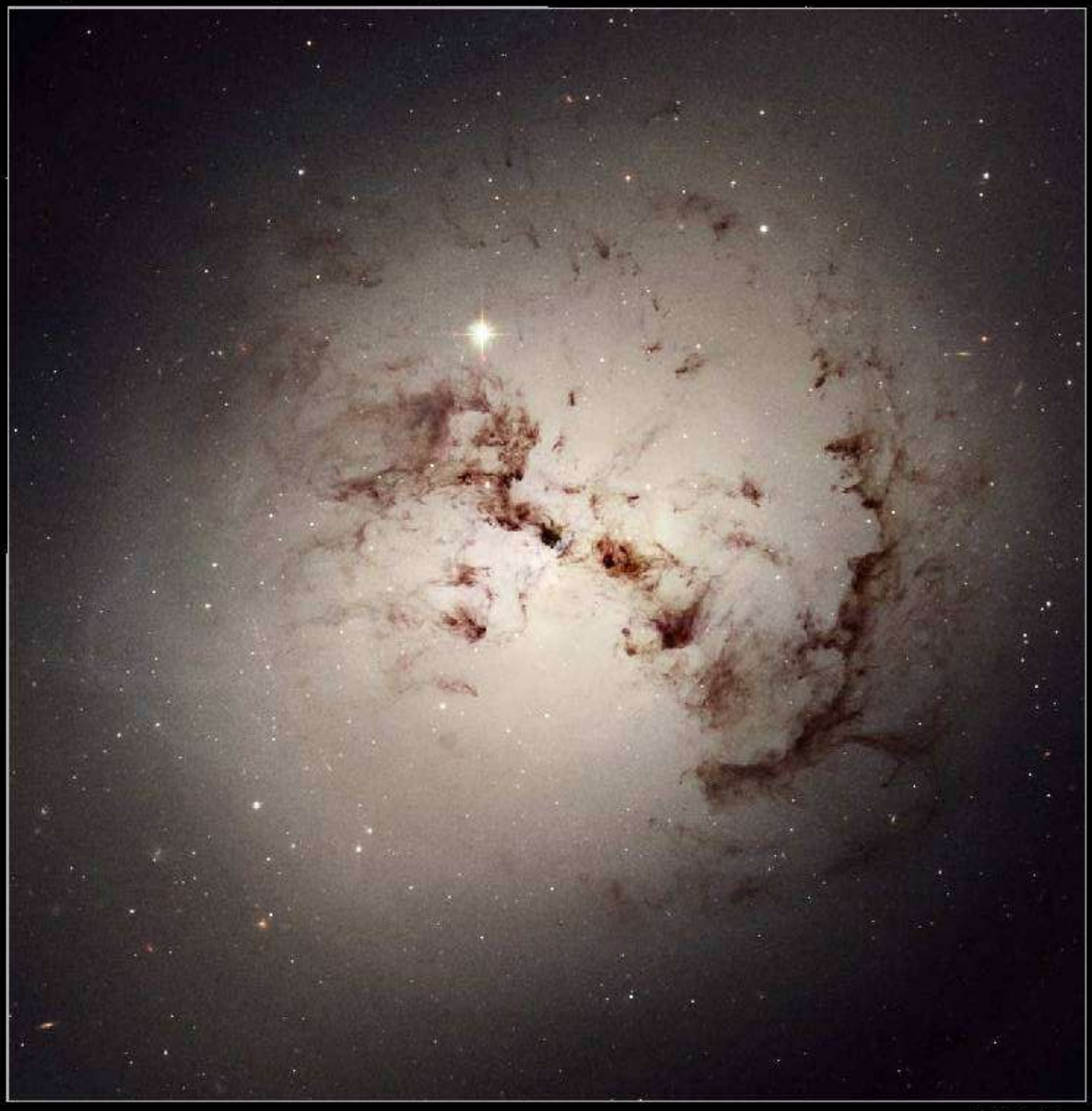

Hubble Heritage

NASA, ESA, and The Hubble Heritage Team (STScI/AURA) • Hubble Space Telescope ACS • STScI-PRC05-11

N
W

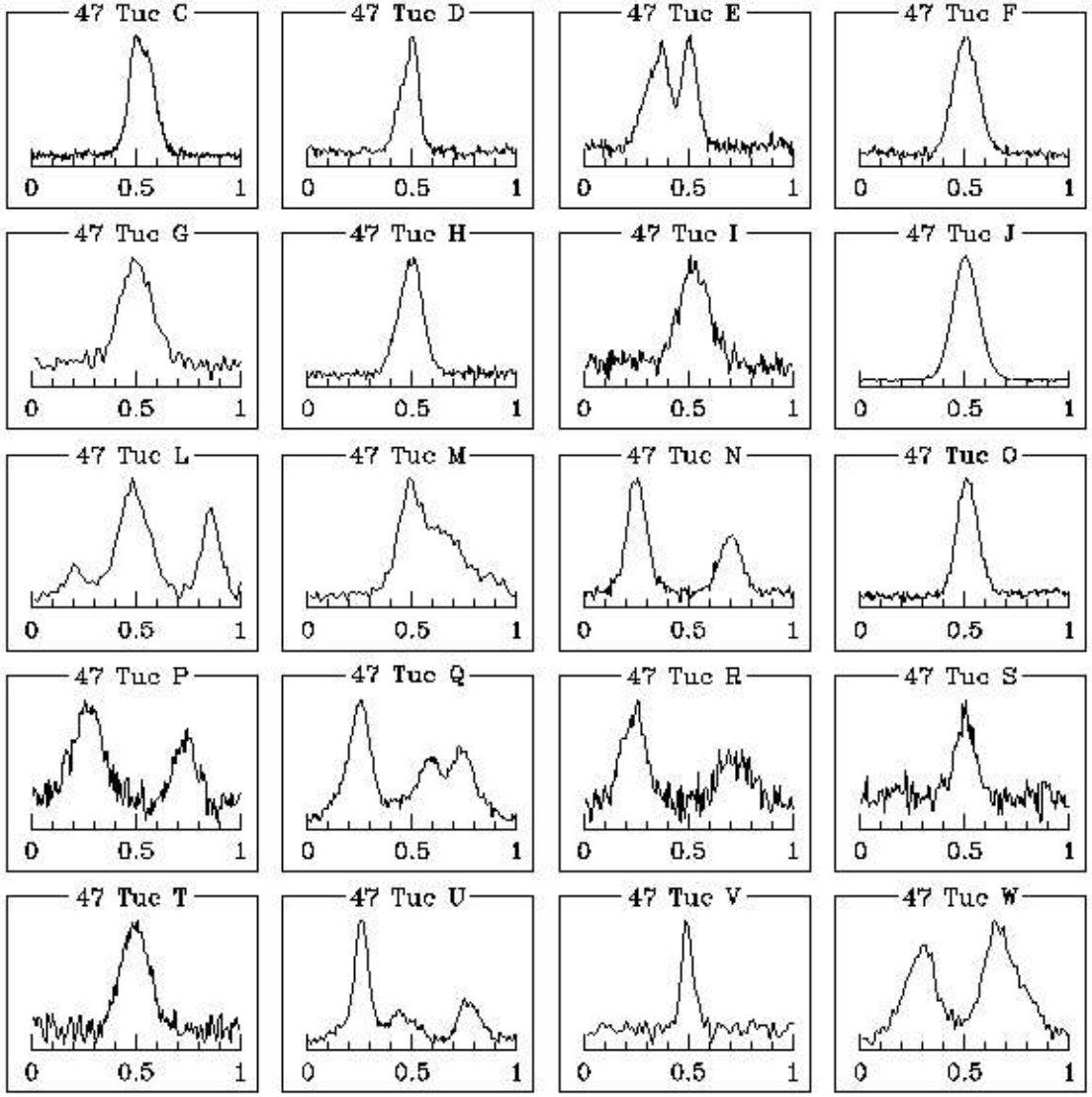

FIG. 5. Average pulse profiles at 20 cm for pulsars in 47 Tuc as a function of rotational phase. The effective time resolution for all profiles displayed is ~0.3 ms, ranging from 0.04 in pulse phase for 47 Tuc T to 0.14 for 47 Tuc J. Some profiles are not resolved (see Table 4).

Finally, from Figure 5 we note that 11 pulsars have essentially simple, single-component profiles; five pulsars have

epoch, although at least one full orbit was covered in each case; 47 Tuc P was seen at all orbital phases, while 47 Tuc R

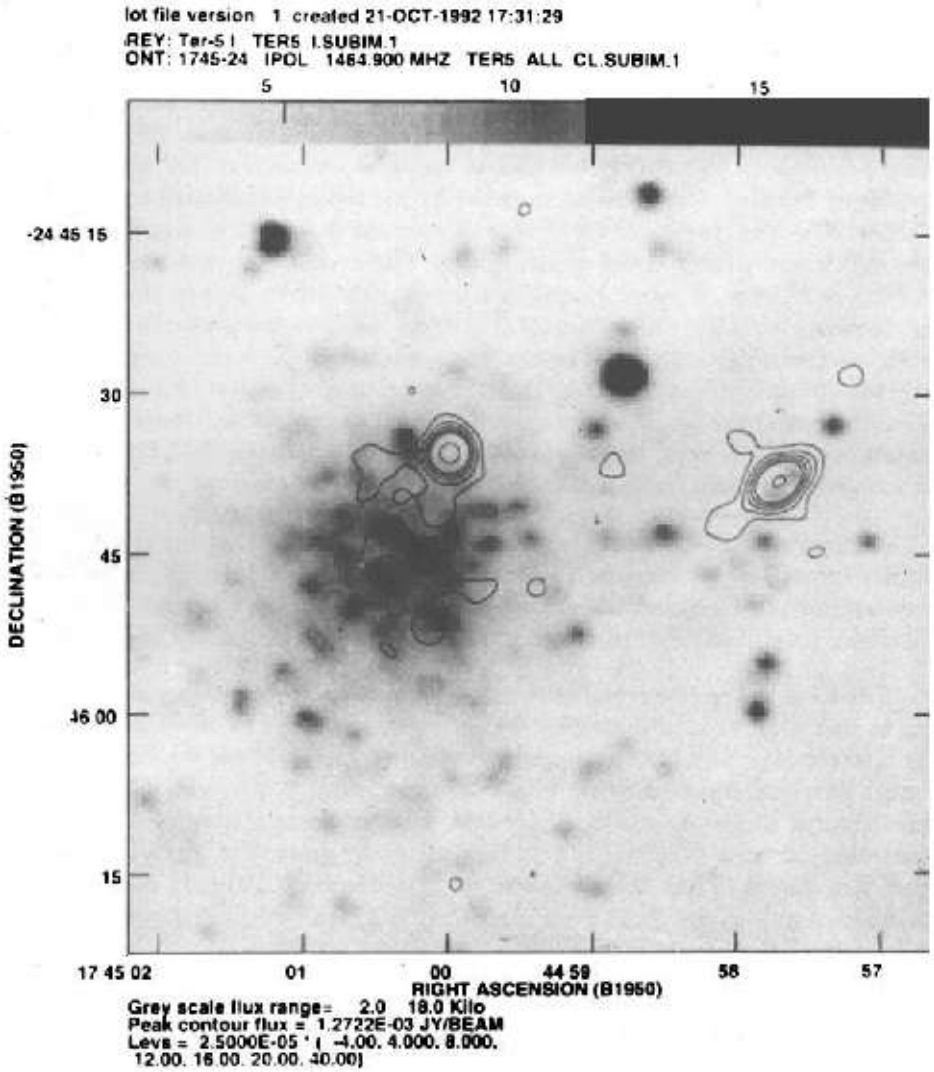

Figure 1: Radio contours are shown superposed on an I band image of the rich cluster Terzan 5. The 20 cm radio image has a beamsize of 3" × 3".

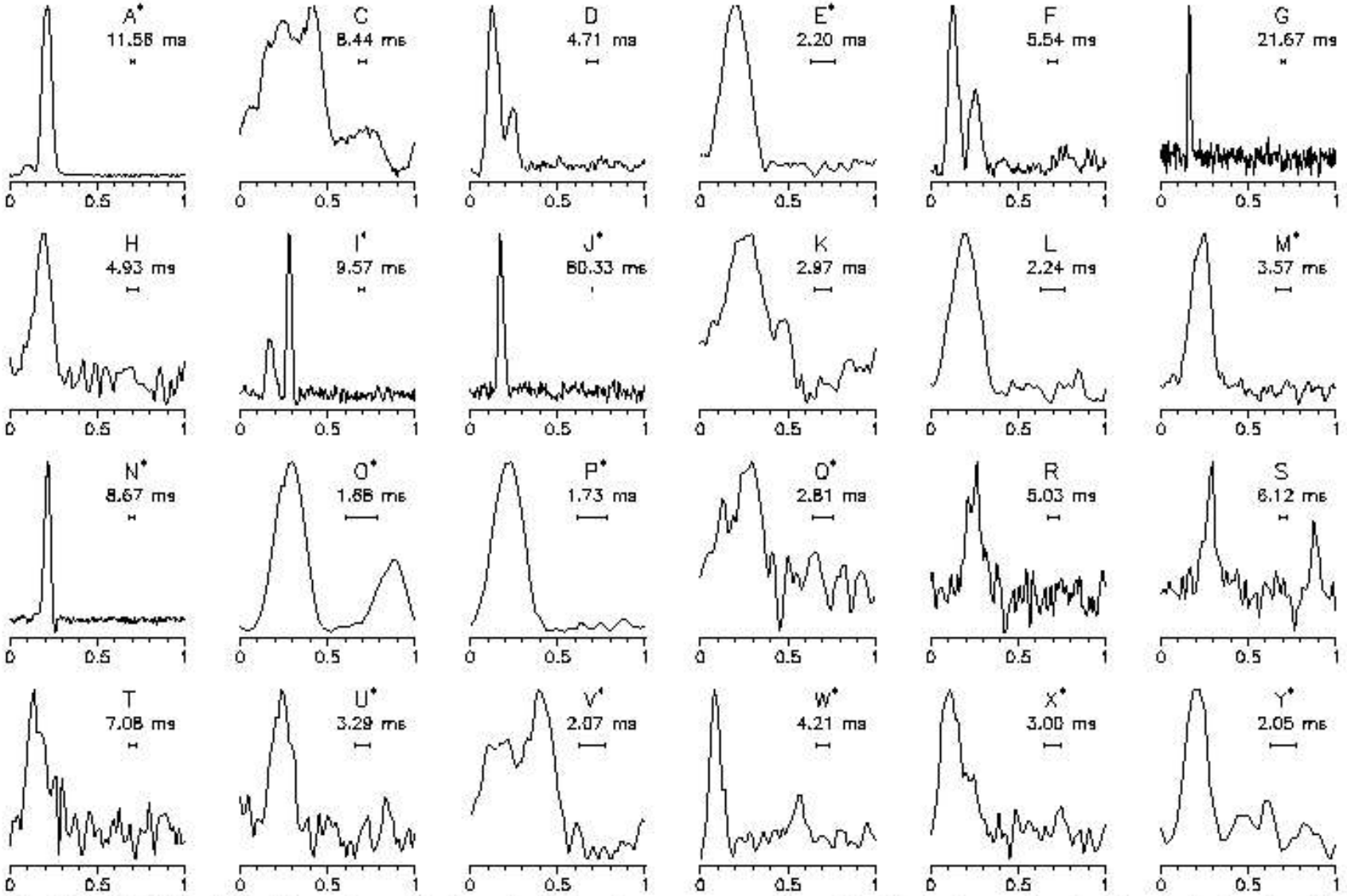

Fig. 1. The 1950 MHz GBT Spigot pulse profiles for each of the pulsars known in Terzan 5. All but Ter 5 A, C, and D are newly discovered (*18*). Each profile is the weighted average of the best detections of that pulsar and is a measure of the relative flux density as a function of rotational phase. Asterisks indicate that the pulsar is the member of a binary system, and the length of the horizontal error bar (0.3 ms) is the effective system time resolution.

Downloaded from www.sciencemag.org

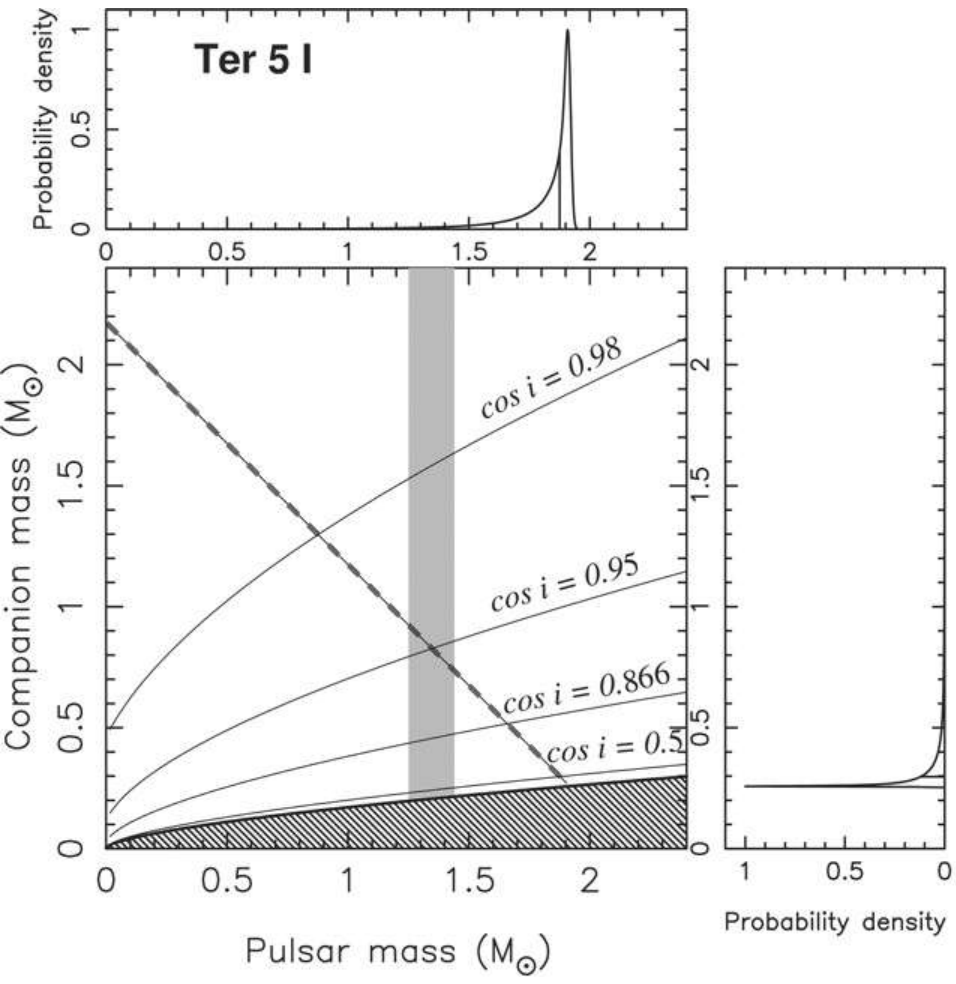
Ter 5 I
Probability density
Companion mass (M⊙)
Pulsar mass (M⊙)
cos i = 0.98
cos i = 0.95
cos i = 0.866
cos i = 0.5
Probability density

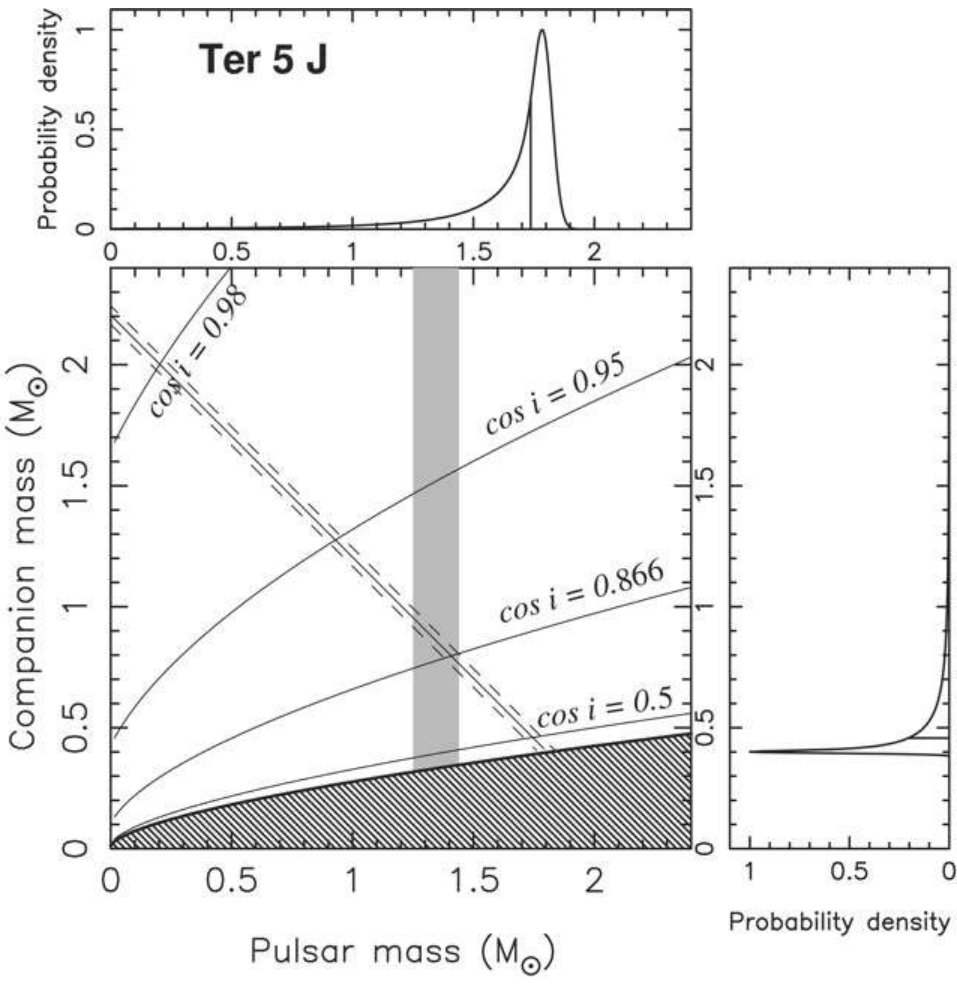
Ter 5 J
Probability density
Companion mass (M⊙)
Pulsar mass (M⊙)
cos i = 0.98
cos i = 0.95
cos i = 0.866
cos i = 0.5
Probability density

R J1748–2446ad in 10
ations of Terzan 5 and
2005 observations using
nd (32) on the GBT. All
pigot with 600 MHz of
red at 1950 MHz, 768
81.92-μs sampling. Ob-
y 6 to 7 hours long and
thly intervals starting
there was a more closely
ns in early May 2005.
rvation showed that the
y system and is eclipsed
of these properties re-
detect the pulsar in our
metheless, we have now
least 18 of the 30 mul-
n thus far (see Fig. 1 for
e derived a reliable or-
11 by initially modeling
of a few good detections
erion and then refining
lse times of arrival to a
al model with arbitrary
ween observing epochs.
l us to detect the pulsar
here it was not initially
iodicity search.
highly circular 26-hour
mass (M_c) companion.
0% of its orbital 2 GHz.
fraction, corresponding
h physical size ~3 to 6
R_c) is extremely rare for
rbit (separation between
n of ~ 4 to 5 times R_c).

which will provide a precise position and observed spin frequency derivative, $\dot{\nu}$. Until then, we have provided an upper limit on $\dot{\nu}$ (Table 1).

We have verified that this signal is not harmonically related to any of the other known pulsars in Terzan 5. We have also carefully investigated the possibility that our searches have identified the second harmonic of a 358-Hz pulsar. When we fold the data at 358 Hz, there are two identical peaks [within the resolution and root mean square (RMS) noise level of the Spigot data] separated by 180° in pulse phase. This is what we expect to see if the pulsar signal is folded at half its intrinsic spin frequency,

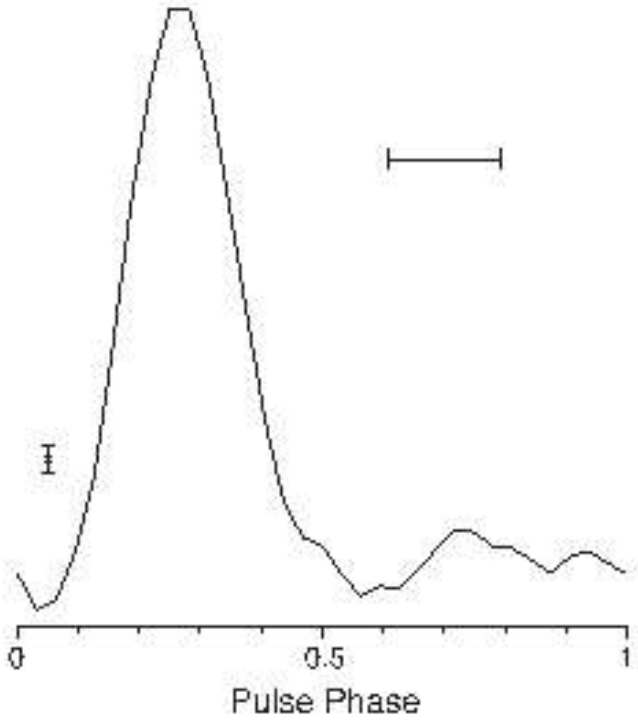

Fig. 1. Master PSR J1748–2446ad pulse profile from the combination of eight GBT Pulsar Spigot observations at 2 GHz with particularly good

provide
the spi
incorpo
due to
suming
wise, ν
derived
and spi
ion ma
$1.4M_{\odot}$
measur
frequer
bandwi
error o

Parame

Pulse p
P (s)
Period
$|\dot{P}|$ (
Pulse f
ν (H
Freque
$|\dot{\nu}|$ (
Epoch

Orbital
P_{orb}
Projecte
x (li
Time o
T_{asc}
Eccentr

Compa
M_c

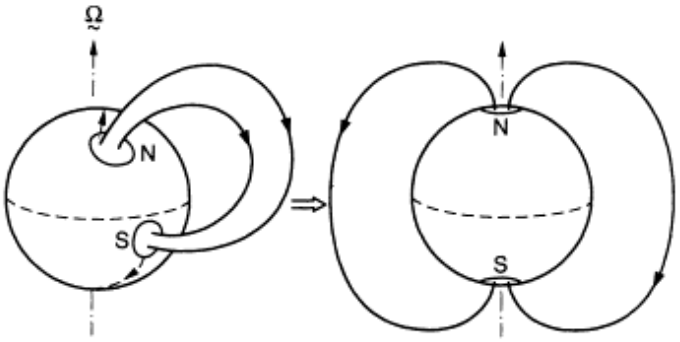

FIG. 1.—Evolution of the surface magnetic field of a short-period spinning-up neutron star when flux lines initially connect the two spin hemisphere.

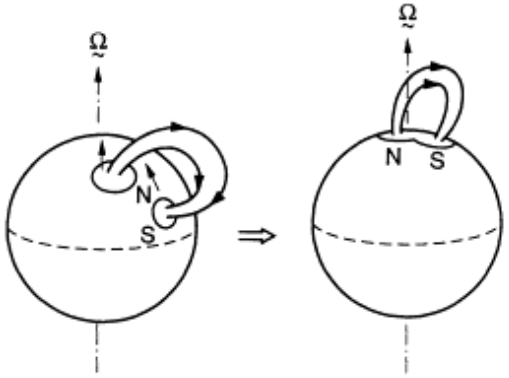

FIG. 2.—Evolution of the magnetic field of a short-period spinning-up neutron star when all flux leaving a hemisphere reenters the same hemisphere.

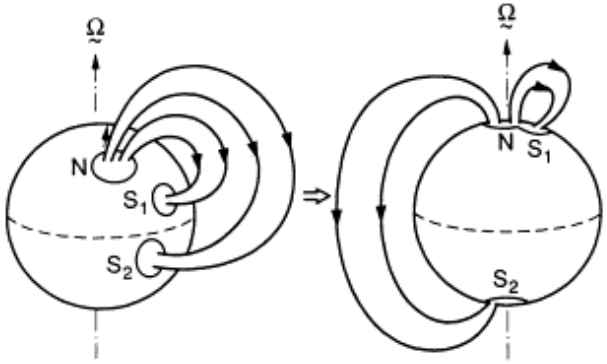

FIG. 3.—Evolution of the magnetic field of a short-period spinning-up neutron star with an initial flux configuration which is intermediate between that of Figs. 1 and 2.

tionary paths shown in Figure 4. The initial neutron star evolution before spin-up is indicated by the dotted line 0 1 2 3 3′ discussed in RII. Here our only concerns are the consequences of spin-up from point 3 (period P_3) to the spin-up line of equation (1). The line 3 7 corresponds to the geometry of Figure 1. The line 3 4 6 corresponds to that of Figure 3 where the dipole is diminished by squeezing field to the spin polar caps until the N-S_2 component, which cannot be further reduced, dominates the dipole moment. It is the sunspot geometry of Figure 2 which leads to the evolution 3 4 5 which would populate the millisecond pulsar area of smallest dipole field (because of almost complete squeezing together of north and south magnetic poles) and smallest period (because spin-up can continue for the longest interval before the spin-up line is reached). It is this region which we shall now consider further (although some of our conclusions may also have application to the other regions).

The original millisecond pulsar PSR 1937+21 (Backer et al. 1982) has the radio pulse profile and the polarization shown in Figure 5. Its polarization properties are still the best known among those of all its subsequently discovered siblings. We concentrate below on trying to understand several of its rare and remarkable properties. These include the following:

1. Two pulse components of comparable intensity which are almost exactly 180° apart at all frequencies (Stinebring 1983). This feature is common among disk millisecond pulsars. In contrast, among the more than 400 observed canonical pulsars, less than a dozen of them have any visible interpulses (Lyne & Manchester 1988). Furthermore, the interpulse intensities of the two fastest millisecond pulsars (PSR 1937+21 and PSR 1957+20) are nearer that of the main pulses than is the case for almost all of the canonical pulsars which have interpulses.

2. A very narrow subpulse width, far below what might have been expected from an extrapolation of the lower bound of pulse width versus P for canonical pulsars.

3. If radio emission is a cone beam, then the probability for observation is very small for such narrow pulse width. If the remarkably large millisecond pulsar/LMXBs (low-mass X-ray binaries) ratio is not to be even larger, radio emission has to be a fan beam, anomalously narrow in its azimuthal width but broad in its polar angle extent.

4. At frequencies below about 10^3 MHz, one of the pulse components is nearly 100% linearly polarized, with an unchanging polarization angle. This is not the case for the other component nor does it hold at higher frequencies (Thorsett 1991).

5. For the other pulse component or at higher frequencies, polarization angles are found in either of two states differing by

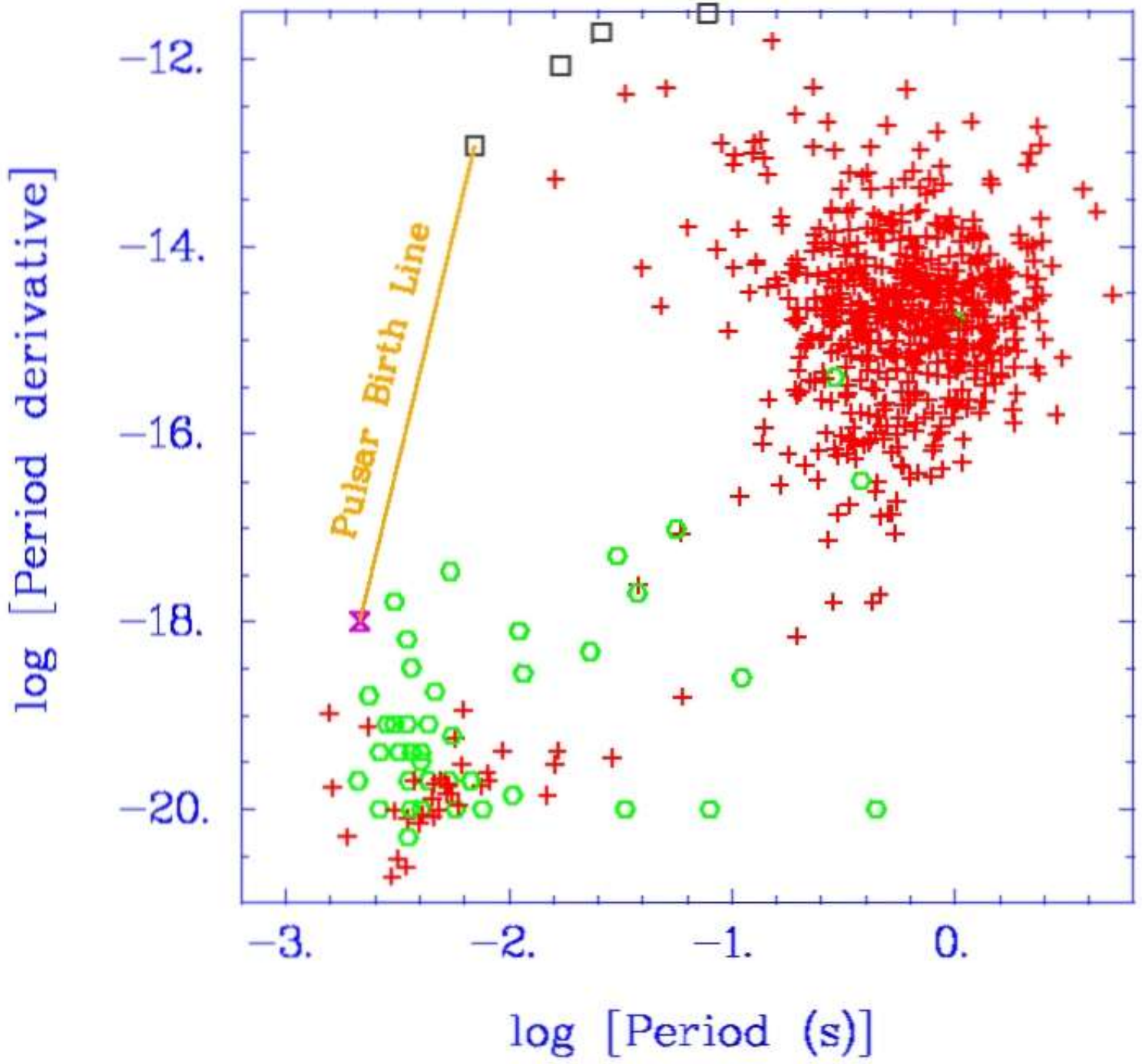
Pulsar Birth Line
log [Period derivative]
log [Period (s)]
−12.
−14.
−16.
−18.
−20.
−3.
−2.
−1.
0.

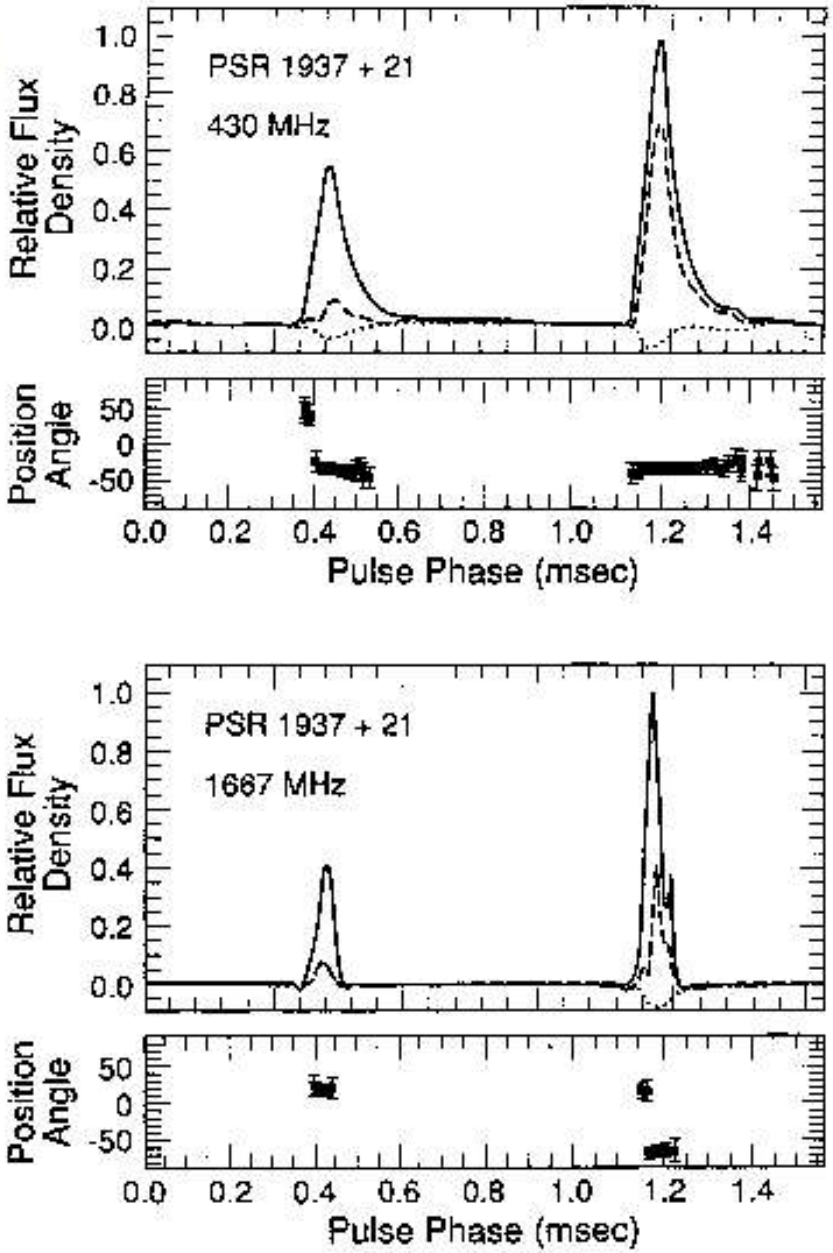

FIG. 5. Pulse shape and polarization for PSR 1937+214 at 430 and 1667 MHz, respectively. The dashed line is the linearly polarized intensity; its position angle is shown below (Thorsett 1991).

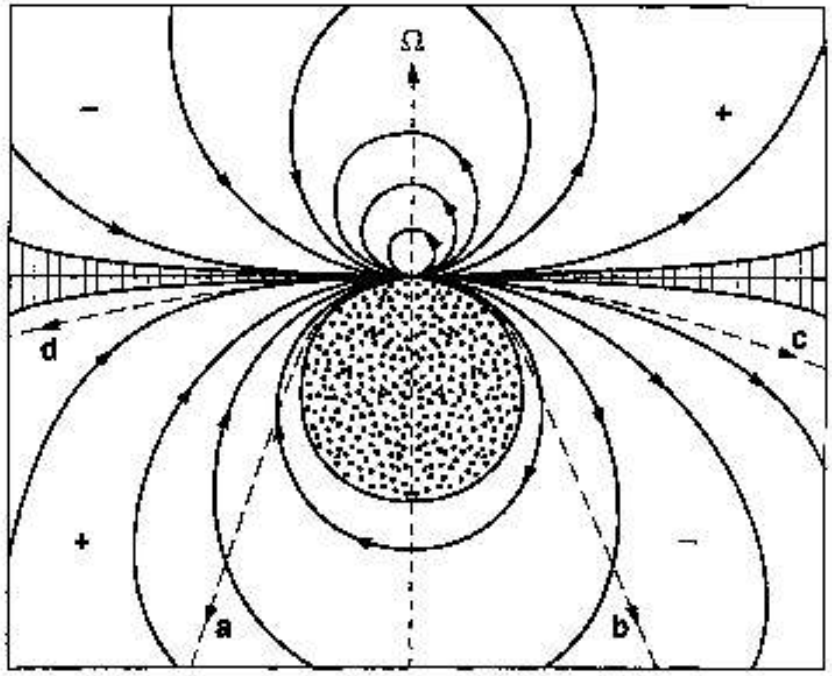

FIG. 6. Magnetosphere of a strongly spun-up diamagnetic (because of core proton superconductivity) neutron star with the initial field geometry of Fig. 2 (or the north hemisphere of Fig. 3).

large viewing angles and the radiation from both sides is symmetric. A two-pulse component would be easily observed with comparable intensity for the main pulse and the interpulse. After bending, the separation between the interpulse and the main pulse should still be 180°.

[In order to spin-up the neutron star to a period near 1 millisecond, a substantial amount of mass ($\geq 0.1\ M_\odot$) has to be transfered onto the neutron star. Then the gravitational bending of millisecond pulsar emission after spin-up should be stronger than that of canonical pulsars even if both had the same magnetic field geometry.]

5. POLARIZATION

The fan beams a–d and b–c of Figure 6 give the observed pulse and interpulse of a millisecond pulsar like PSR 1937+21.

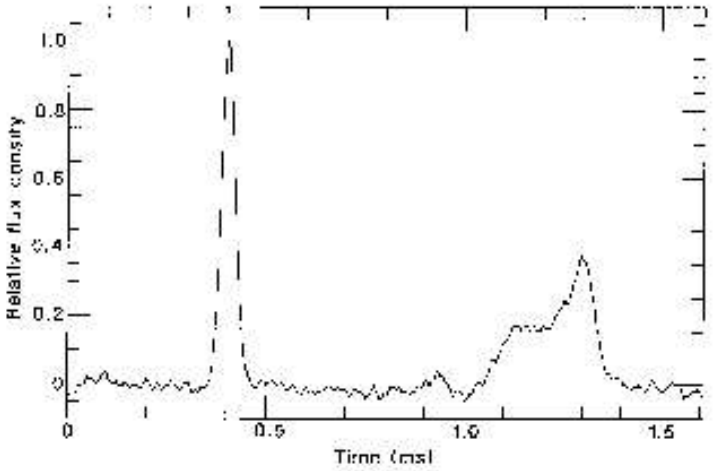

Fig. 1 Integrated profile of PSR1957+20 at 430 MHz. Instrumental smoothing amounts to ≈15 μs, mostly a result of drifting pulse phase during the integration caused by imperfect knowledge of the period.

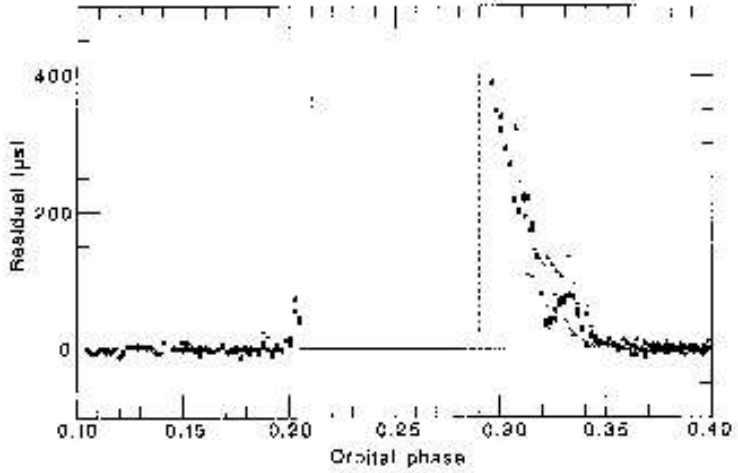

Fig. 3 Excess group delays in the pulsar signal at 430 MHz relative to a model based on our best-fit parameters, plotted as a function of orbital phase near the centre of eclipse. Different symbols correspond to different observing days.

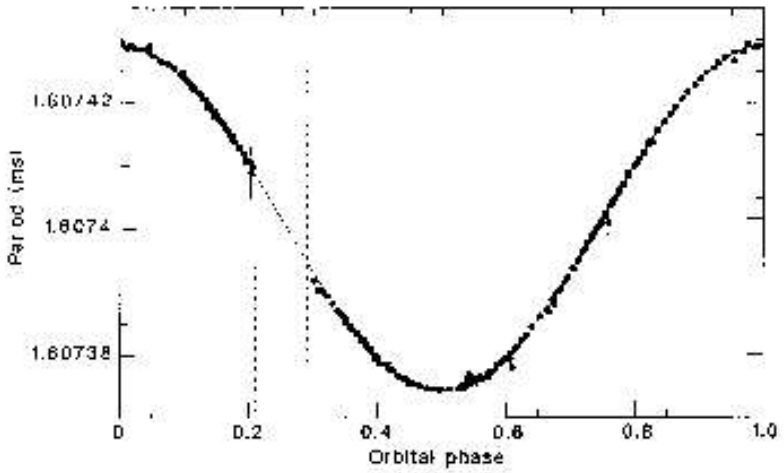

Fig. 2 Orbital velocity curve of PSR1957+20. The pulsar is eclipsed by its companion between phases 0.21–0.29. Points with visible error bars were taken using the pulsar survey system; all other points were obtained with the data acquisition system designed for timing millisecond pulsars.

segments of ~5 min duration, the arrival times (reduced to the solar system barycentre) yield periods which, when folded modulo the 9.17 hour orbital period, comprise the velocity curve illustrated in Fig. 2. A linearized least-squares fit to the period data yielded the pulsar and orbital parameters quoted in Table 1. A 'phase-connected' solution to the observed pulse arrival times, with no pulse-numbering ambiguities between observing days, should be achievable soon and will provide much more accurate pulsar and orbital parameters.

The entire orbit has now been observed. Good observations exist on five different days for all or part of the region $0.15 \lesssim \phi \lesssim 0.35$, where orbital phase ϕ is measured from the time of the ascending node. On all of these days the pulsar signal has disappeared completely between the orbital phases 0.21 and 0.29. At $\phi = 0.25$, the pulsar is at its greatest distance from Earth, and closest to being directly behind the companion star. We conclude that the intervals of missing signal are the result of eclipses by a surprisingly large, though very low-mass, companion.

During the few minutes immediately before eclipse, and for ~20 min after the eclipse, the pulsar signal is delayed by as much as 400 μs relative to arrival times predicted from a model

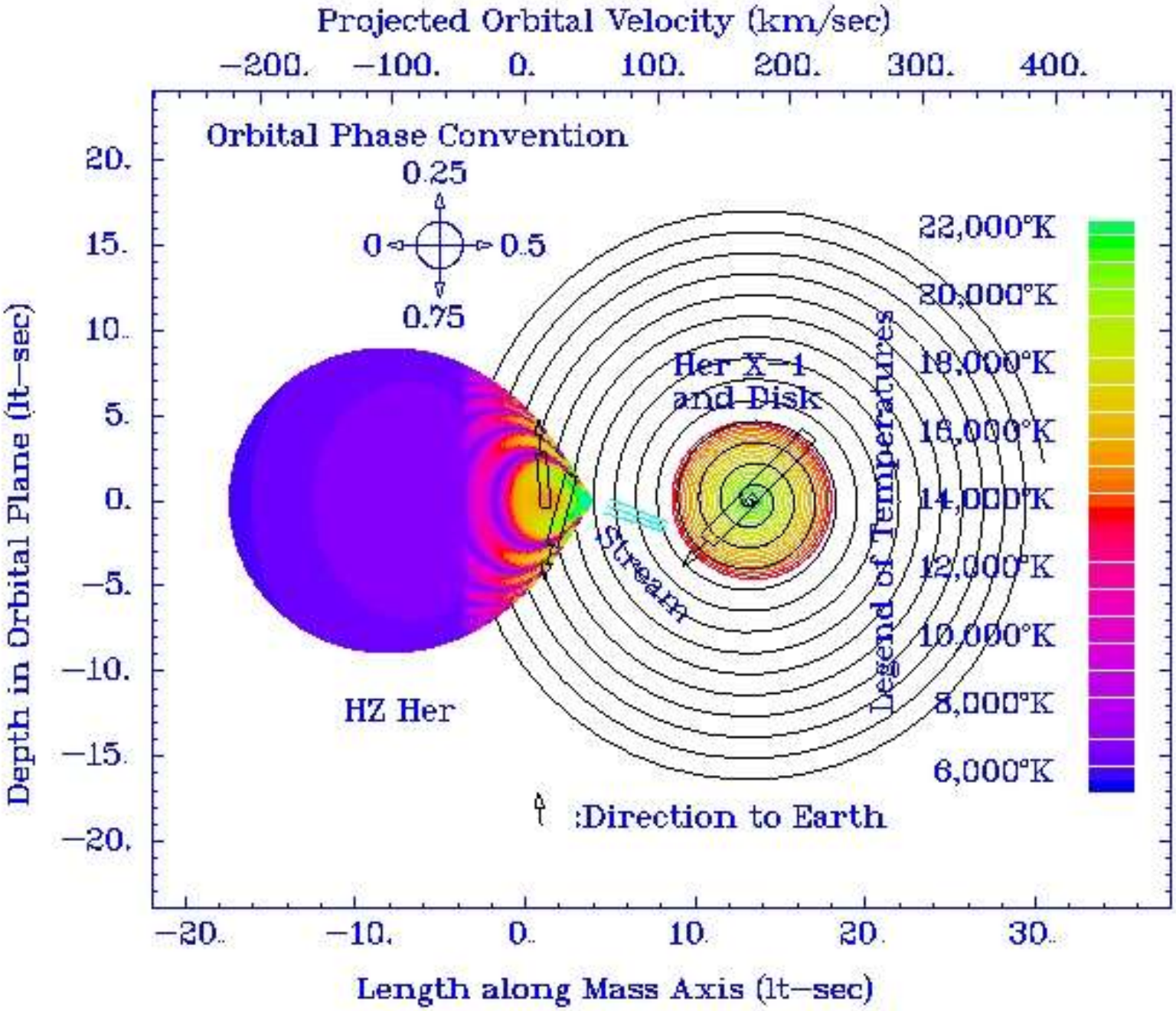
Projected Orbital Velocity (km/sec)
−200.
−100.
0.
100.
200.
300.
400.
Orbital Phase Convention
0.25
0
0.5
0.75
20.
15.
10.
5.
0.
−5.
−10.
−15.
−20.
Depth in Orbital Plane (lt−sec)
Her X−1
and Disk
Stream
HZ Her
Legend of Temperatures
22,000°K
20,000°K
18,000°K
16,000°K
14,000°K
12,000°K
10,000°K
8,000°K
6,000°K
:Direction to Earth
−20.
−10.
0.
10.
20.
30.
Length along Mass Axis (lt−sec)

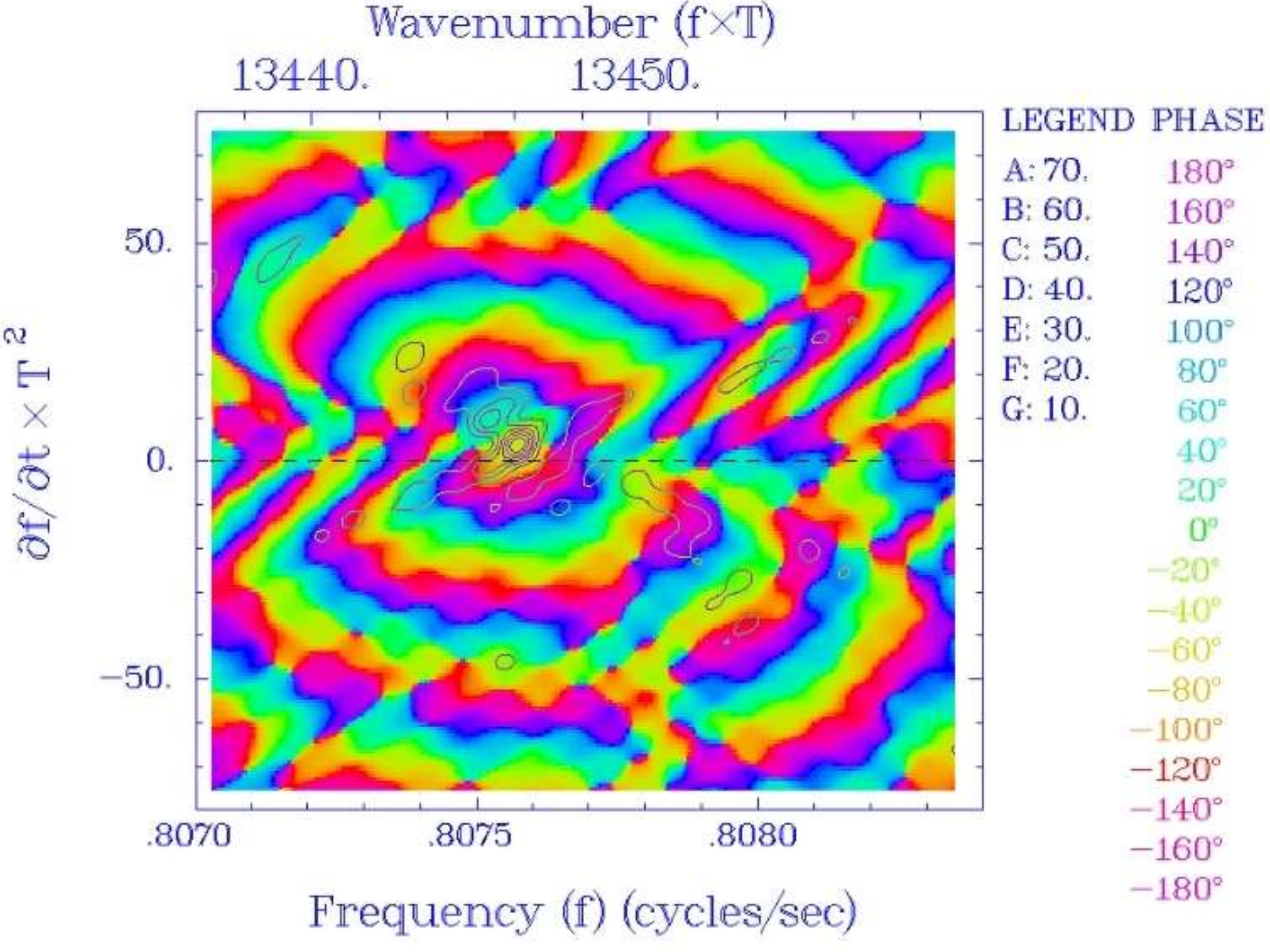
Wavenumber (f×T)
13440.
13450.
50.
0.
−50.
∂f/∂t × T²
.8070
.8075
.8080
Frequency (f) (cycles/sec)
LEGEND PHASE
A: 70. 180°
B: 60. 160°
C: 50. 140°
D: 40. 120°
E: 30. 100°
F: 20. 80°
G: 10. 60°
40°
20°
0°
−20°
−40°
−60°
−80°
−100°
−120°
−140°
−160°
−180°

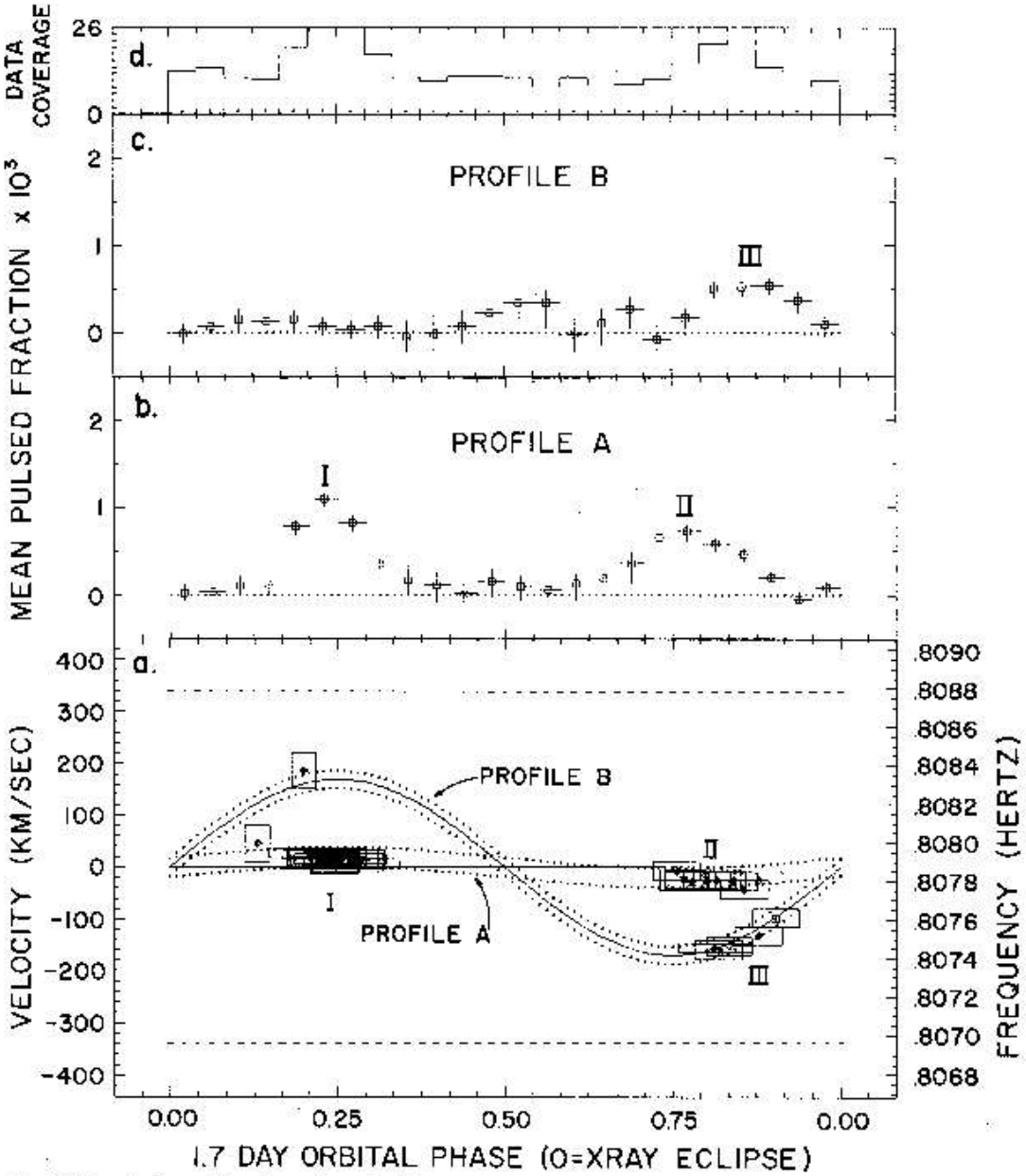

FIG. 2.—(*a*) The significant bins chosen from all of the power spectra are shown plotted as boxes on the orbital phase-frequency plane. Features I, II, and III are labeled. The horizontal solid line and the solid sine curve indicate the average pulse frequency of Her X-1 and its Doppler-shifted pulse frequency, respectively. The horizontal dashed lines at the top and bottom of the frame indicate the frequency region examined and are at twice the extent of the maximum Her X-1 Doppler shift. The dotted lines indicate the regions on the phase-frequency plane which were applied to all of the spectra to calculate the amplitude profiles in (*b*) and (*c*). (*b*) The profile of amplitude versus orbital phase for Features I and II from HZ Her. (*c*) The amplitude profile following the Doppler track of Her X-1. Feature III is indicated near phase 0.85. (*d*) The data coverage histogram over 24 equal parts of the 1.7 orbital phase. The profiles in (*b*) and (*c*) have had this unevenness normalized out.

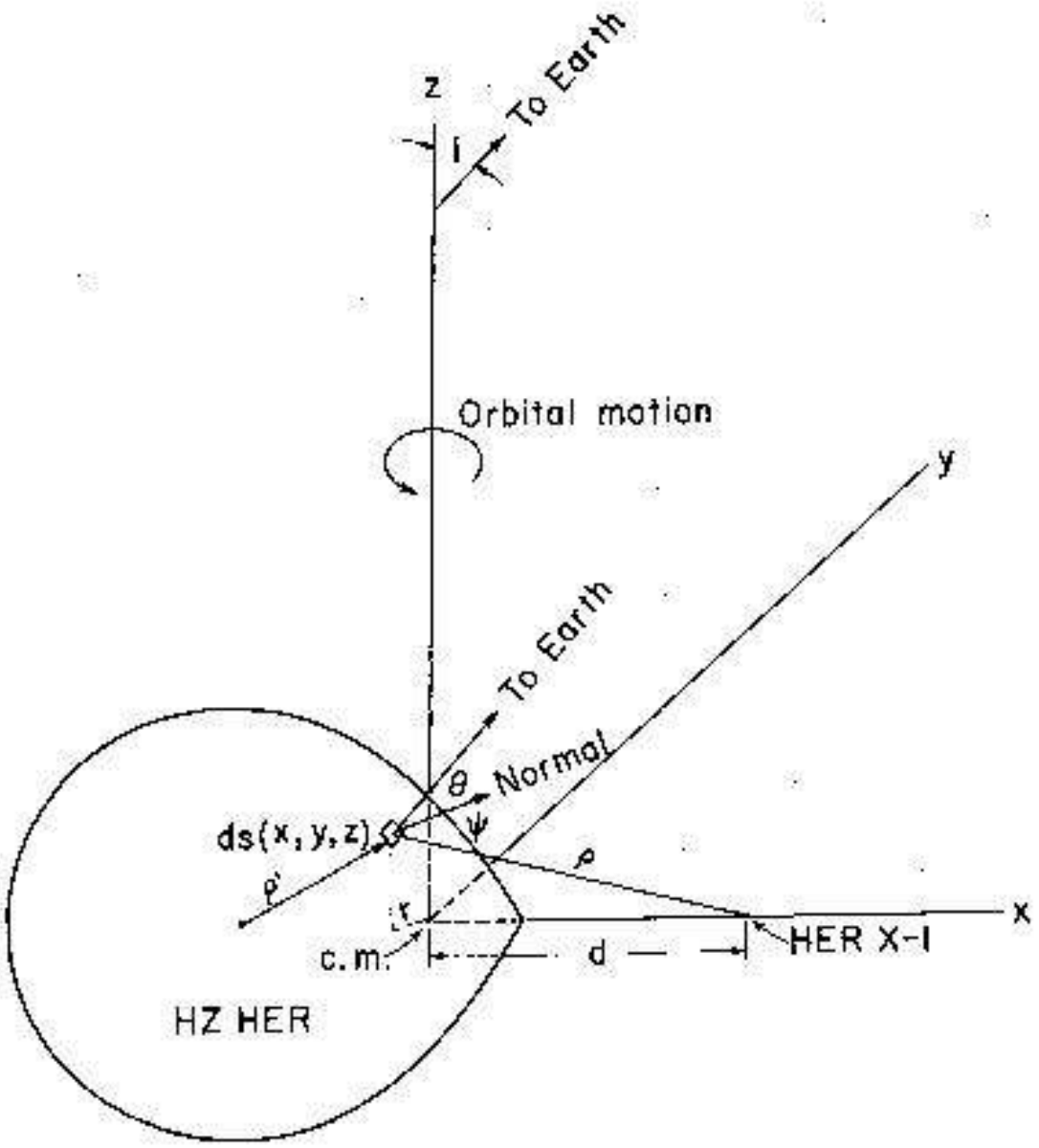

FIG. 6.—The geometry for the reprocessing-reflection model calculations. HZ Her, Her X-1, and the x- and y-axes are shown to be rotating counterclockwise (right-handedly) about the z-axis.

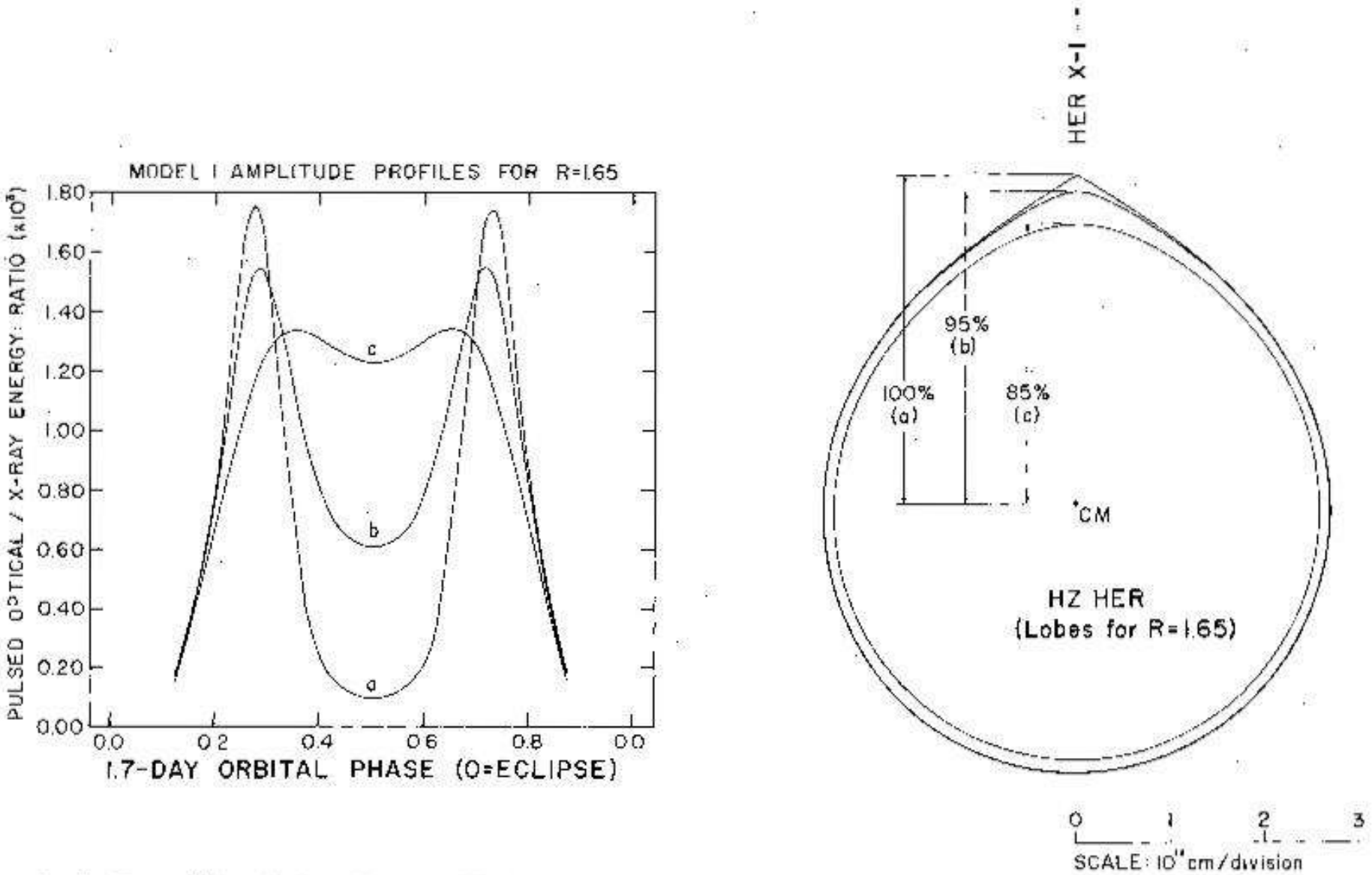

FIG. 8.—The model 1 amplitude profiles versus 1.7 orbital phase for three Roche equipotential contours with $R = 1.65$ are plotted together on the left for comparison. The right-hand side shows the three contours associated with the profiles *a*, *b*, and *c* labeled according to their extent from the HZ Her center of mass toward Her X-1 along the mass axis. The critical Roche lobe defines 100% for this extent.

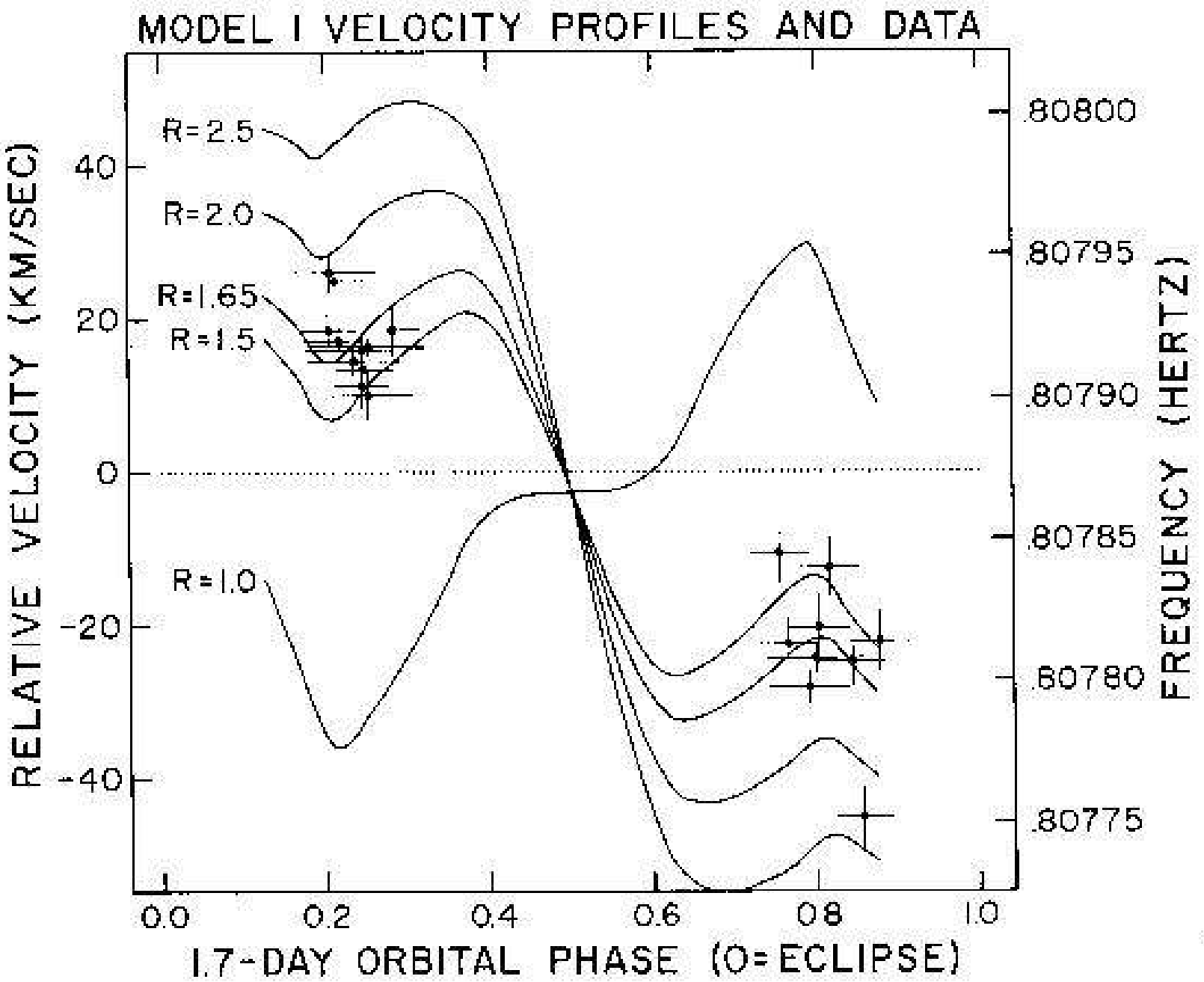

FIG. 10.—The model I frequency tracks over 1d7 orbital phase for various mass ratios are plotted with the data even features I and II.

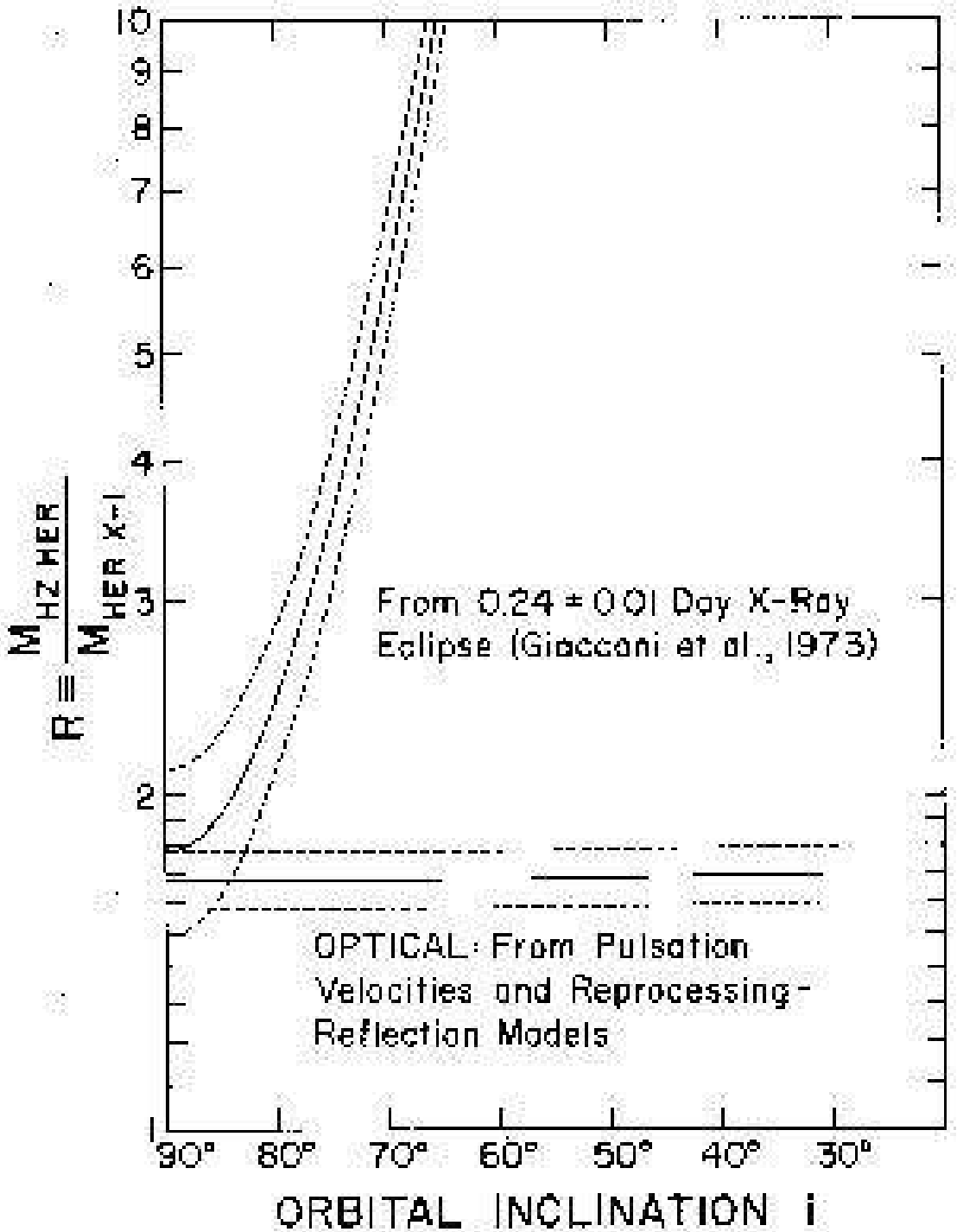
10
9
8
7
6
5
4
3
2
1
$R \equiv \frac{M_{HZ\ HER}}{M_{HER\ X-1}}$
From 0.24 ± 0.01 Day X-Ray Eclipse (Giacconi et al., 1973)
OPTICAL: From Pulsation Velocities and Reprocessing-Reflection Models
90°
80°
70°
60°
50°
40°
30°
ORBITAL INCLINATION i

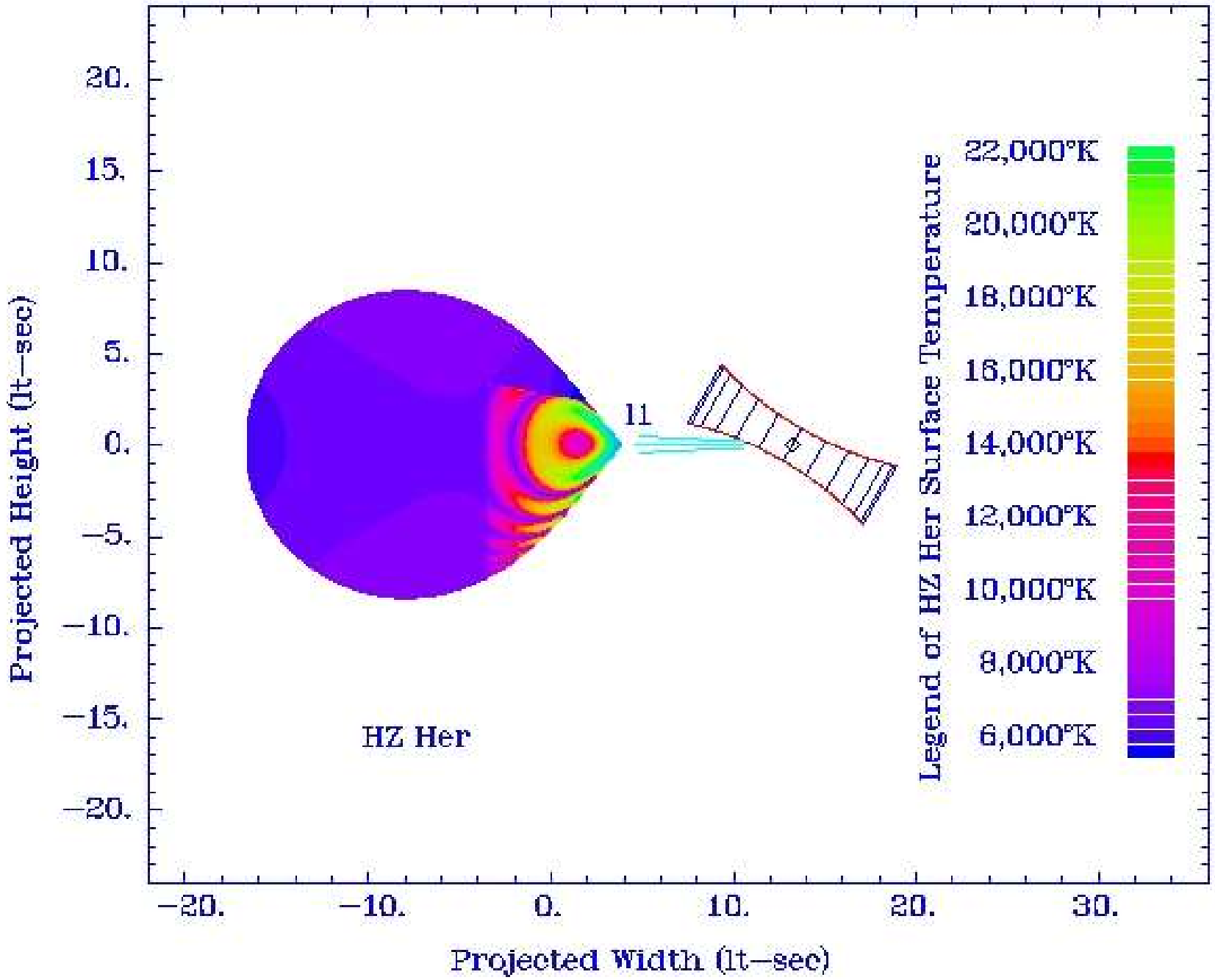
20.
15.
10.
5.
0.
−5.
−10.
−15.
−20.
Projected Height (lt−sec)
−20.
−10.
0.
10.
20.
30.
Projected Width (lt−sec)
11
HZ Her
Legend of HZ Her Surface Temperature
22,000°K
20,000°K
18,000°K
16,000°K
14,000°K
12,000°K
10,000°K
8,000°K
6,000°K

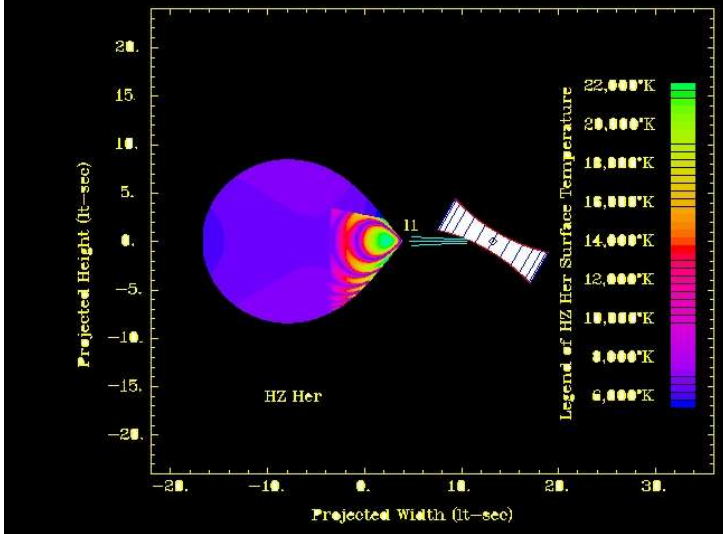
Projected Height (lt-sec)
20.
15.
10.
5.
0.
-5.
-10.
-15.
-20.
-20.
-10.
0.
10.
20.
30.
Projected Width (lt-sec)
HZ Her
11
4
Legend of HZ Her Surface Temperature
22,000°K
20,000°K
18,000°K
16,000°K
14,000°K
12,000°K
10,000°K
8,000°K
6,000°K

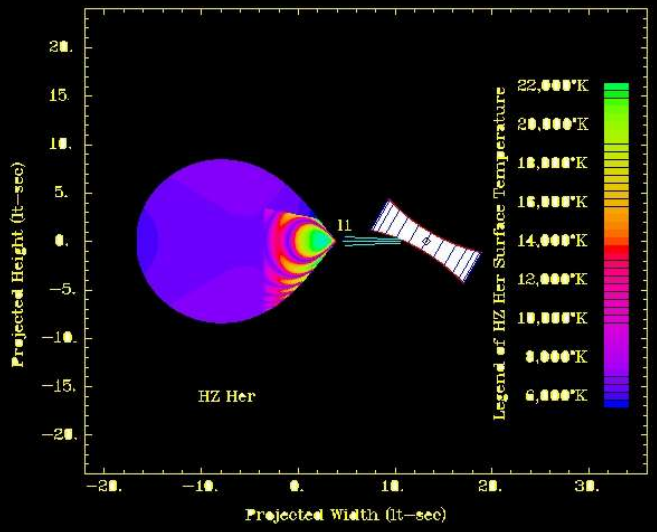
Projected Height (lt-sec)
20.
15.
10.
5.
0.
-5.
-10.
-15.
-20.
-20.
-10.
0.
10.
20.
30.
Projected Width (lt-sec)
HZ Her
11
4
Legend of HZ Her Surface Temperature
22,000°K
20,000°K
18,000°K
16,000°K
14,000°K
12,000°K
10,000°K
8,000°K
6,000°K

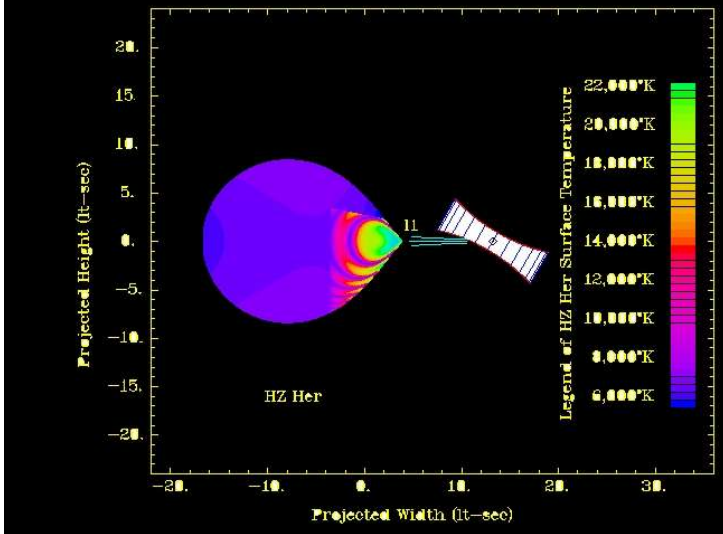
Projected Height (lt-sec)
20.
15.
10.
5.
0.
-5.
-10.
-15.
-20.
-20.
-10.
0.
10.
20.
30.
Projected Width (lt-sec)
HZ Her
11
4
Legend of HZ Her Surface Temperature
22,000°K
20,000°K
18,000°K
16,000°K
14,000°K
12,000°K
10,000°K
8,000°K
6,000°K

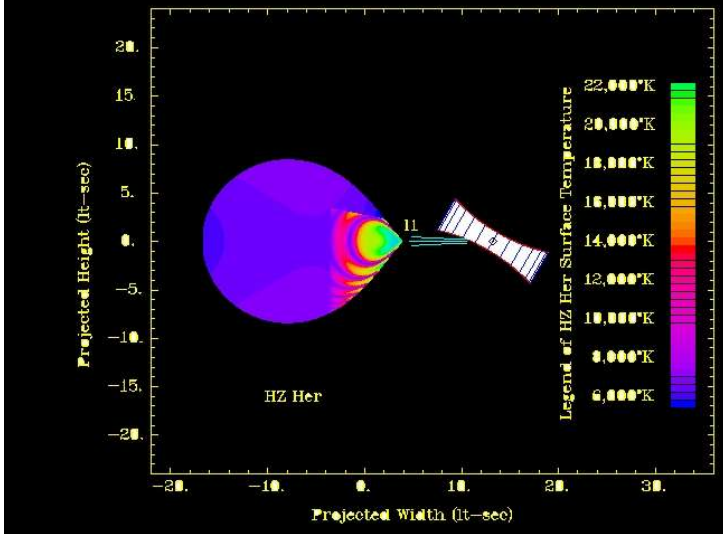
Projected Height (lt-sec)
20.
15.
10.
5.
0.
-5.
-10.
-15.
-20.
-20.
-10.
0.
10.
20.
30.
Projected Width (lt-sec)
HZ Her
11
4
Legend of HZ Her Surface Temperature
22,000°K
20,000°K
18,000°K
16,000°K
14,000°K
12,000°K
10,000°K
8,000°K
6,000°K

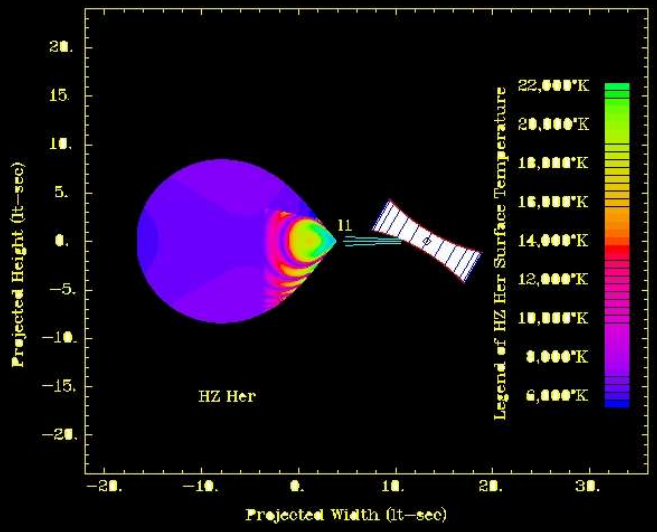
Projected Height (lt-sec)
20.
15.
10.
5.
0.
-5.
-10.
-15.
-20.
-20.
-10.
0.
10.
20.
30.
Projected Width (lt-sec)
HZ Her
11
4
Legend of HZ Her Surface Temperature
22,000°K
20,000°K
18,000°K
16,000°K
14,000°K
12,000°K
10,000°K
8,000°K
6,000°K

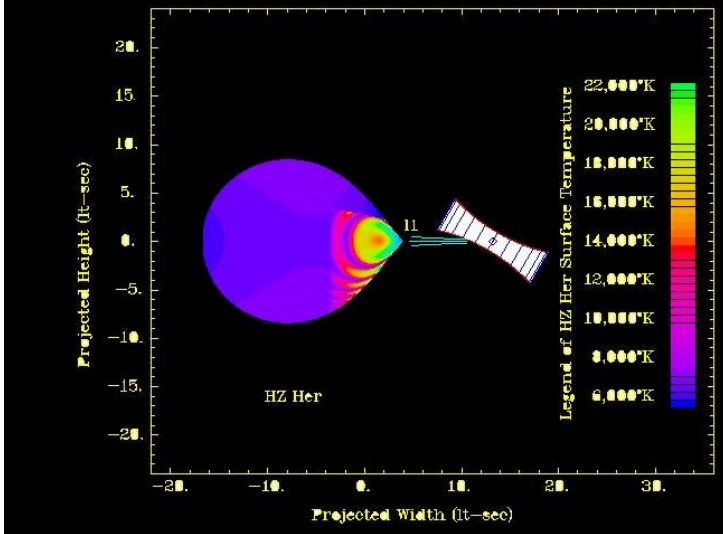
Projected Height (lt-sec)
20.
15.
10.
5.
0.
-5.
-10.
-15.
-20.
-20.
-10.
0.
10.
20.
30.
Projected Width (lt-sec)
HZ Her
11
4
Legend of HZ Her Surface Temperature
22,000°K
20,000°K
18,000°K
16,000°K
14,000°K
12,000°K
10,000°K
8,000°K
6,000°K

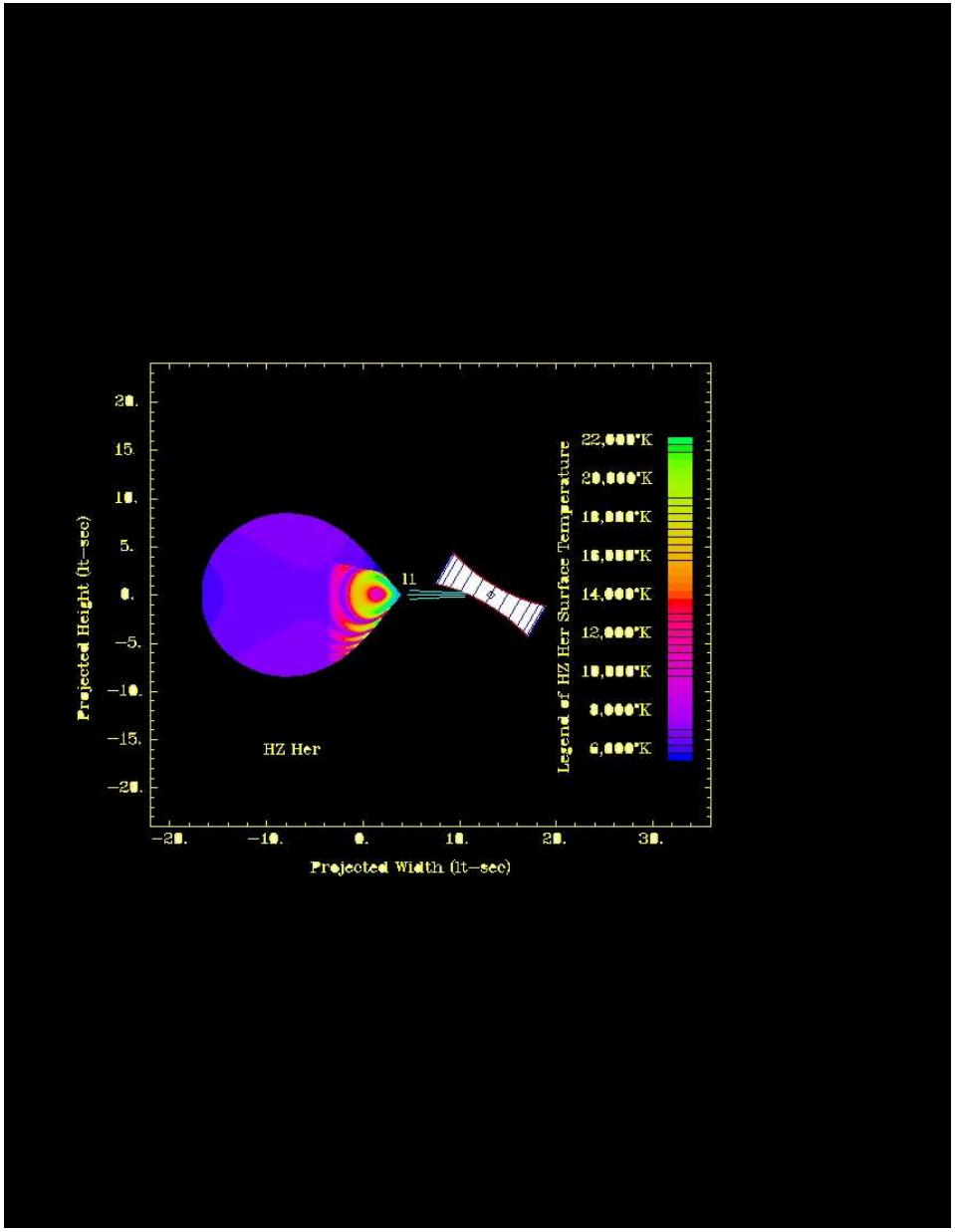
Projected Height (lt-sec)
20.
15.
10.
5.
0.
-5.
-10.
-15.
-20.
-20.
-10.
0.
10.
20.
30.
Projected Width (lt-sec)
HZ Her
11
4
Legend of HZ Her Surface Temperature
22,000°K
20,000°K
18,000°K
16,000°K
14,000°K
12,000°K
10,000°K
8,000°K
6,000°K

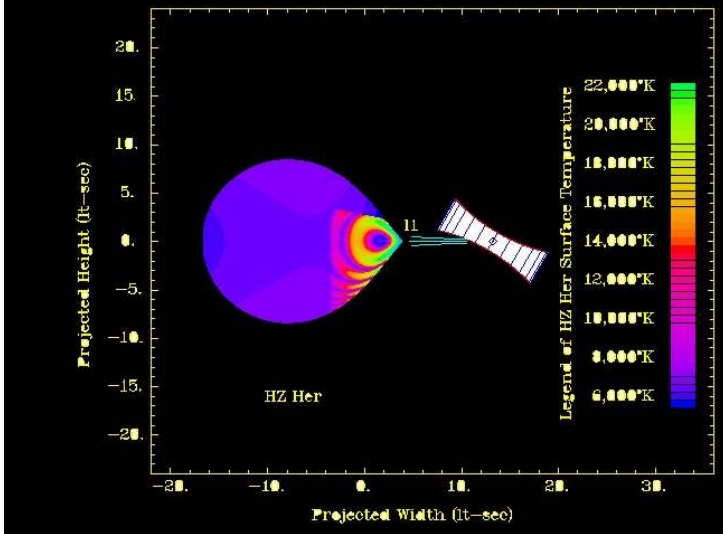
Projected Height (lt-sec)
20.
15.
10.
5.
0.
-5.
-10.
-15.
-20.
-20.
-10.
0.
10.
20.
30.
Projected Width (lt-sec)
HZ Her
11
4
Legend of HZ Her Surface Temperature
22,000°K
20,000°K
18,000°K
16,000°K
14,000°K
12,000°K
10,000°K
8,000°K
6,000°K

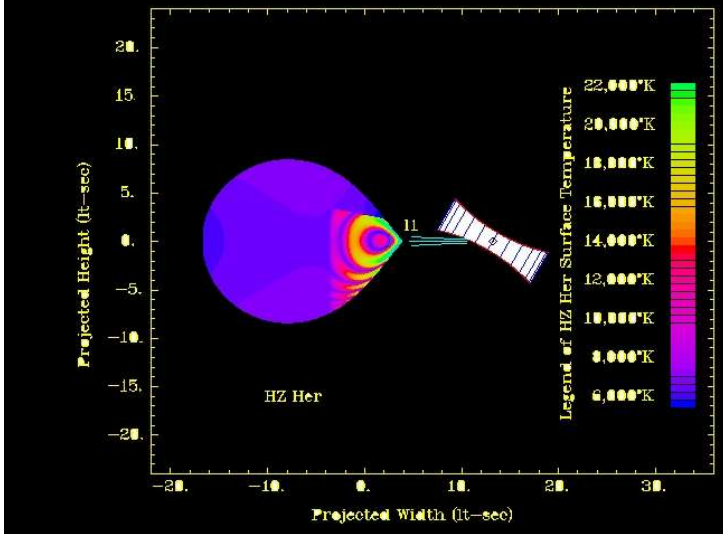
Projected Height (lt-sec)
20.
15.
10.
5.
0.
-5.
-10.
-15.
-20.
-20.
-10.
0.
10.
20.
30.
Projected Width (lt-sec)
HZ Her
11
4
Legend of HZ Her Surface Temperature
22,000°K
20,000°K
18,000°K
16,000°K
14,000°K
12,000°K
10,000°K
8,000°K
6,000°K

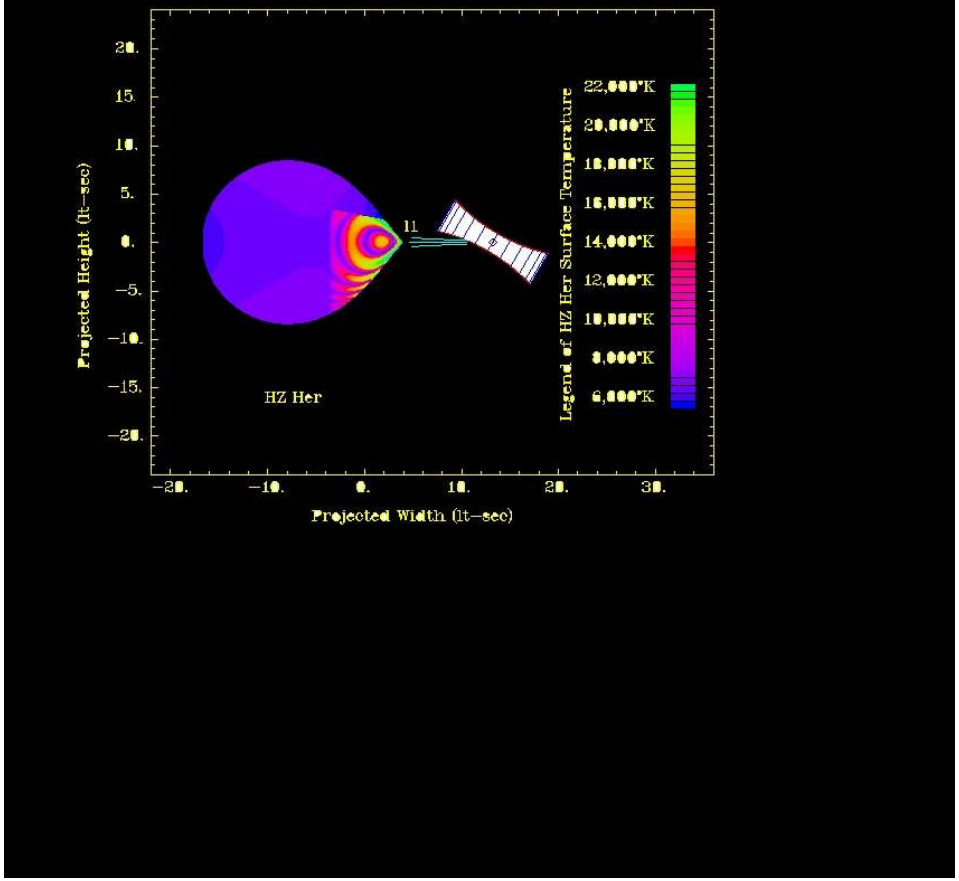
Projected Height (lt-sec)
20.
15.
10.
5.
0.
-5.
-10.
-15.
-20.
-20.
-10.
0.
10.
20.
30.
Projected Width (lt-sec)
HZ Her
11
4
Legend of HZ Her Surface Temperature
22,000°K
20,000°K
18,000°K
16,000°K
14,000°K
12,000°K
10,000°K
8,000°K
6,000°K

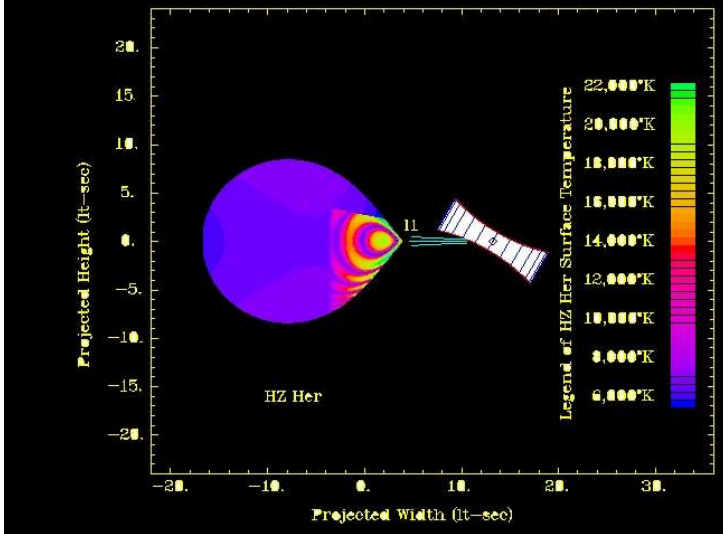
Projected Height (lt-sec)
20.
15.
10.
5.
0.
-5.
-10.
-15.
-20.
-20.
-10.
0.
10.
20.
30.
Projected Width (lt-sec)
HZ Her
11
4
Legend of HZ Her Surface Temperature
22,000°K
20,000°K
18,000°K
16,000°K
14,000°K
12,000°K
10,000°K
8,000°K
6,000°K

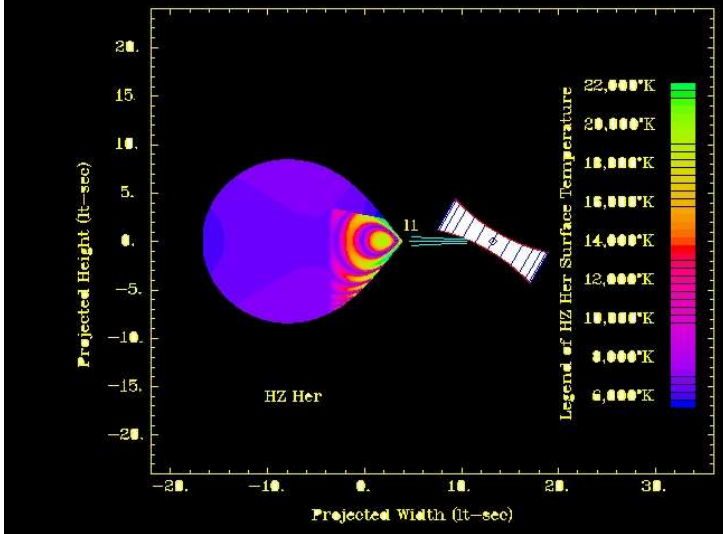
Projected Height (lt-sec)
20.
15.
10.
5.
0.
-5.
-10.
-15.
-20.
-20.
-10.
0.
10.
20.
30.
Projected Width (lt-sec)
HZ Her
11
4
Legend of HZ Her Surface Temperature
22,000°K
20,000°K
18,000°K
16,000°K
14,000°K
12,000°K
10,000°K
8,000°K
6,000°K

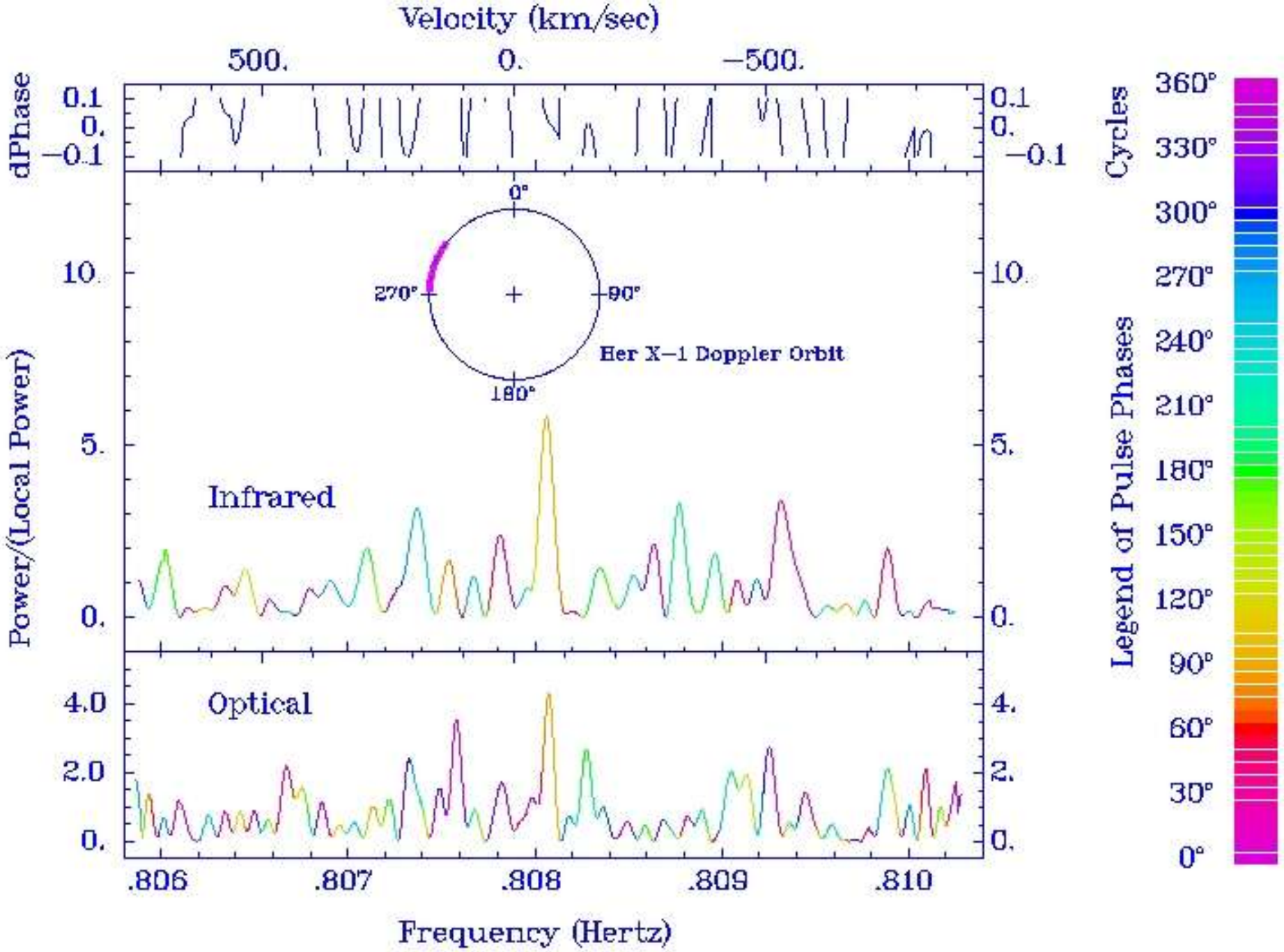
Velocity (km/sec)
500.
0.
−500.
dPhase
0.1
0.
−0.1
0°
270°
90°
180°
Her X−1 Doppler Orbit
Power/(Local Power)
10.
5.
0.
Infrared
4.0
2.0
Optical
.806
.807
.808
.809
.810
Frequency (Hertz)
Cycles
Legend of Pulse Phases
360°
330°
300°
270°
240°
210°
180°
150°
120°
90°
60°
30°
0°

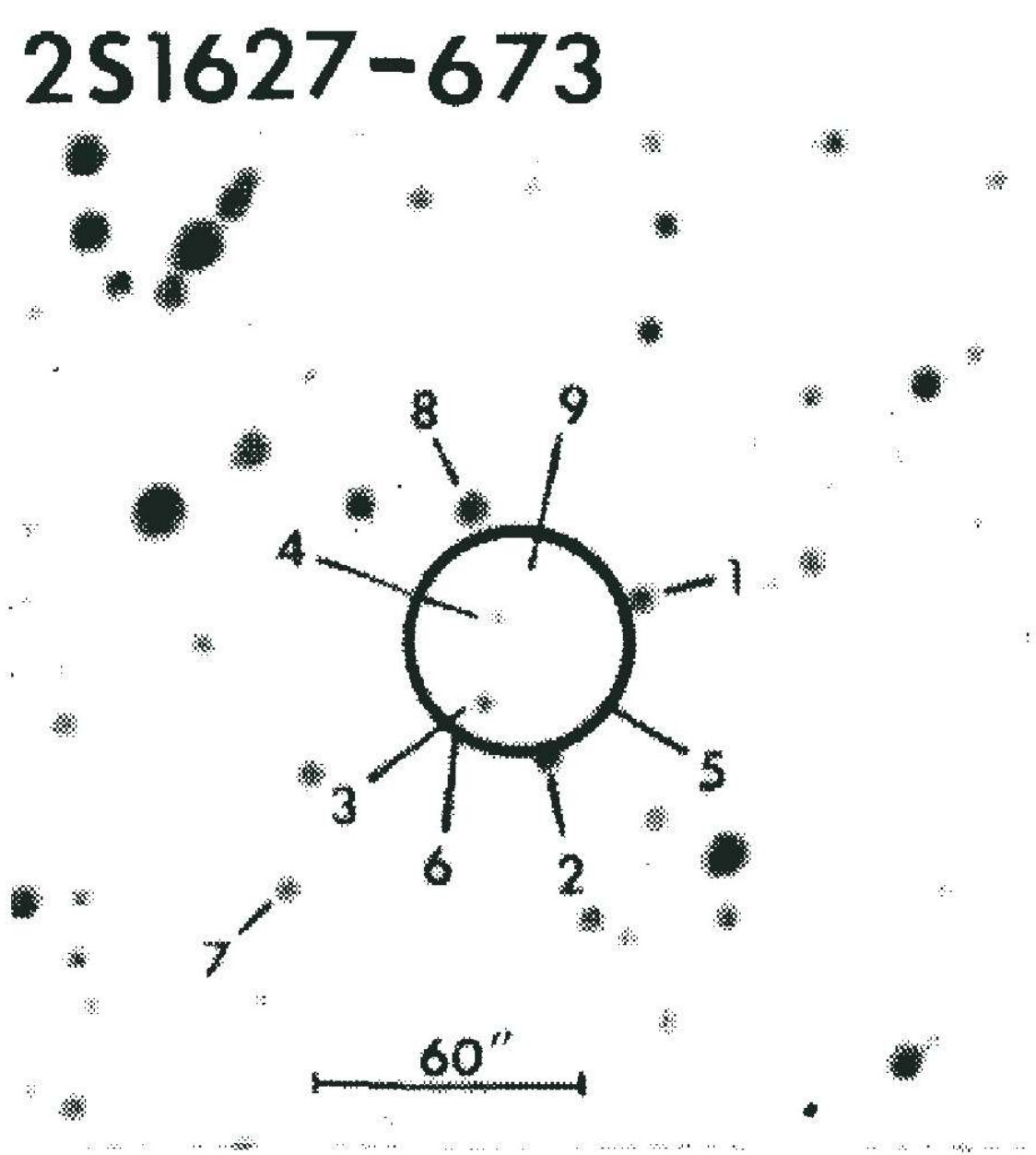

Fig. 2 Finding charts for the source 3U1626−67 — 2S1627-673. The optical candidate is star 4 (ref. 9).

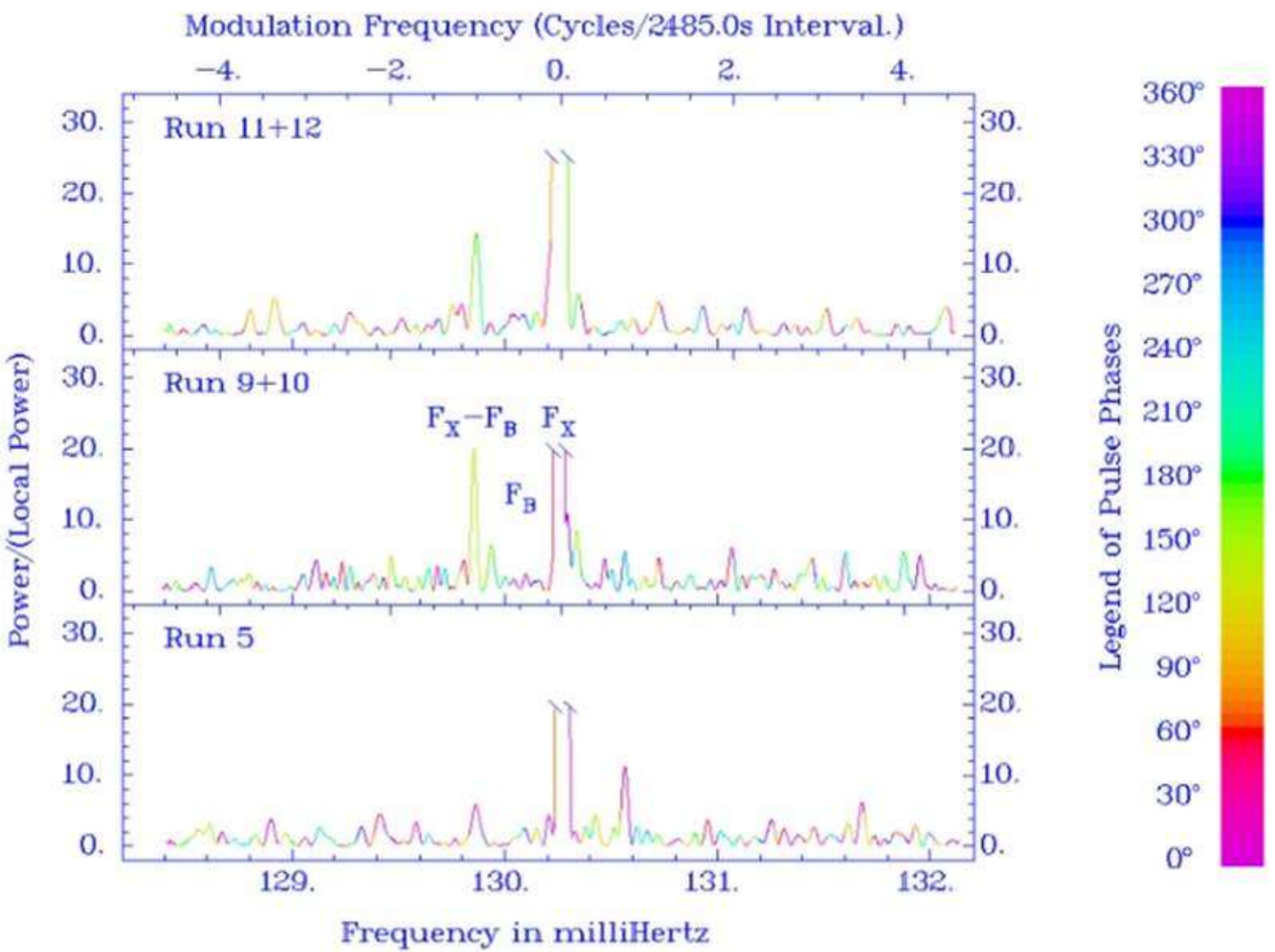
Modulation Frequency (Cycles/2485.0s Interval.)
−4.
−2.
0.
2.
4.
Run 11+12
Run 9+10
Run 5
$F_X - F_B$
F_X
F_B
30.
20.
10.
0.
Power/(Local Power)
129.
130.
131.
132.
Frequency in milliHertz
Legend of Pulse Phases
360°
330°
300°
270°
240°
210°
180°
150°
120°
90°
60°
30°
0°

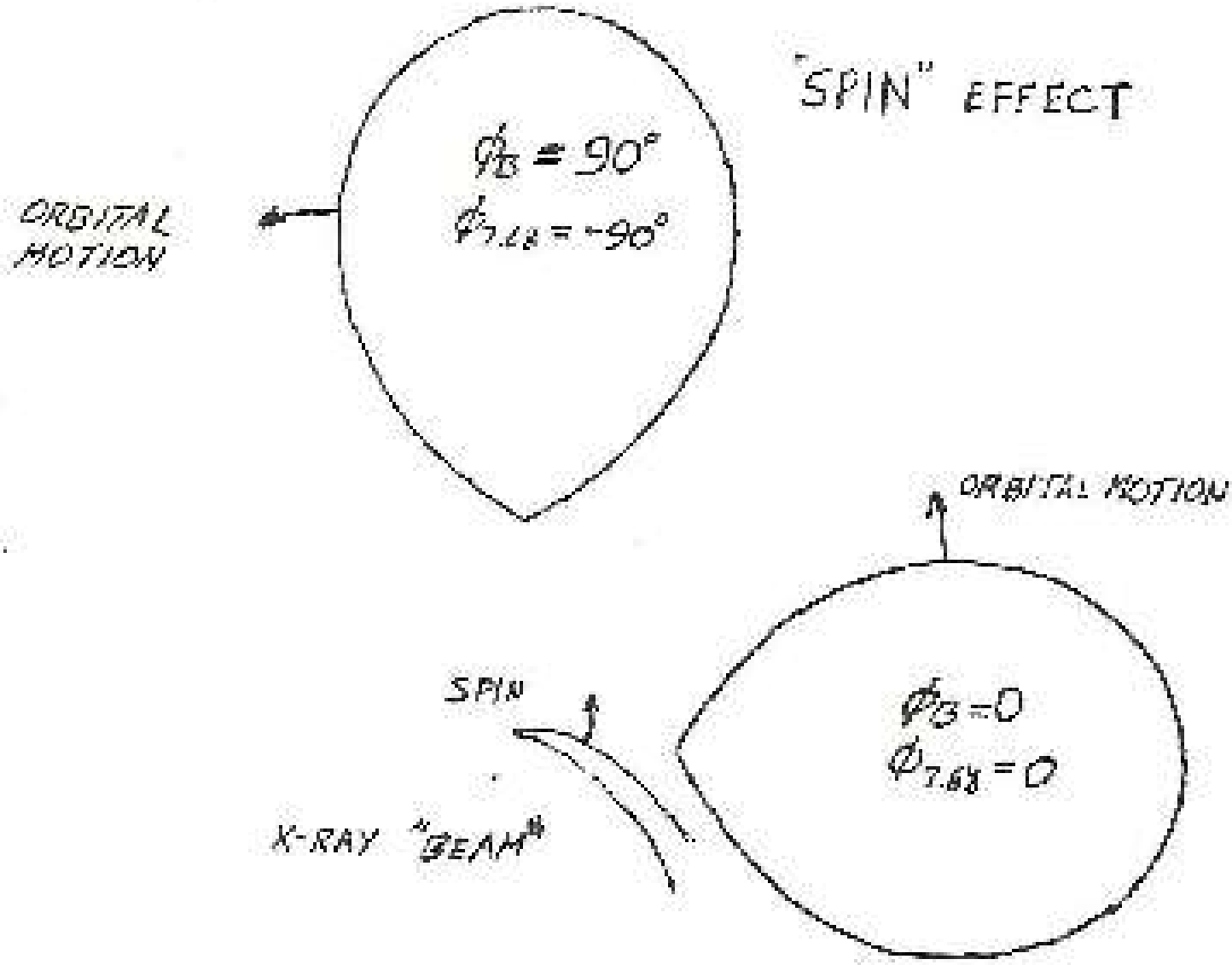
"SPIN" EFFECT
ORBITAL MOTION
$\phi_E = 90°$
$\phi_{7.68} = -90°$
ORBITAL MOTION
SPIN
X-RAY "BEAM"
$\phi_E = 0$
$\phi_{7.68} = 0$

Fig 15

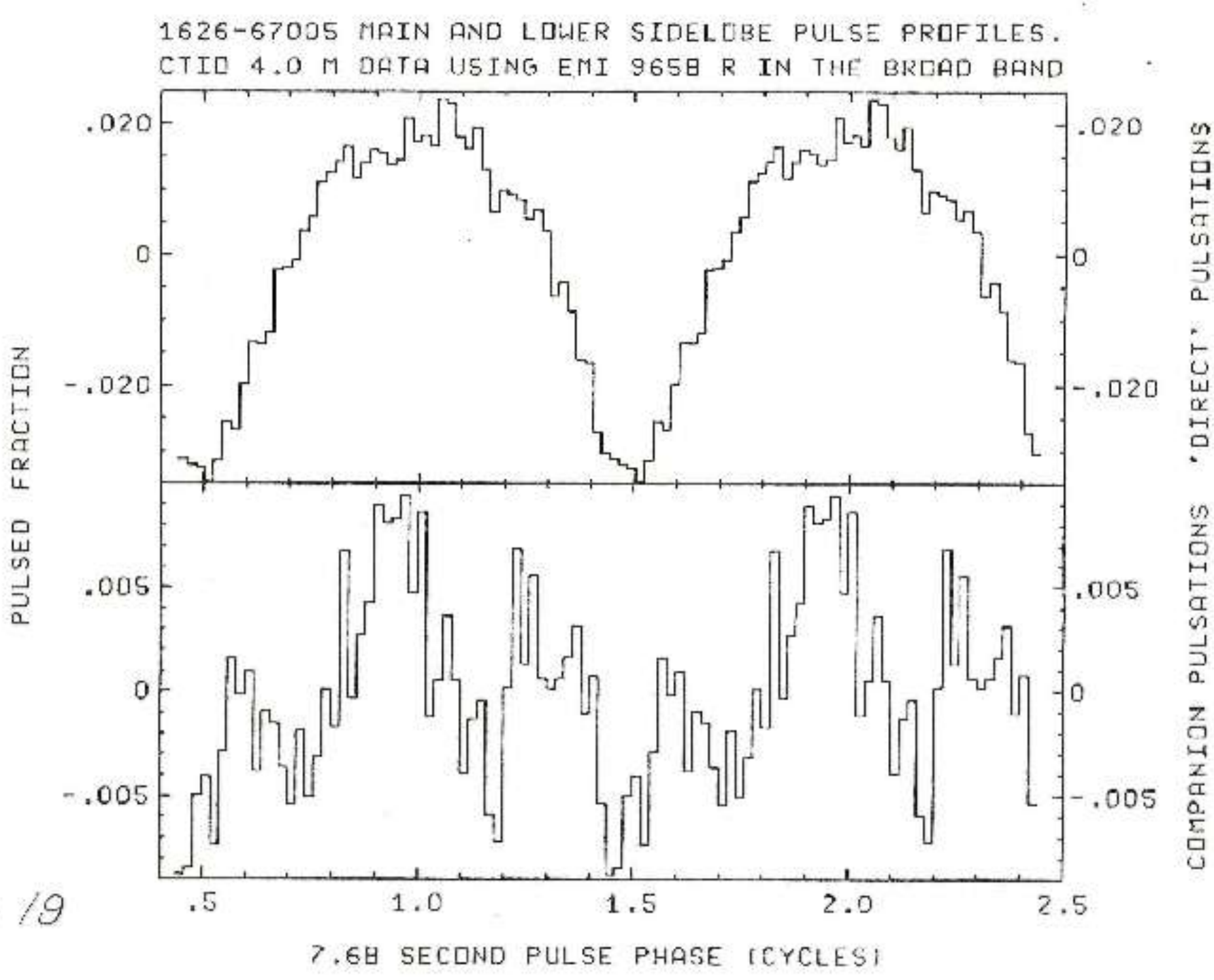
1626-67005 MAIN AND LOWER SIDELOBE PULSE PROFILES.
CTIO 4.0 M DATA USING EMI 9658 R IN THE BROAD BAND
.020
0
-.020
.005
0
-.005
PULSED FRACTION
COMPANION PULSATIONS 'DIRECT' PULSATIONS
.5
1.0
1.5
2.0
2.5
7.68 SECOND PULSE PHASE (CYCLES)

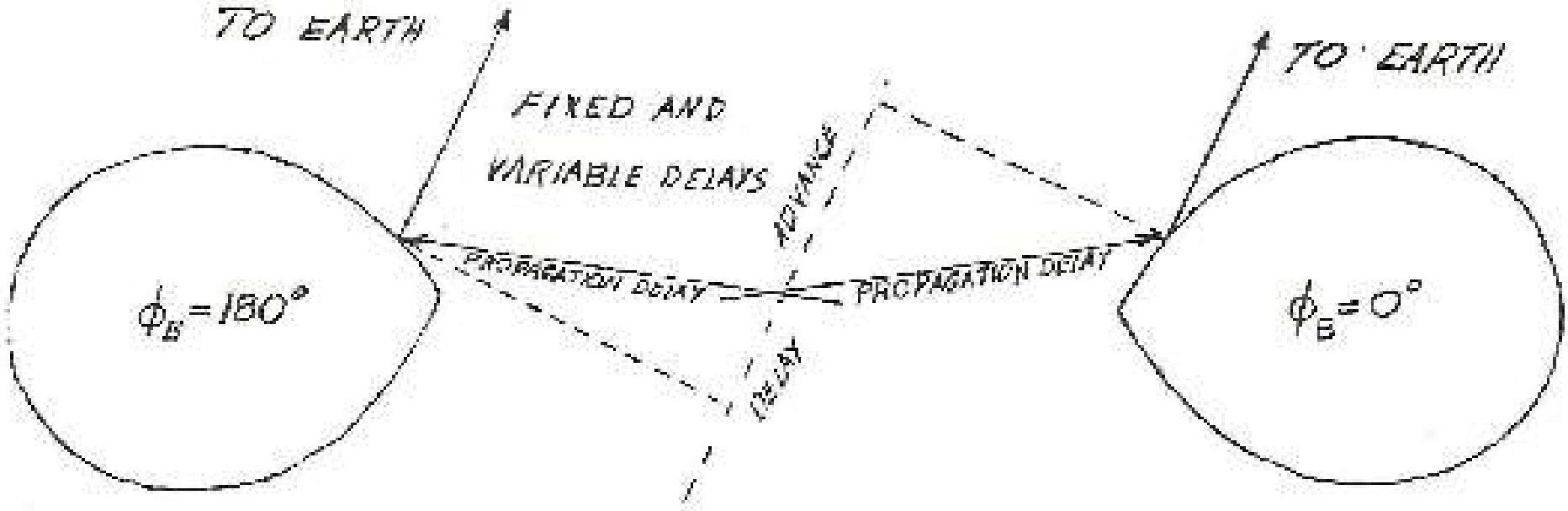
TO EARTH
FIXED AND
VARIABLE DELAYS
ADVANCE
TO EARTH
PROPAGATION DELAY
PROPAGATION DELAY
DELAY
$\phi_B = 180°$
$\phi_B = 0°$

Fig. 21

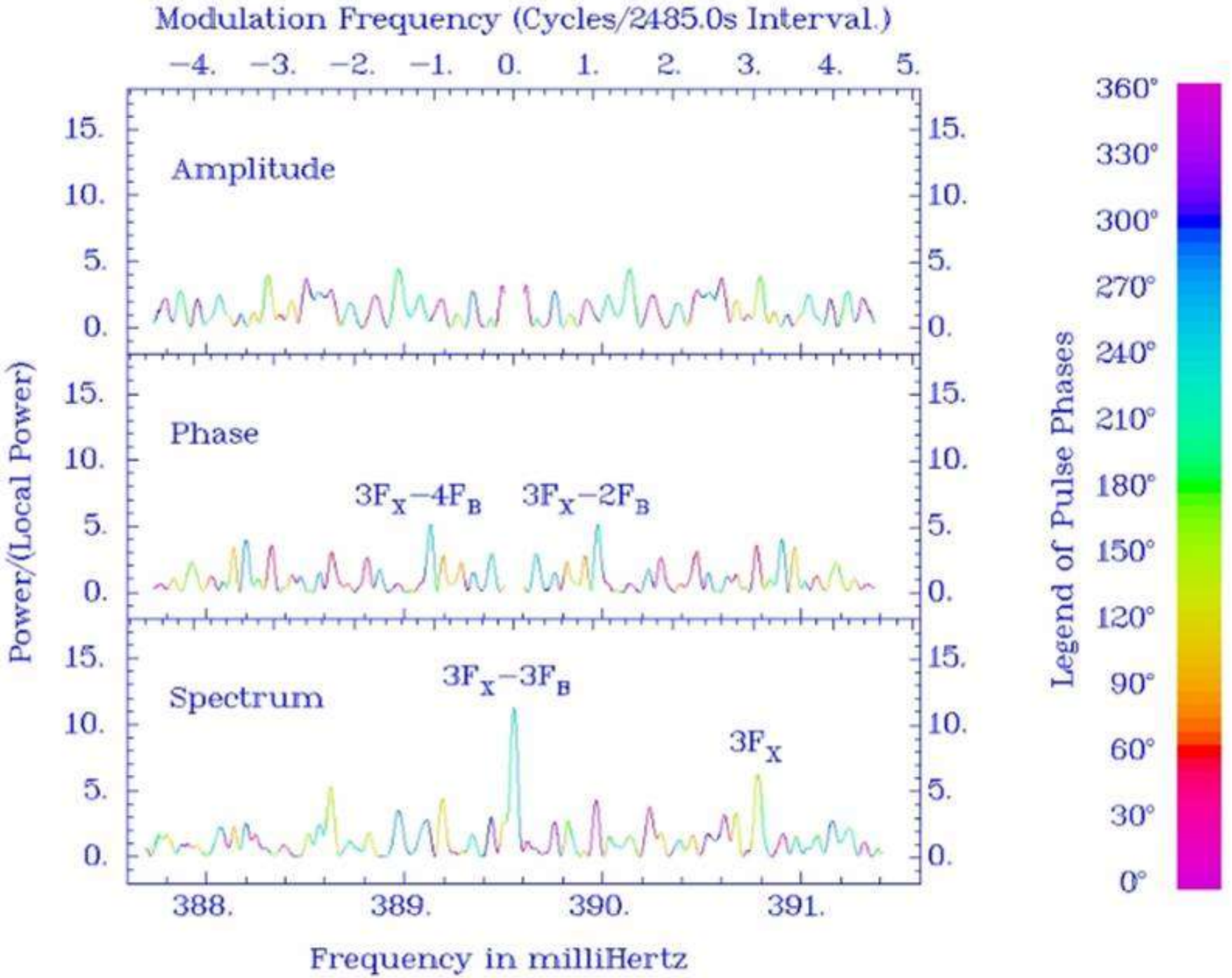
Modulation Frequency (Cycles/2485.0s Interval.)
−4. −3. −2. −1. 0. 1. 2. 3. 4. 5.
Amplitude
Phase
3F_X−4F_B
3F_X−2F_B
Spectrum
3F_X−3F_B
3F_X
15.
10.
5.
0.
Power/(Local Power)
388. 389. 390. 391.
Frequency in milliHertz
Legend of Pulse Phases
360°
330°
300°
270°
240°
210°
180°
150°
120°
90°
60°
30°
0°

No other orbital period (or any other periodic modulation of the direct pulsations at 130.26 mHz) is evident

where T_{FFT} is the total time spanned by the Fourier transform. Equation (1) represents a good approxima-

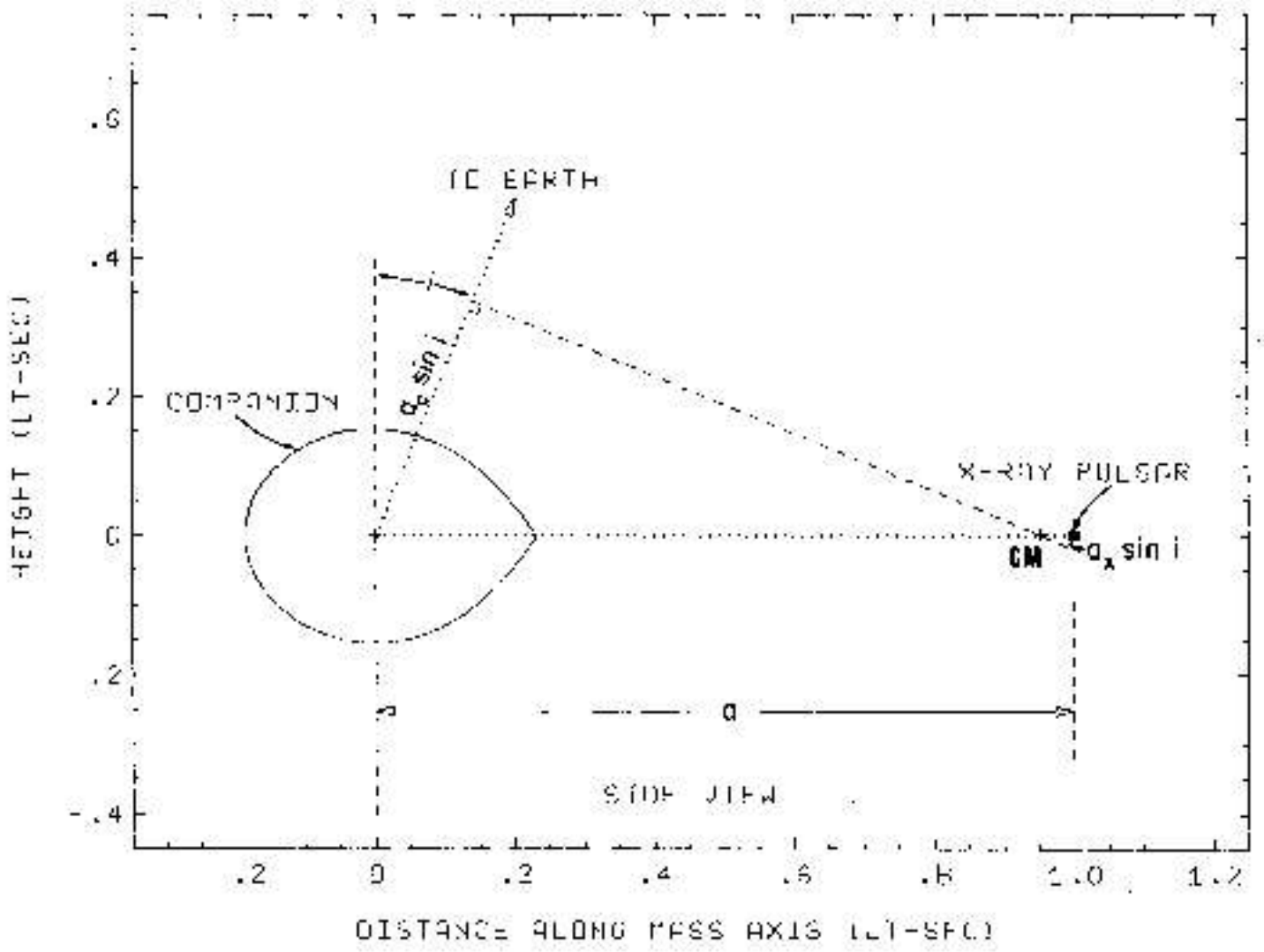

FIG. 3.—The orbital geometry of the 4U 1626–67 binary system with $R = M_c/M_x = 0.05$, an inclination $i = 22.^\circ5$ and with an orientation corresponding to orbital phase, $\phi_B = 180^\circ$. The projected orbital radii for the Roche filling companion star and the X-ray pulsar, $a_c \sin i$ and $a_x \sin i$, are shown along with the total orbital separation, a.

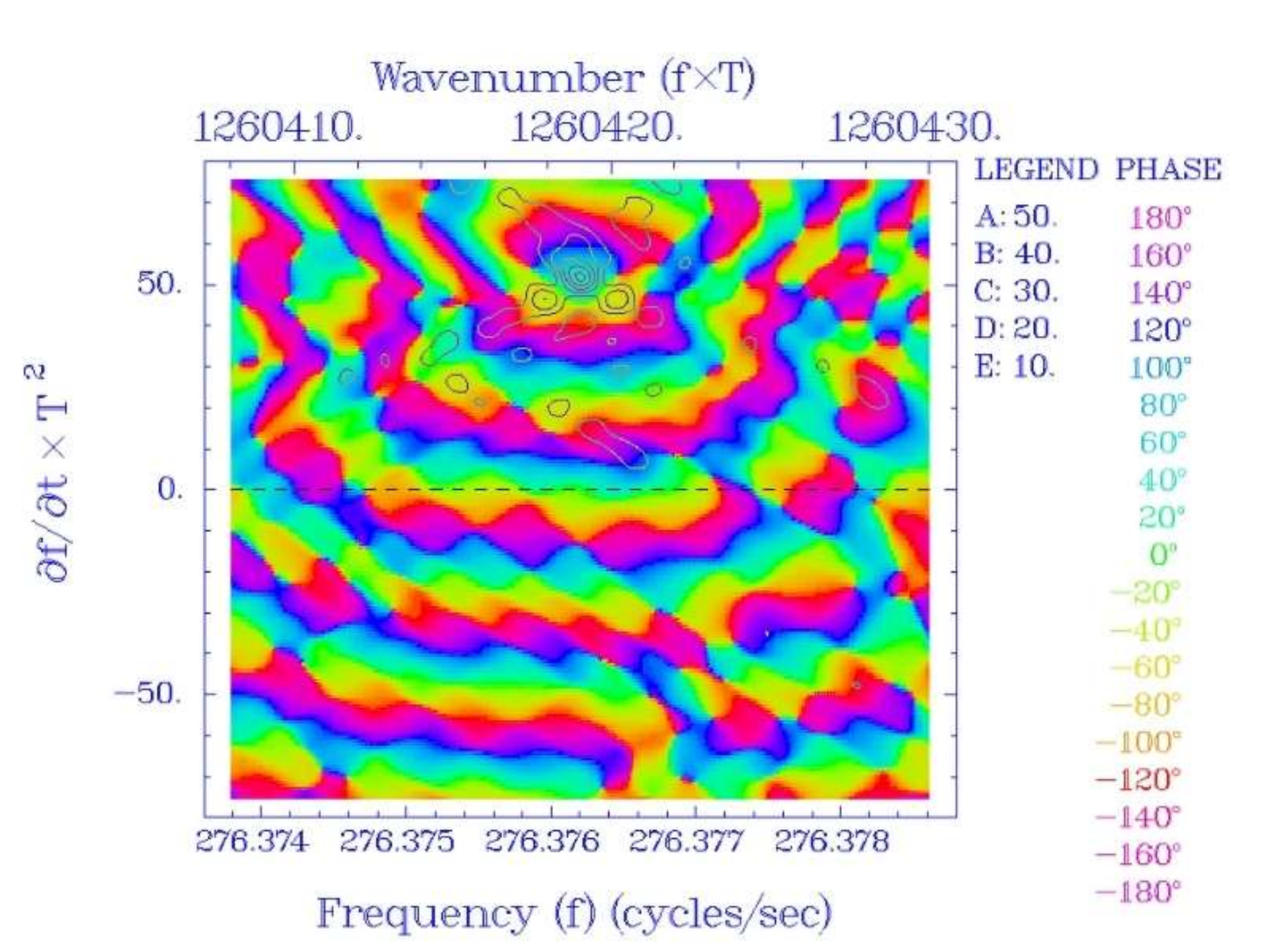
Wavenumber (f×T)
1260410.
1260420.
1260430.
LEGEND PHASE
A: 50.
B: 40.
C: 30.
D: 20.
E: 10.
180°
160°
140°
120°
100°
80°
60°
40°
20°
0°
−20°
−40°
−60°
−80°
−100°
−120°
−140°
−160°
−180°
50.
0.
−50.
∂f/∂t × T²
276.374
276.375
276.376
276.377
276.378
Frequency (f) (cycles/sec)

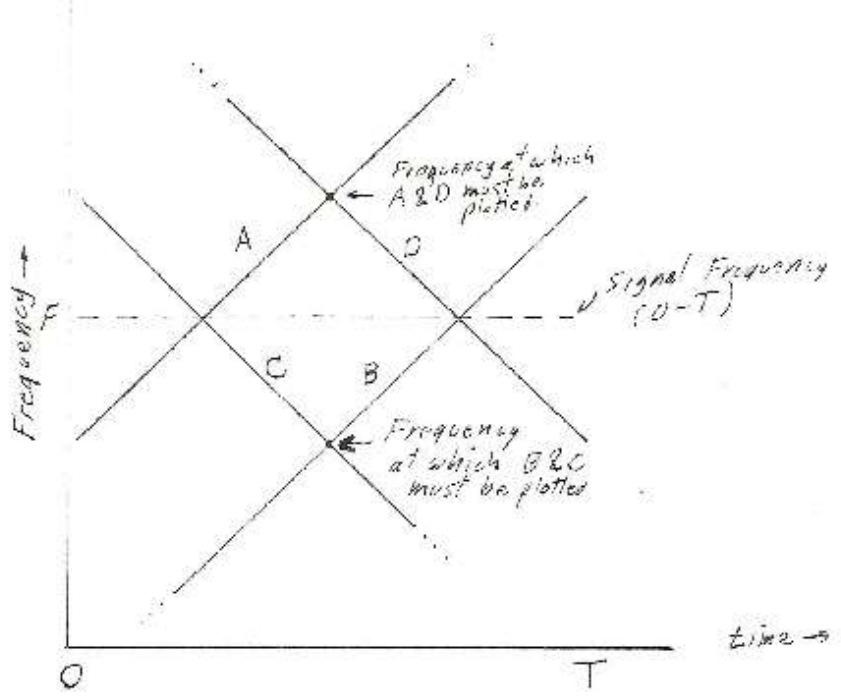
Frequency at which A & D must be plotted
A
D
Signal Frequency (O-T)
Frequency
F
C
B
Frequency at which B & C must be plotted
time →
O
T

Figure 25

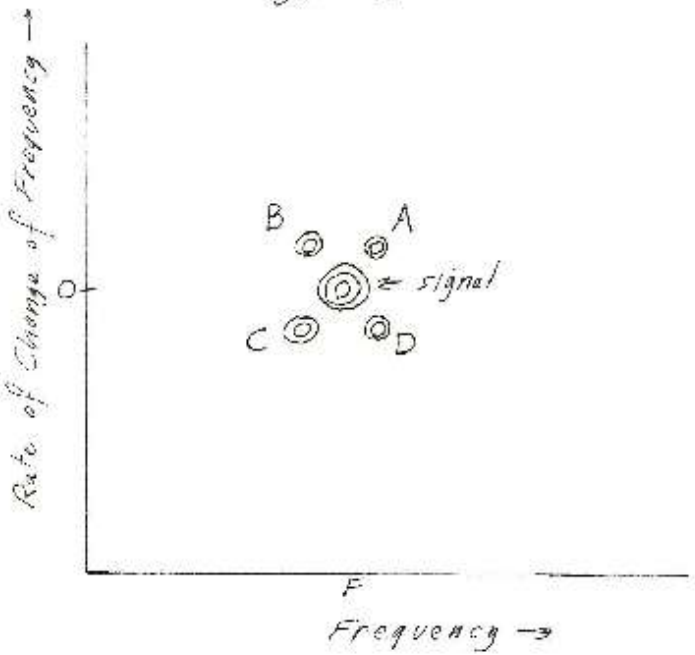
Rate of Change of Frequency →
B
A
signal
O
C
D
F
Frequency →

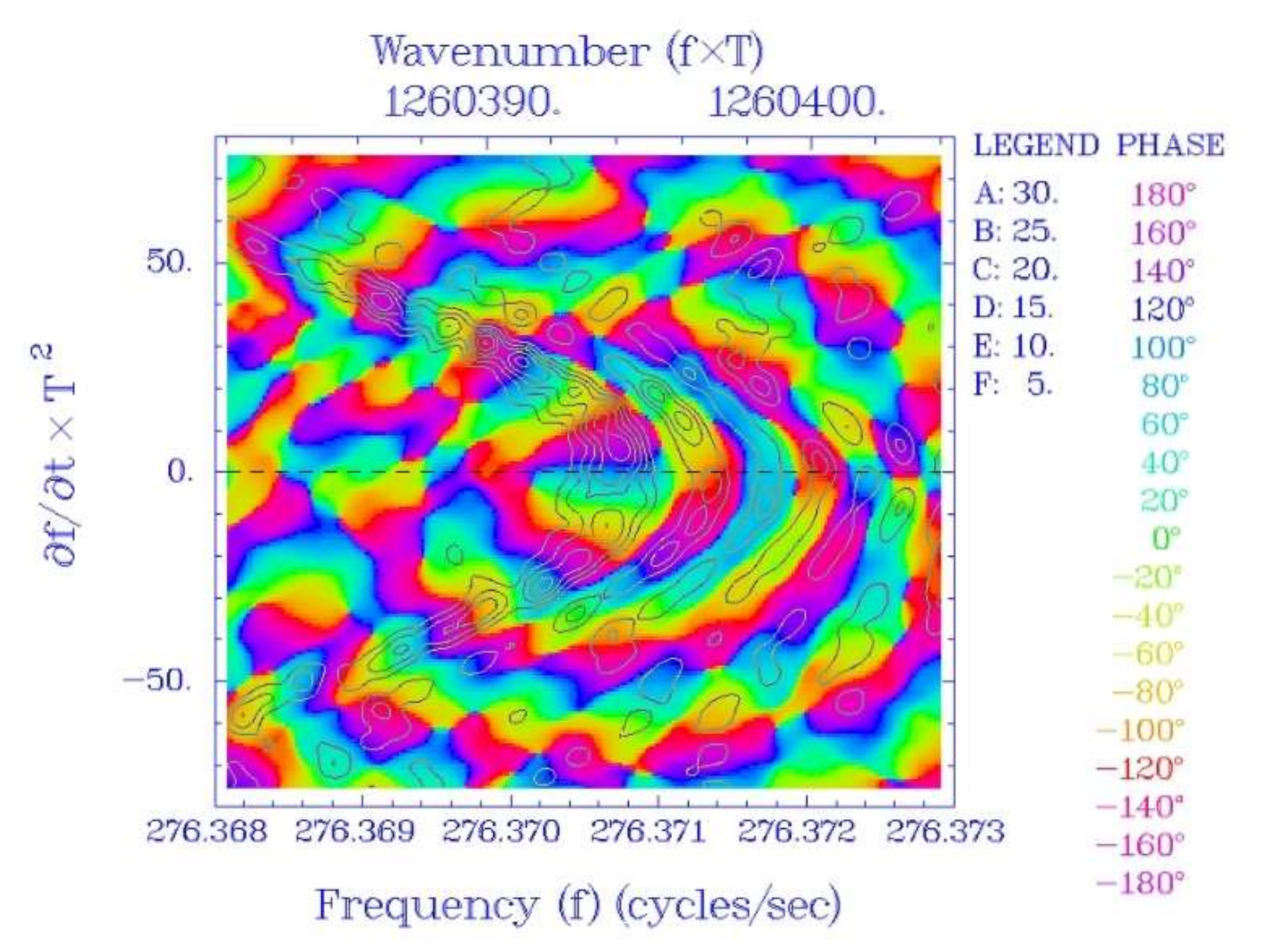
Wavenumber (f×T)
1260390.
1260400.
LEGEND PHASE
A: 30.
B: 25.
C: 20.
D: 15.
E: 10.
F: 5.
180°
160°
140°
120°
100°
80°
60°
40°
20°
0°
−20°
−40°
−60°
−80°
−100°
−120°
−140°
−160°
−180°
50.
0.
−50.
∂r/∂t × T²
276.368
276.369
276.370
276.371
276.372
276.373
Frequency (f) (cycles/sec)

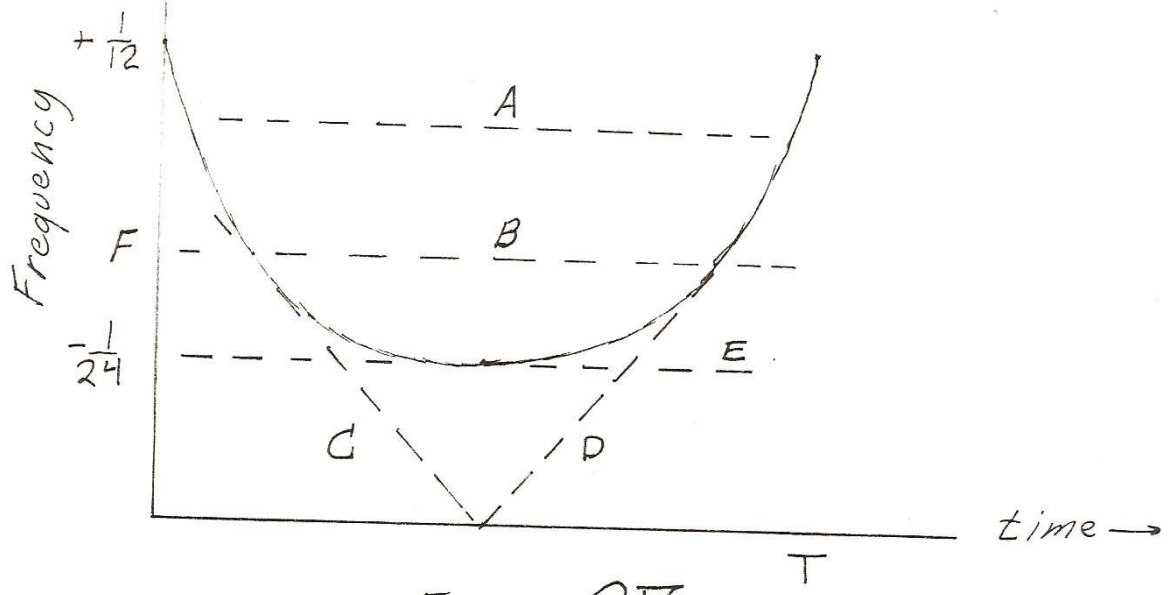
+1/12
Frequency
A
F
B
-1/24
E
C
D
time
T

Figure 28

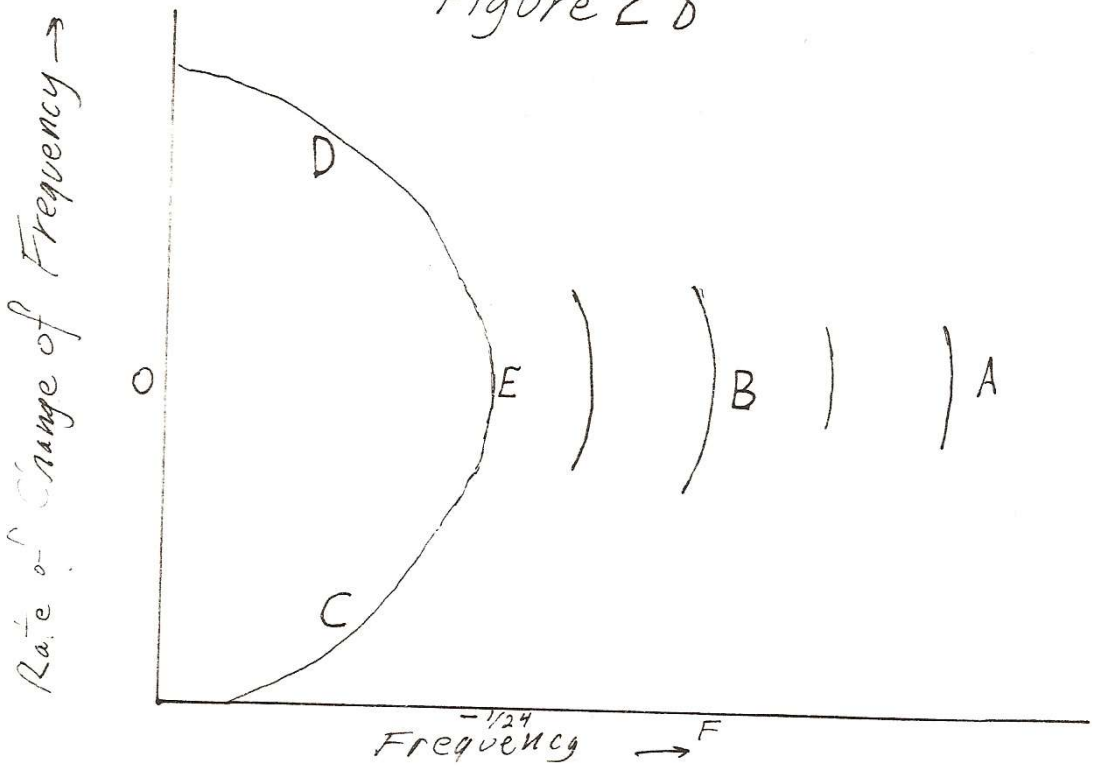
Rate of Change of Frequency
D
O
E
B
A
C
-1/24
Frequency
F

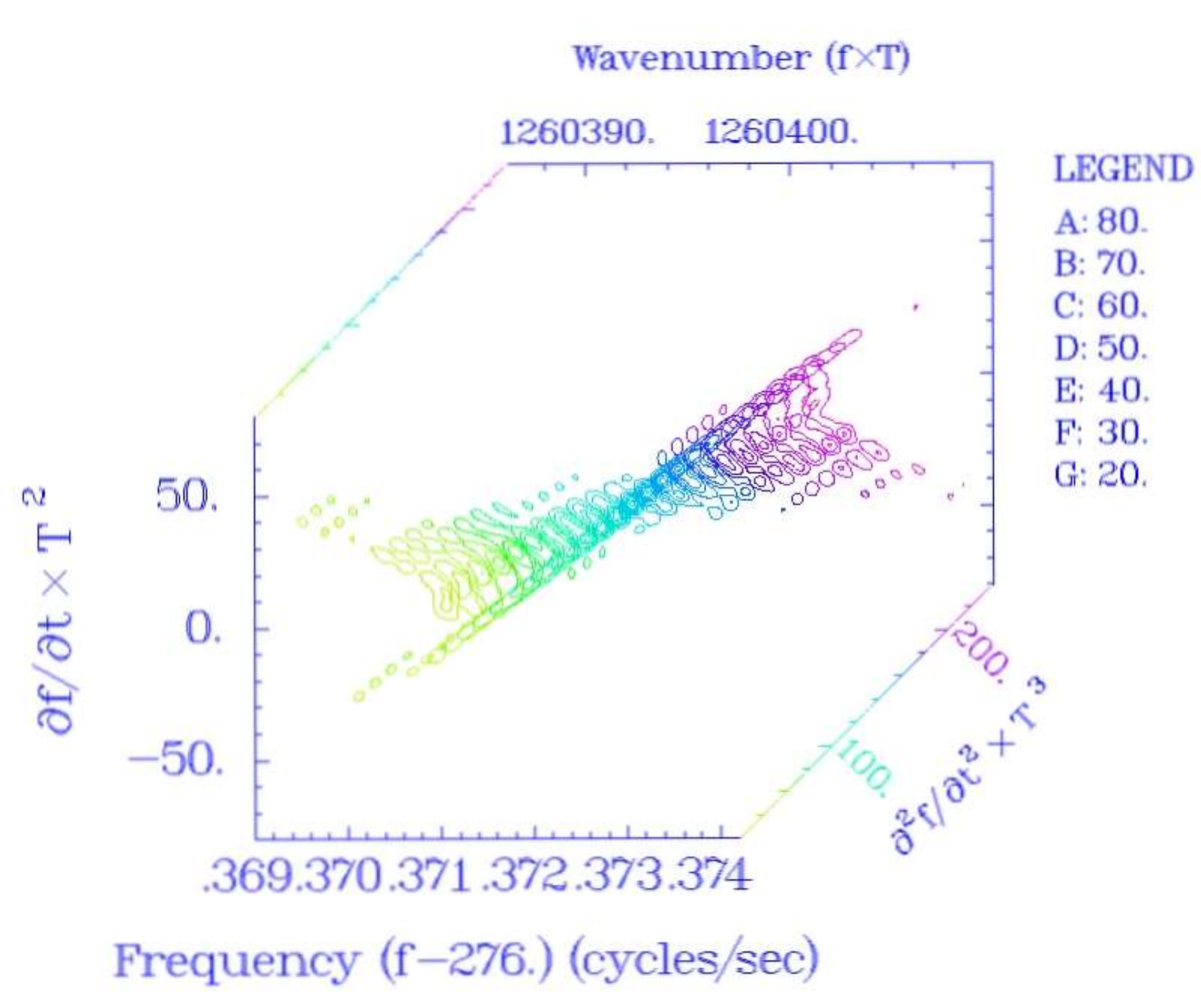
Wavenumber (f×T)
1260390.
1260400.
LEGEND
A: 80.
B: 70.
C: 60.
D: 50.
E: 40.
F: 30.
G: 20.
50.
0.
−50.
∂f/∂t × T²
200.
100.
∂²f/∂t² × T³
.369.370.371.372.373.374
Frequency (f−276.) (cycles/sec)

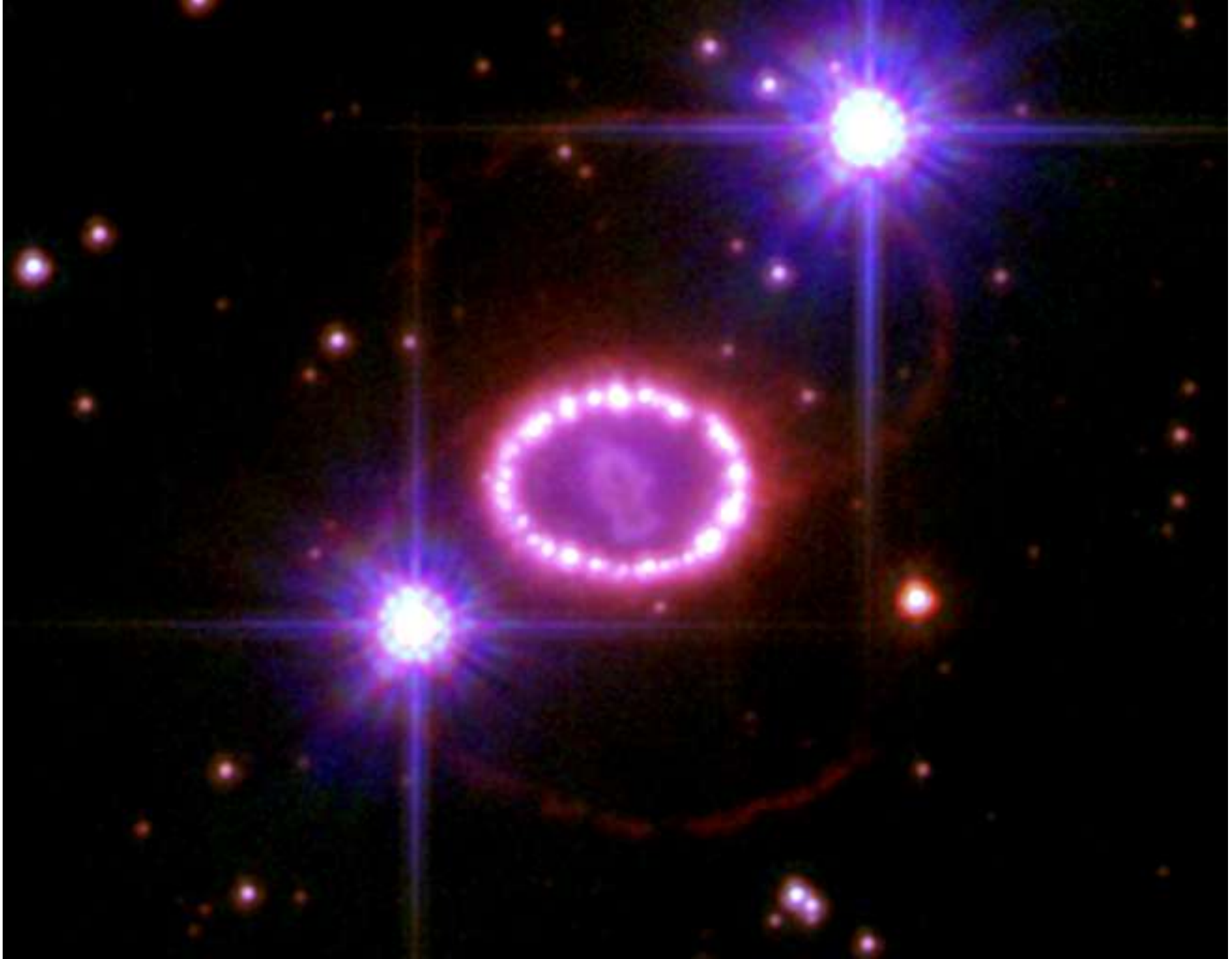

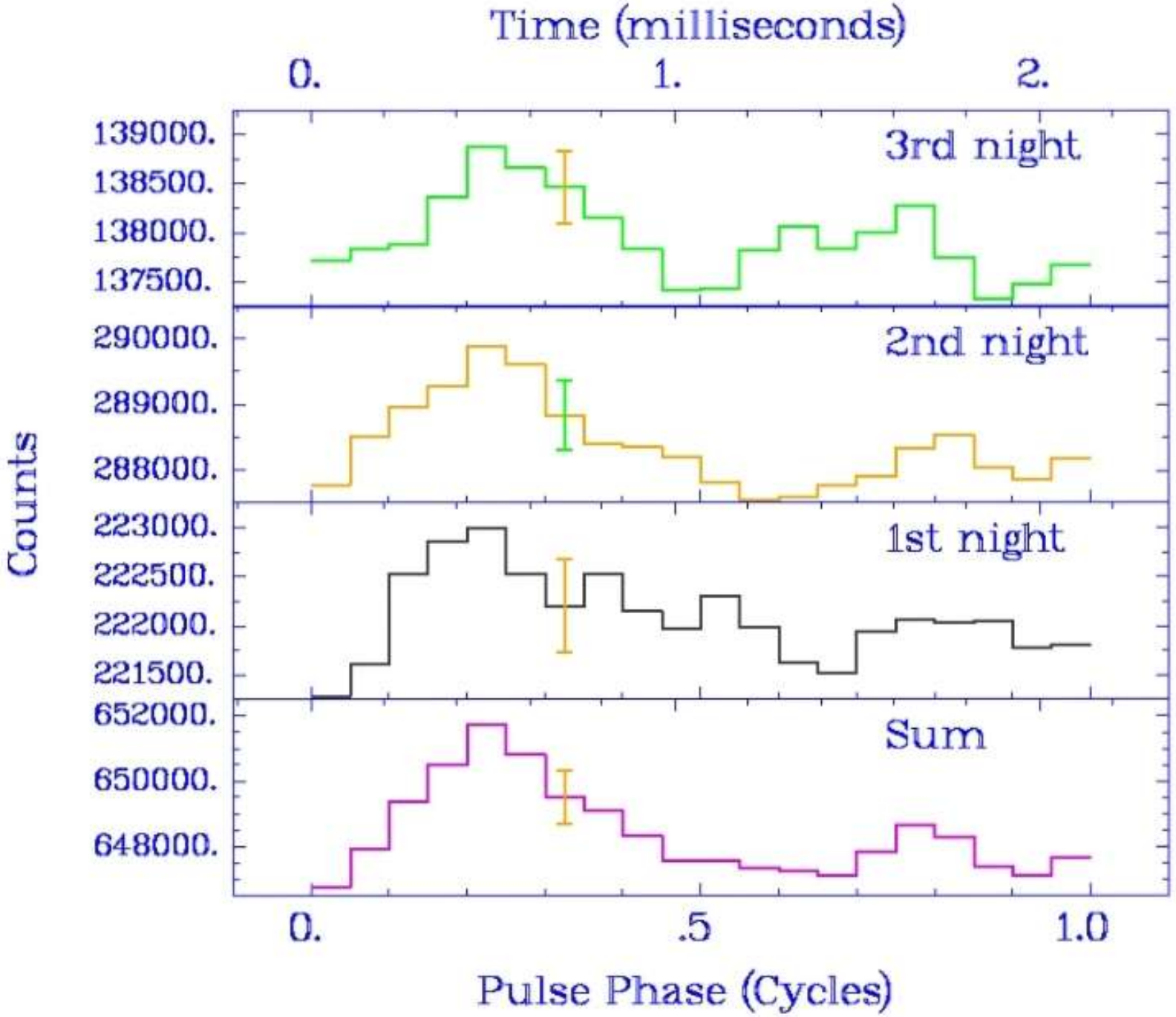
Time (milliseconds)
0.
1.
2.
Counts
139000.
138500.
138000.
137500.
3rd night
290000.
289000.
288000.
2nd night
223000.
222500.
222000.
221500.
1st night
652000.
650000.
648000.
Sum
0.
.5
1.0
Pulse Phase (Cycles)

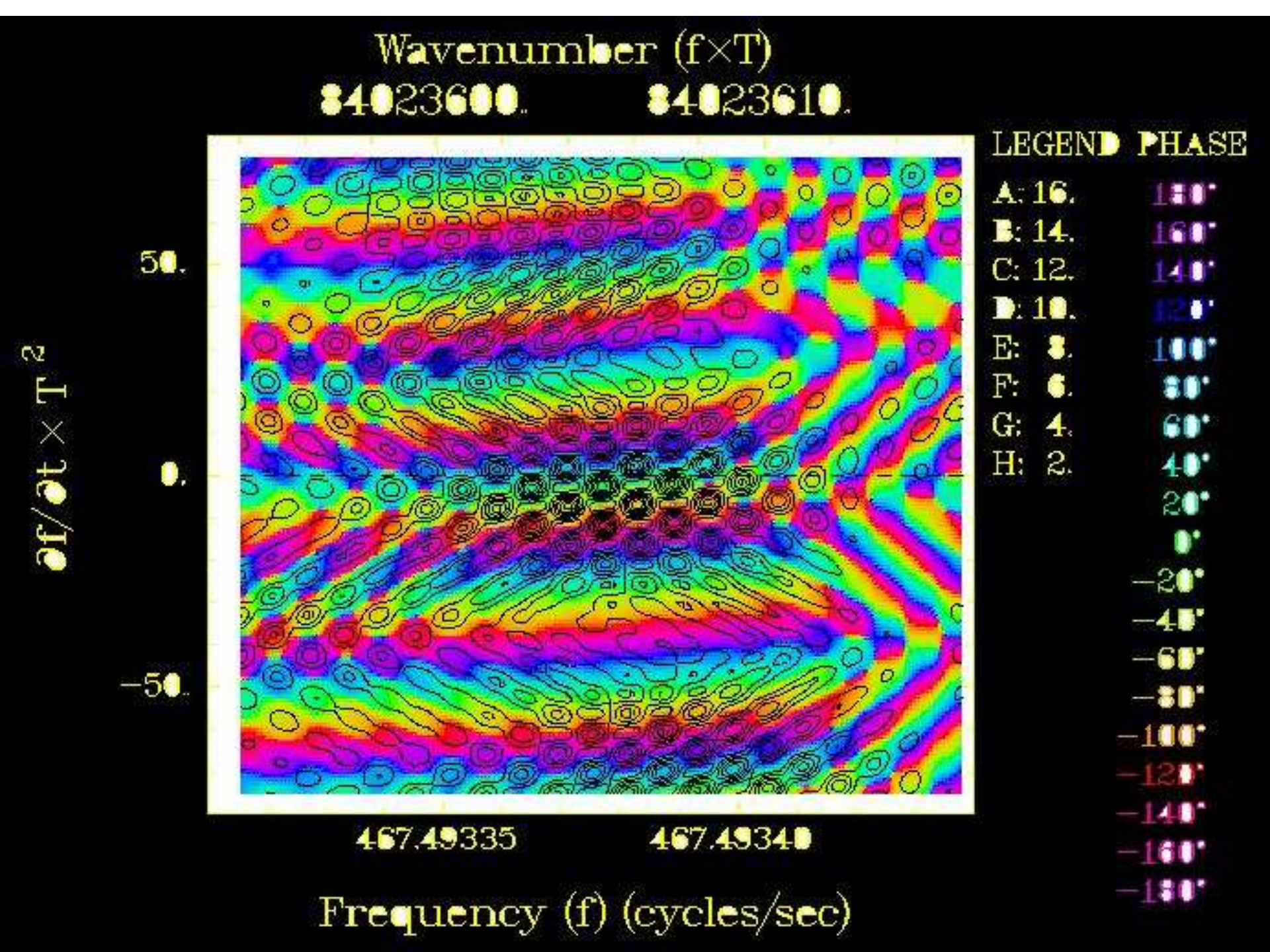
Wavenumber (f×T)
8402360.
8402361.
50.
0.
-50.
af/at × T²
LEGEND PHASE
A: 16.
B: 14.
C: 12.
D: 10.
E: 8.
F: 6.
G: 4.
H: 2.
180°
160°
140°
120°
100°
80°
60°
40°
20°
0°
-20°
-40°
-60°
-80°
-100°
-120°
-140°
-160°
-180°
467.49335
467.49340
Frequency (f) (cycles/sec)

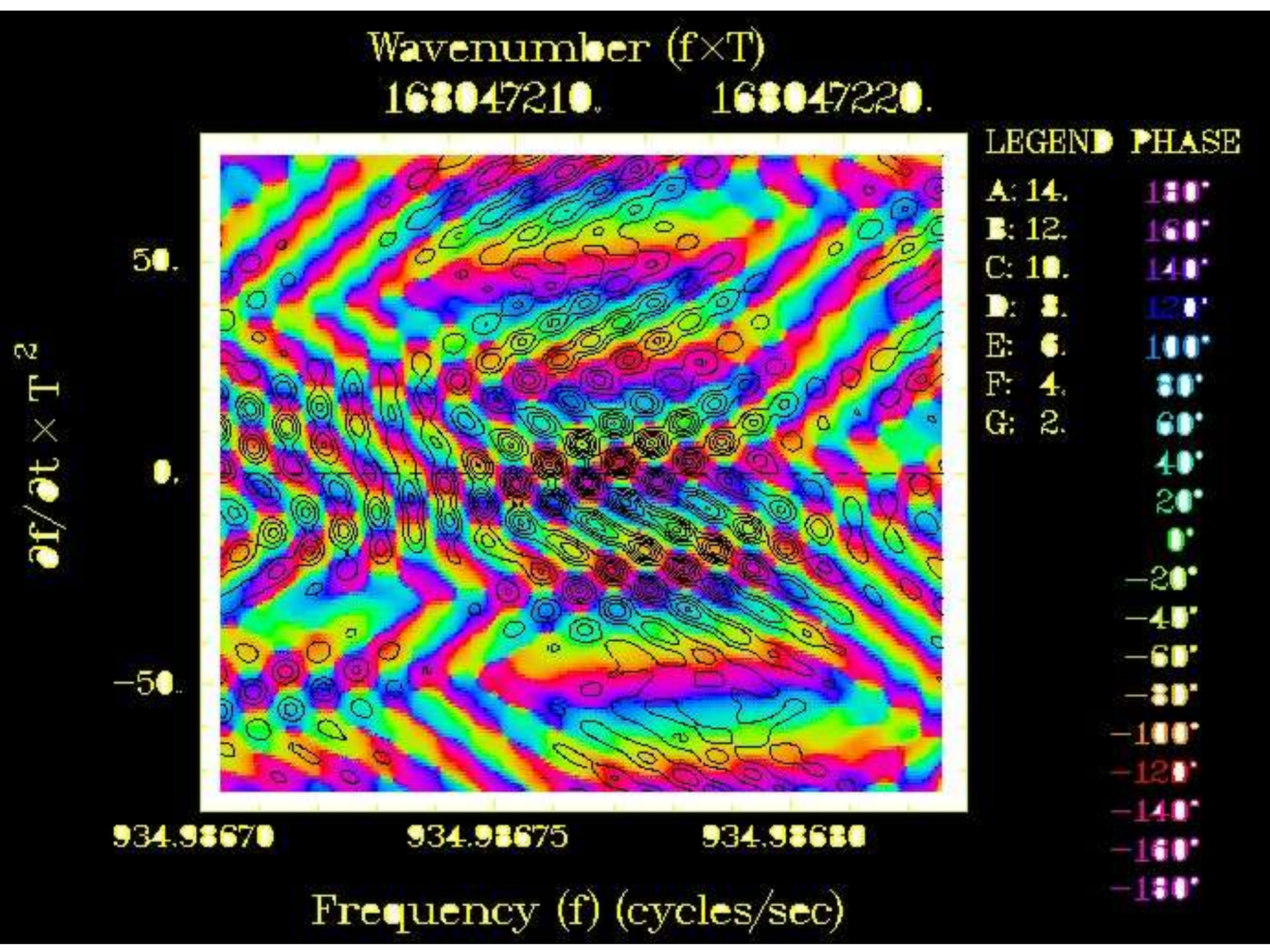
Wavenumber (f×T)
168047210.
168047220.
LEGEND PHASE
A: 14.
B: 12.
C: 10.
D: 8.
E: 6.
F: 4.
G: 2.
180°
160°
140°
120°
100°
80°
60°
40°
20°
0°
−20°
−40°
−60°
−80°
−100°
−120°
−140°
−160°
−180°
50.
0.
−50.
∂f/∂t × T²
934.98670
934.98675
934.98680
Frequency (f) (cycles/sec)

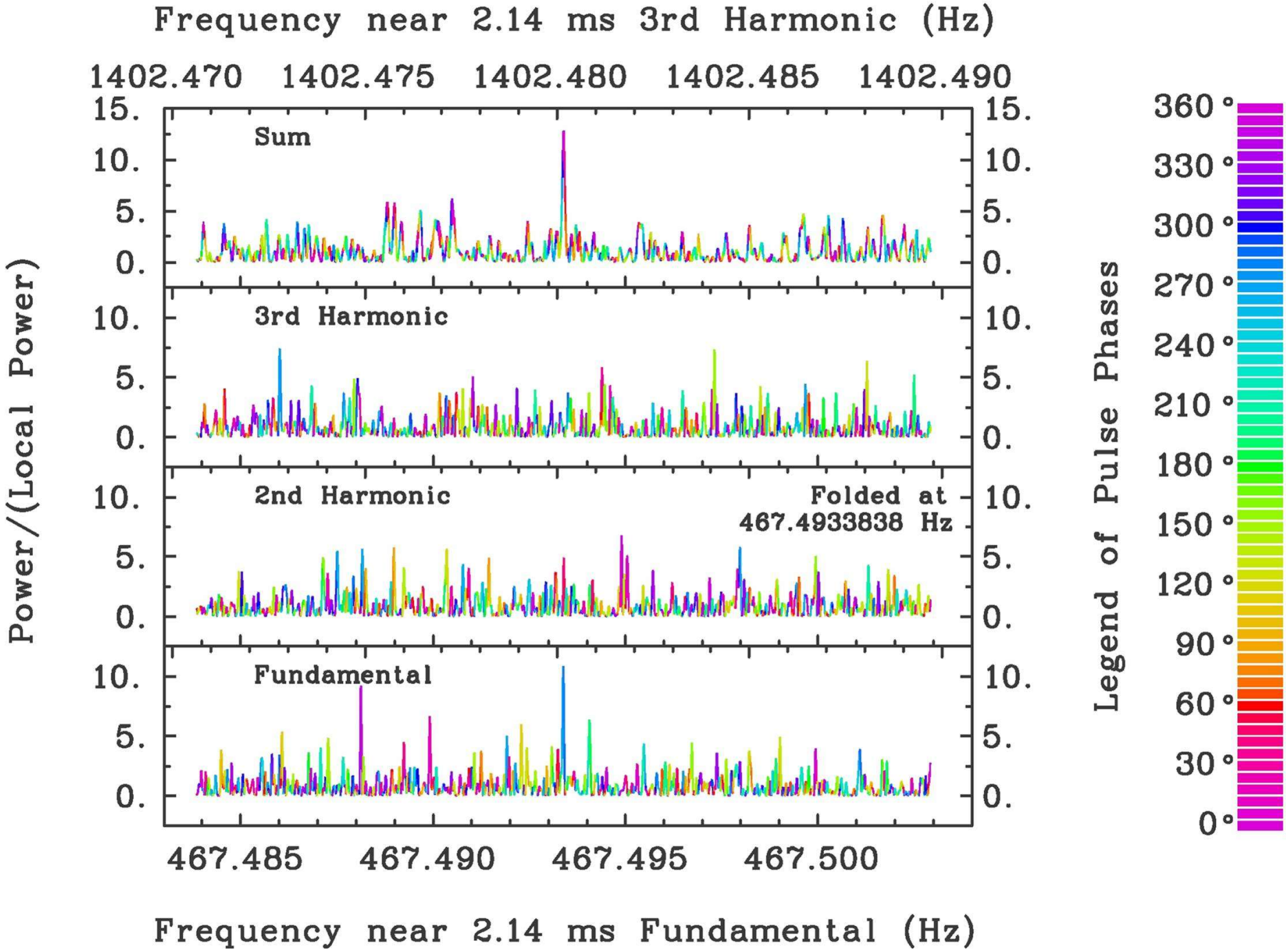
Frequency near 2.14 ms 3rd Harmonic (Hz)
1402.470
1402.475
1402.480
1402.485
1402.490
Sum
3rd Harmonic
2nd Harmonic
Folded at
467.4933838 Hz
Fundamental
Power/(Local Power)
15.
10.
5.
0.
467.485
467.490
467.495
467.500
Frequency near 2.14 ms Fundamental (Hz)
Legend of Pulse Phases
360 °
330 °
300 °
270 °
240 °
210 °
180 °
150 °
120 °
90 °
60 °
30 °
0 °

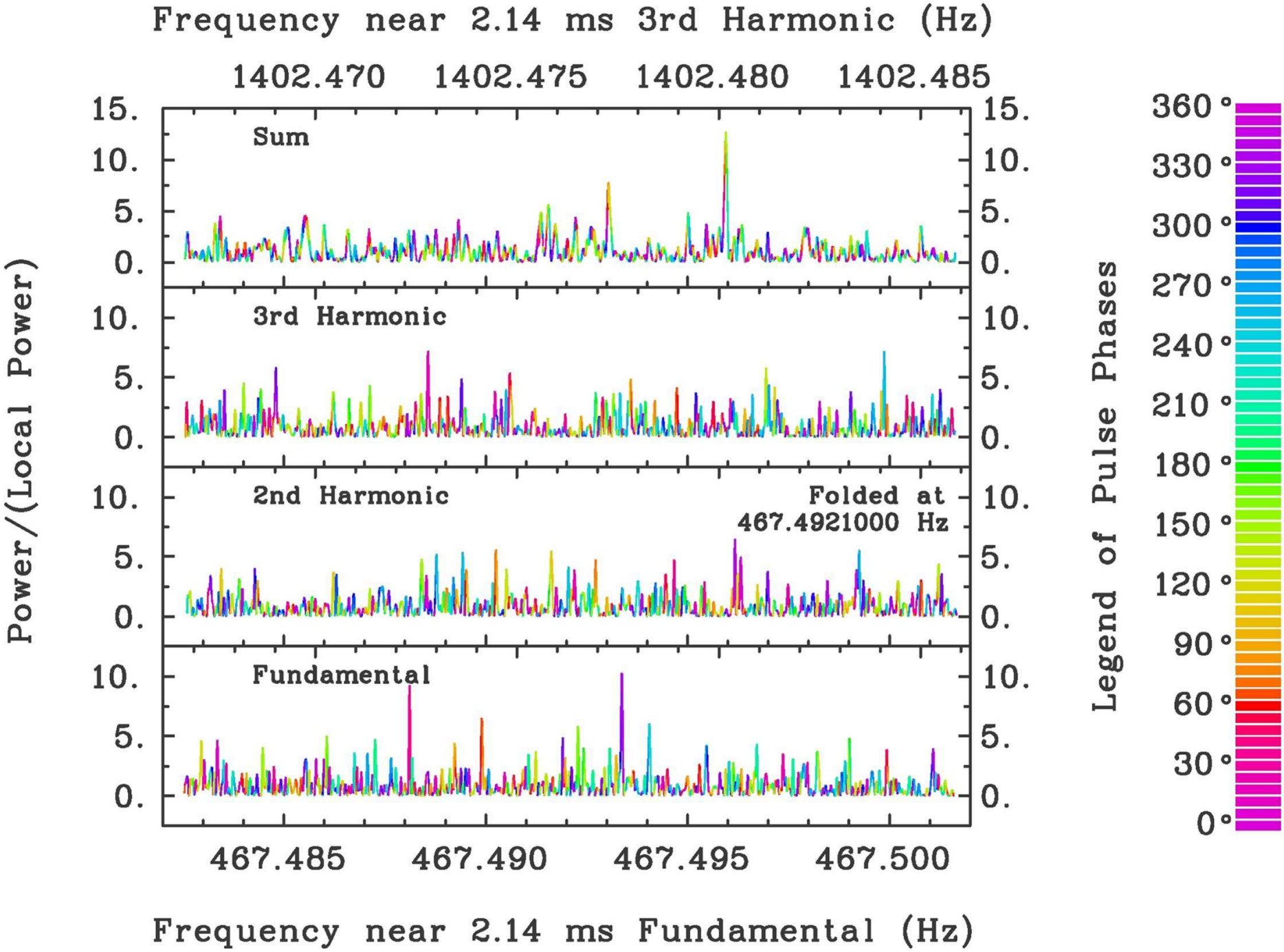
Frequency near 2.14 ms 3rd Harmonic (Hz)
1402.470
1402.475
1402.480
1402.485
Sum
3rd Harmonic
2nd Harmonic
Folded at
467.4921000 Hz
Fundamental
15.
10.
5.
0.
Power/(Local Power)
467.485
467.490
467.495
467.500
Frequency near 2.14 ms Fundamental (Hz)
Legend of Pulse Phases
360 °
330 °
300 °
270 °
240 °
210 °
180 °
150 °
120 °
90 °
60 °
30 °
0 °

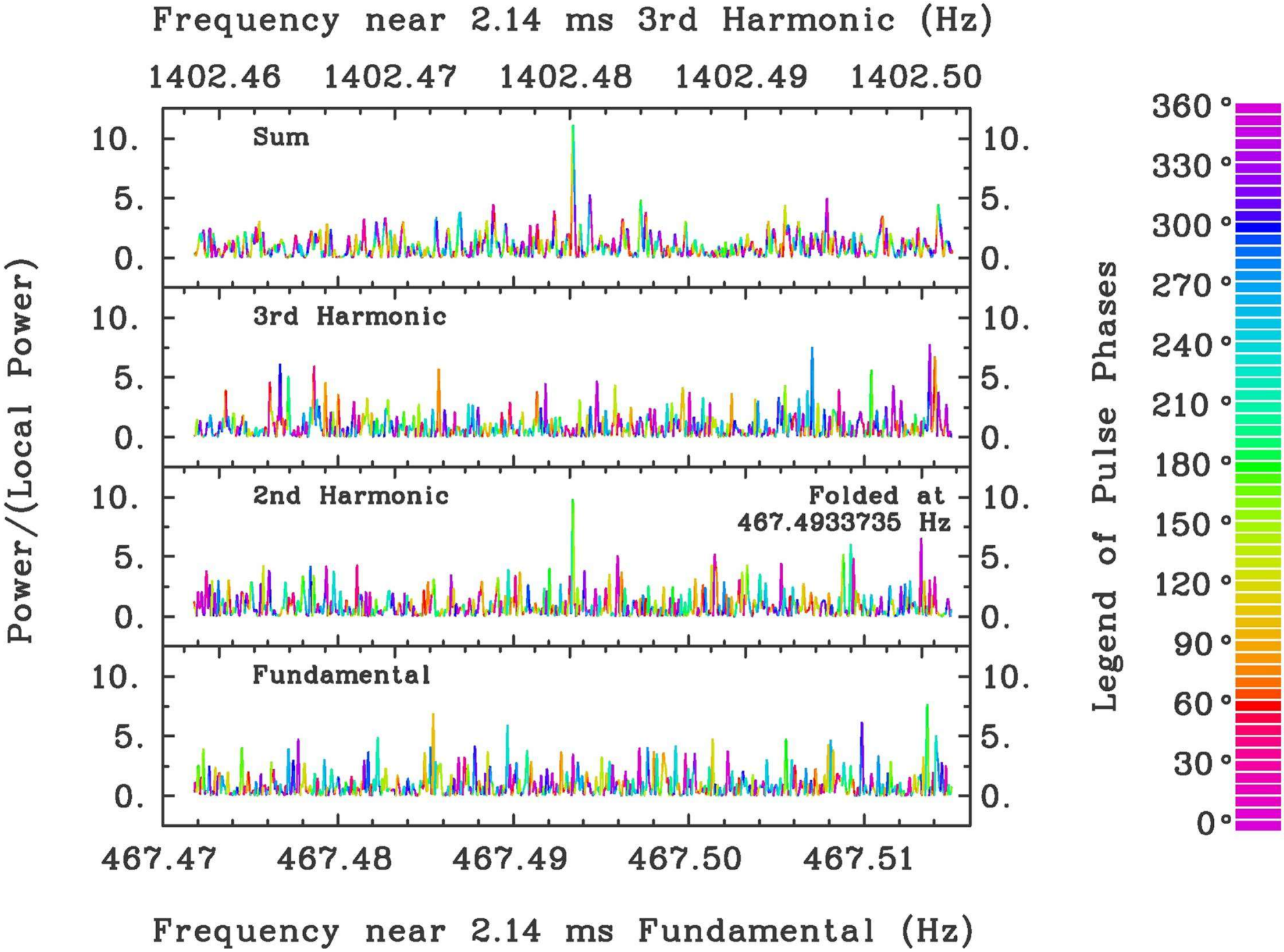
Frequency near 2.14 ms 3rd Harmonic (Hz)
1402.46
1402.47
1402.48
1402.49
1402.50
Sum
3rd Harmonic
2nd Harmonic
Folded at
467.4933735 Hz
Fundamental
10.
5.
0.
Power/(Local Power)
467.47
467.48
467.49
467.50
467.51
Frequency near 2.14 ms Fundamental (Hz)
Legend of Pulse Phases
360 °
330 °
300 °
270 °
240 °
210 °
180 °
150 °
120 °
90 °
60 °
30 °
0 °

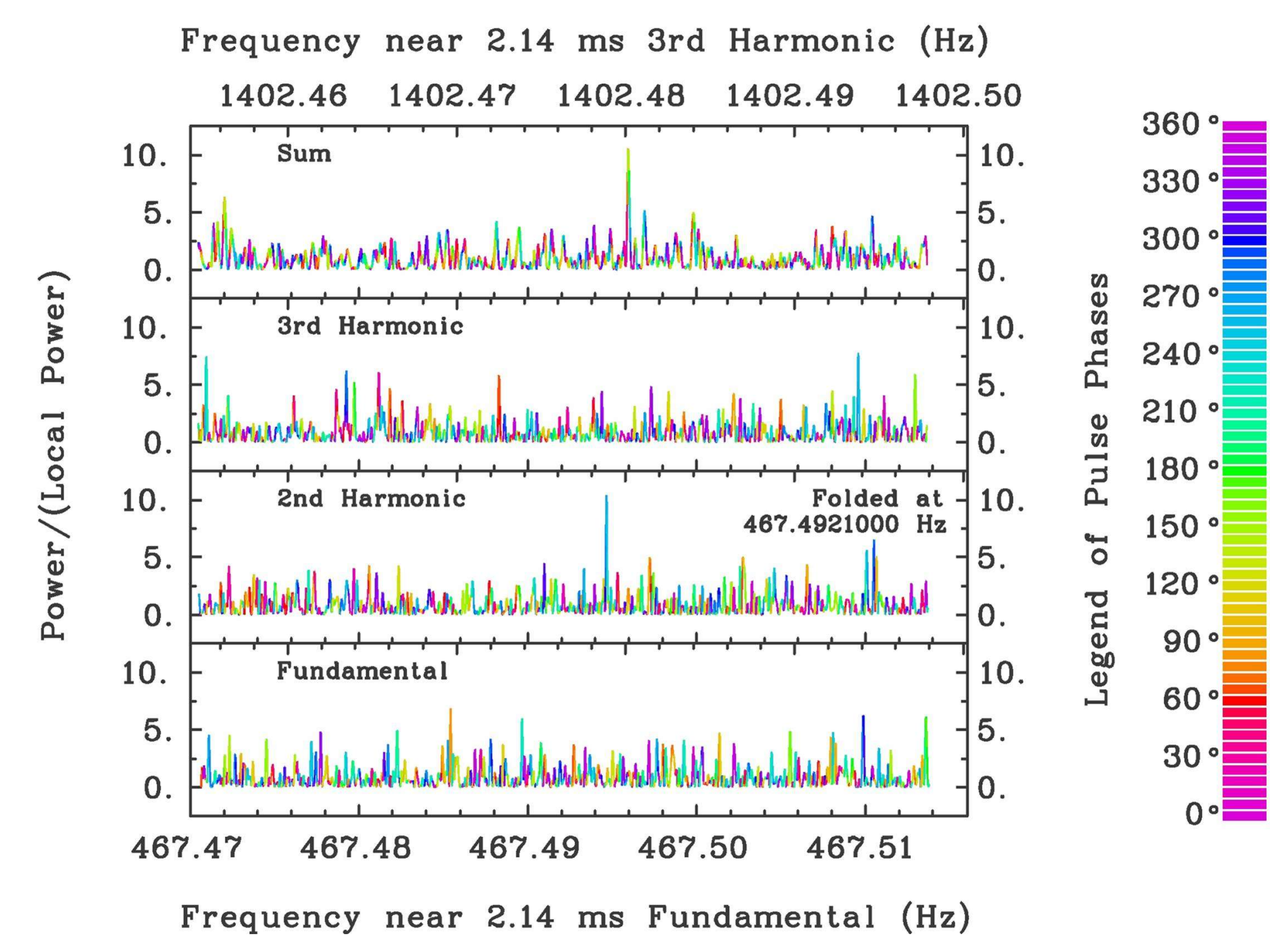
Frequency near 2.14 ms 3rd Harmonic (Hz)
1402.46
1402.47
1402.48
1402.49
1402.50
Sum
3rd Harmonic
2nd Harmonic
Folded at
467.4921000 Hz
Fundamental
10.
5.
0.
Power/(Local Power)
467.47
467.48
467.49
467.50
467.51
Frequency near 2.14 ms Fundamental (Hz)
Legend of Pulse Phases
360 °
330 °
300 °
270 °
240 °
210 °
180 °
150 °
120 °
90 °
60 °
30 °
0 °

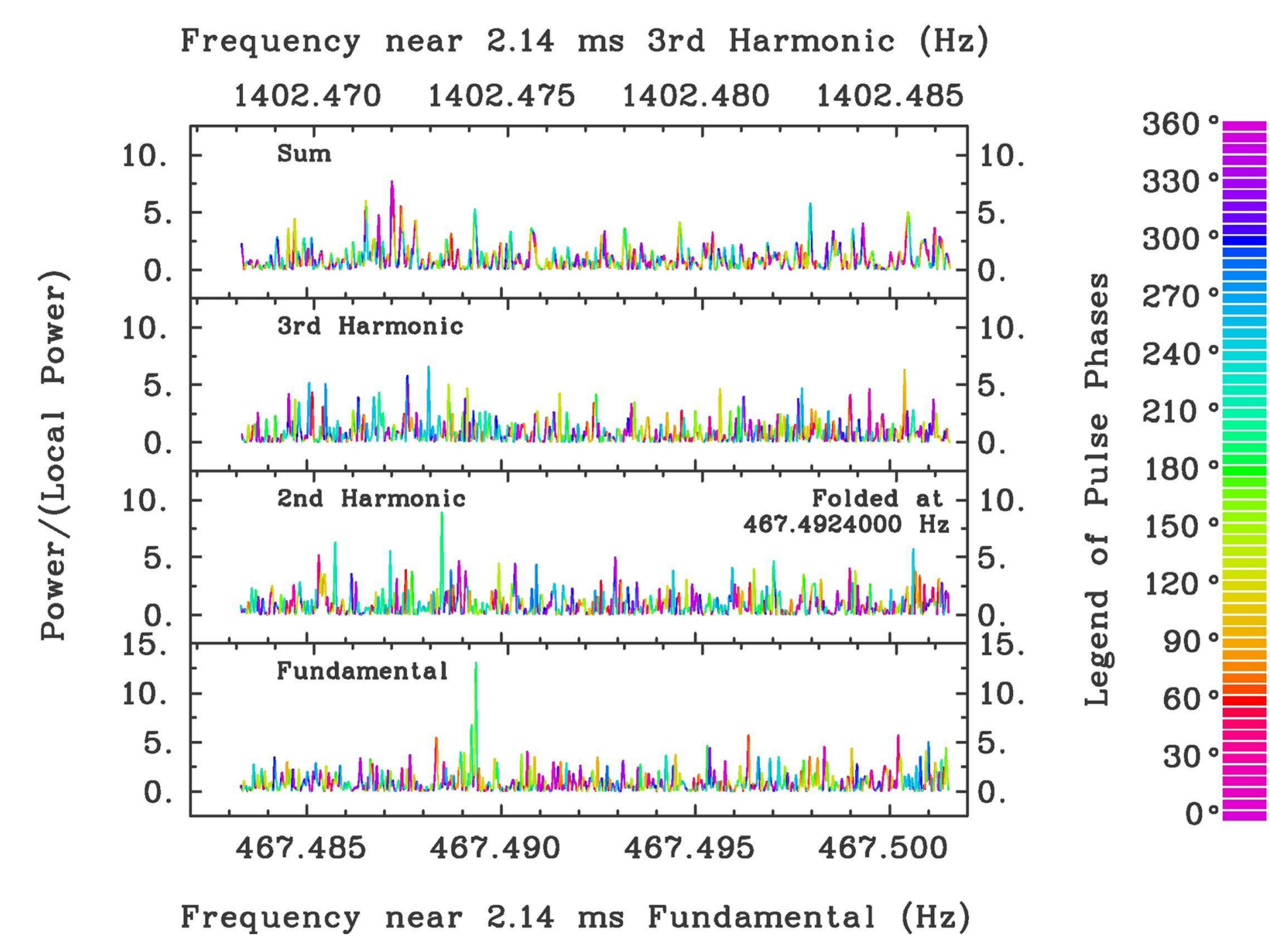
Frequency near 2.14 ms 3rd Harmonic (Hz)
1402.470
1402.475
1402.480
1402.485
Sum
3rd Harmonic
2nd Harmonic
Folded at
467.4924000 Hz
Fundamental
Power/(Local Power)
10.
5.
0.
15.
467.485
467.490
467.495
467.500
Frequency near 2.14 ms Fundamental (Hz)
Legend of Pulse Phases
360 °
330 °
300 °
270 °
240 °
210 °
180 °
150 °
120 °
90 °
60 °
30 °
0 °

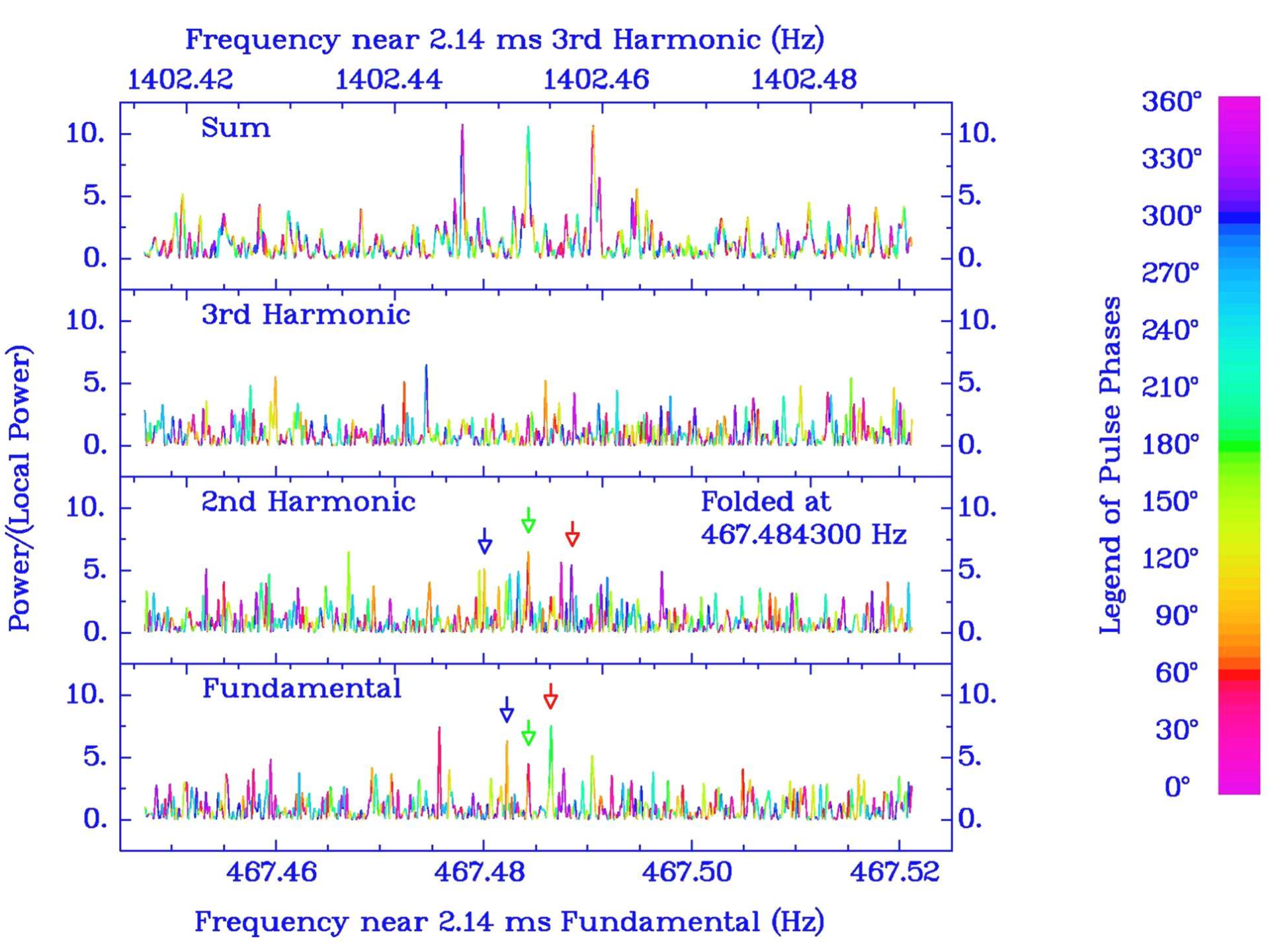
Frequency near 2.14 ms 3rd Harmonic (Hz)
1402.42
1402.44
1402.46
1402.48
Sum
3rd Harmonic
2nd Harmonic
Folded at
467.484300 Hz
Fundamental
10.
5.
0.
Power/(Local Power)
467.46
467.48
467.50
467.52
Frequency near 2.14 ms Fundamental (Hz)
Legend of Pulse Phases
360°
330°
300°
270°
240°
210°
180°
150°
120°
90°
60°
30°
0°

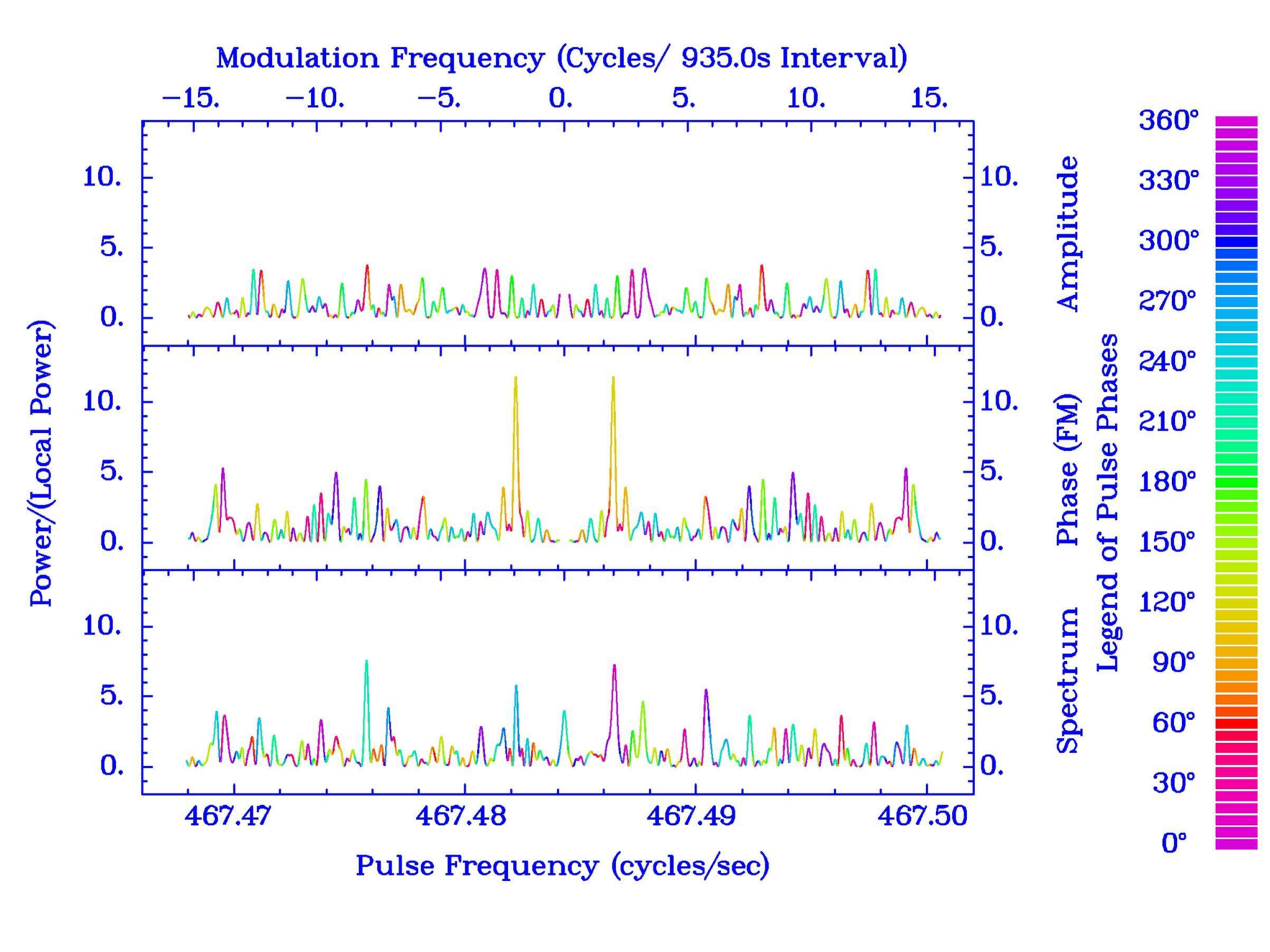
Modulation Frequency (Cycles/ 935.0s Interval)
−15.
−10.
−5.
0.
5.
10.
15.
Power/(Local Power)
10.
5.
0.
Amplitude
Phase (FM)
Spectrum
Legend of Pulse Phases
360°
330°
300°
270°
240°
210°
180°
150°
120°
90°
60°
30°
0°
467.47
467.48
467.49
467.50
Pulse Frequency (cycles/sec)

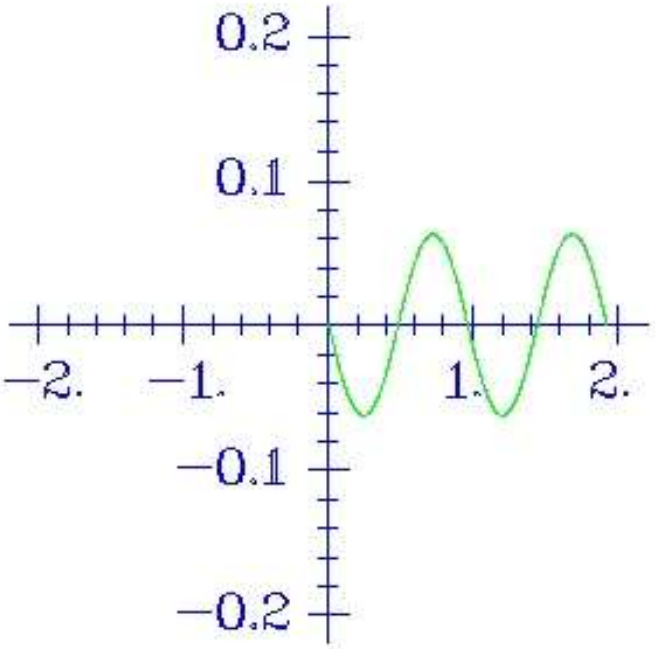
0.2
0.1
−2.
−1.
1.
2.
−0.1
−0.2

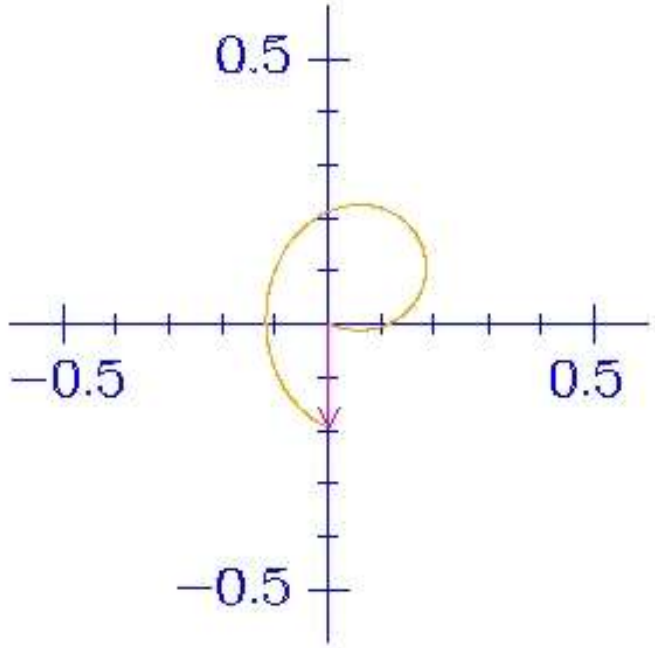
0.5
−0.5
0.5
−0.5

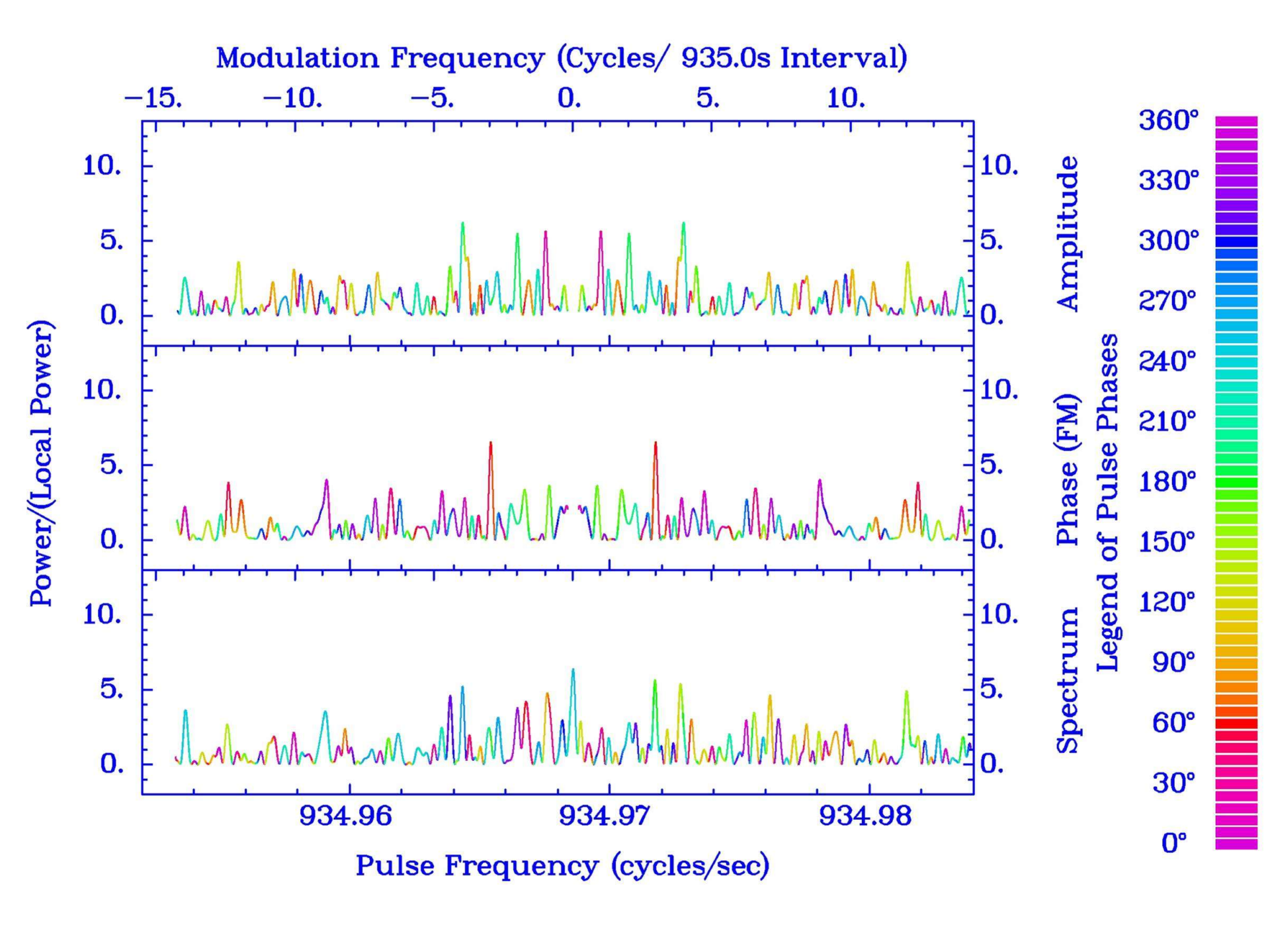
Modulation Frequency (Cycles/ 935.0s Interval)
−15.
−10.
−5.
0.
5.
10.
Power/(Local Power)
10.
5.
0.
Amplitude
Phase (FM)
Spectrum
Legend of Pulse Phases
360°
330°
300°
270°
240°
210°
180°
150°
120°
90°
60°
30°
0°
934.96
934.97
934.98
Pulse Frequency (cycles/sec)

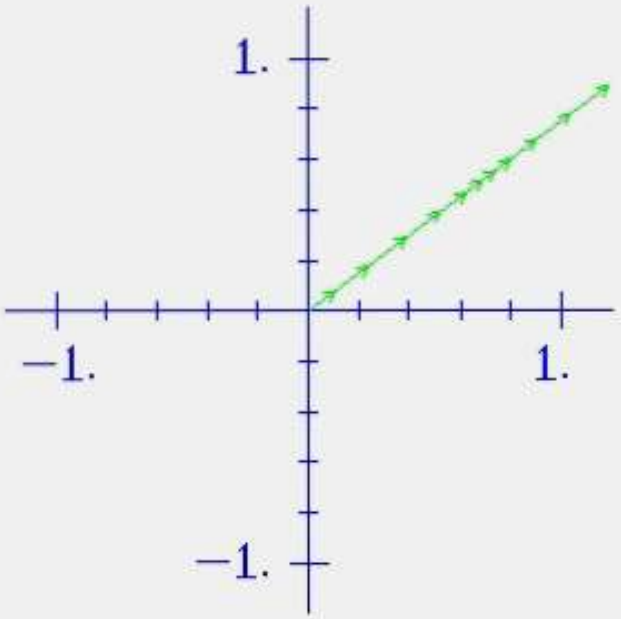
1.
−1.
1.
−1.

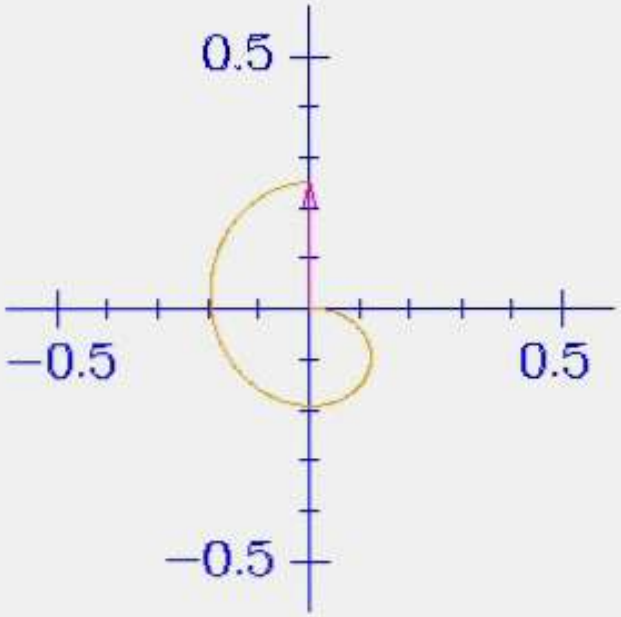
0.5
−0.5
0.5
−0.5

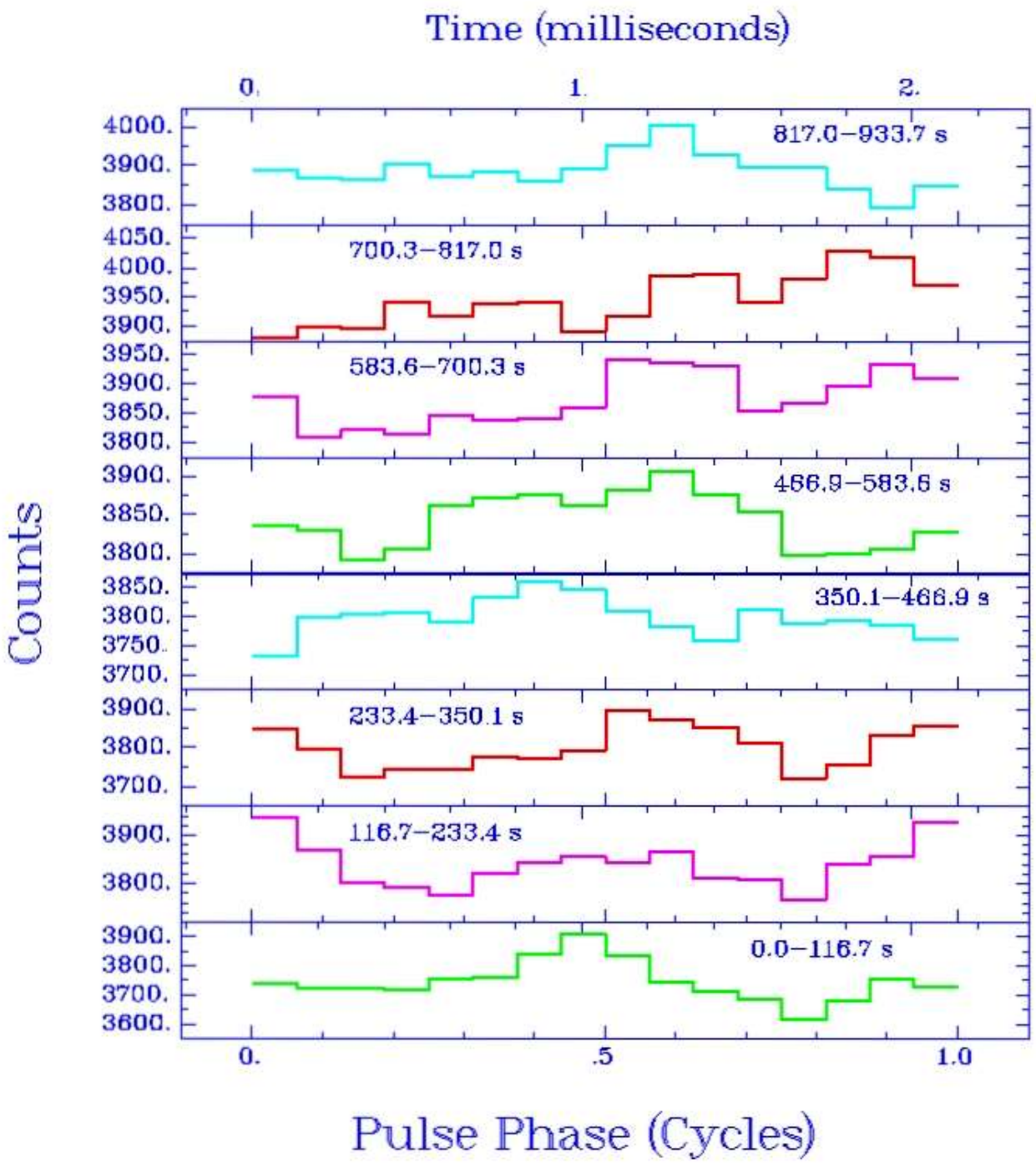
Time (milliseconds)
0.
1.
2.
817.0–933.7 s
700.3–817.0 s
583.6–700.3 s
466.9–583.6 s
350.1–466.9 s
233.4–350.1 s
116.7–233.4 s
0.0–116.7 s
Counts
0.
.5
1.0
Pulse Phase (Cycles)

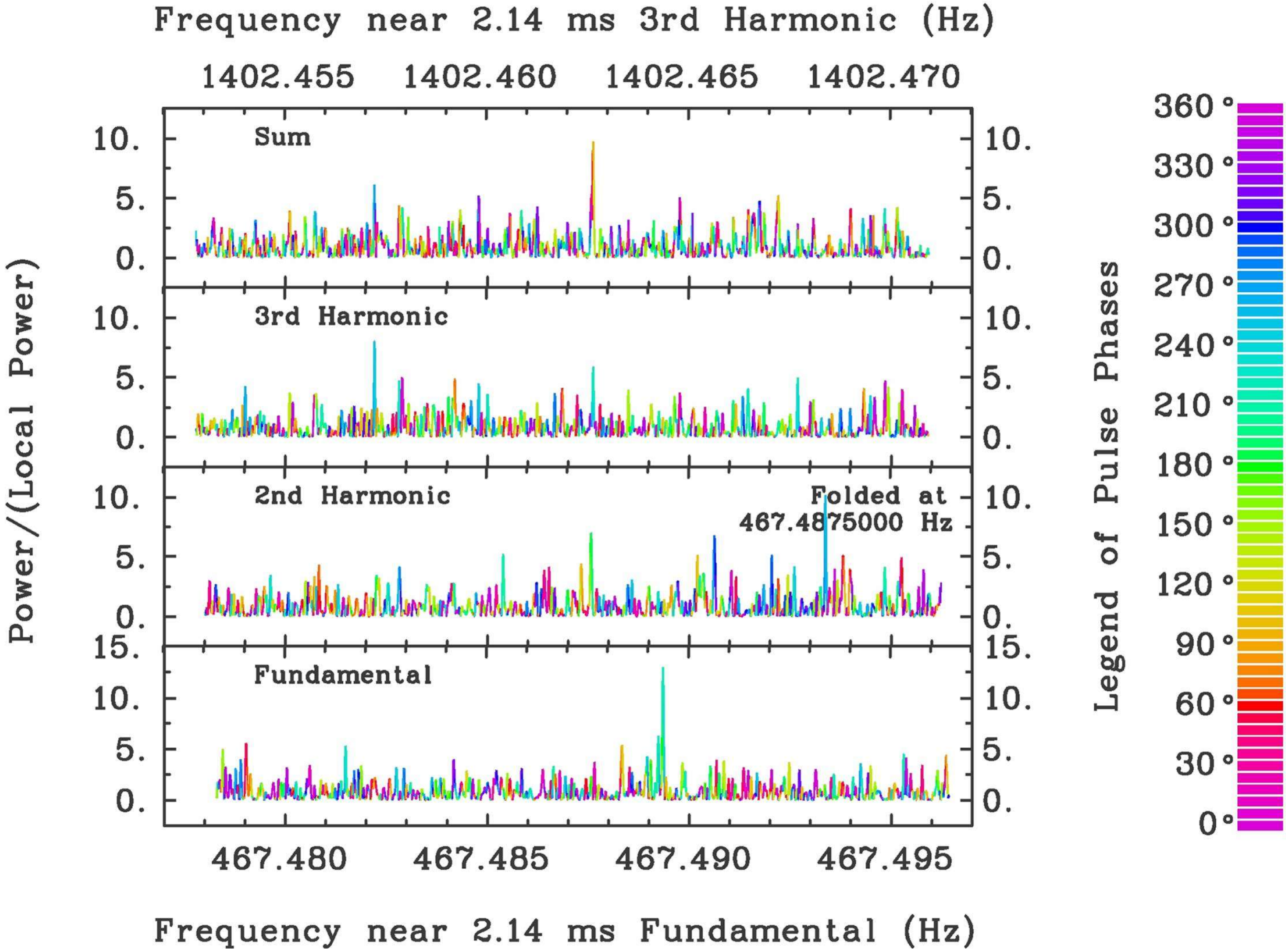
Frequency near 2.14 ms 3rd Harmonic (Hz)
1402.455
1402.460
1402.465
1402.470
Sum
3rd Harmonic
2nd Harmonic
Folded at
467.4875000 Hz
Fundamental
Power/(Local Power)
10.
5.
0.
15.
467.480
467.485
467.490
467.495
Frequency near 2.14 ms Fundamental (Hz)
Legend of Pulse Phases
360 °
330 °
300 °
270 °
240 °
210 °
180 °
150 °
120 °
90 °
60 °
30 °
0 °

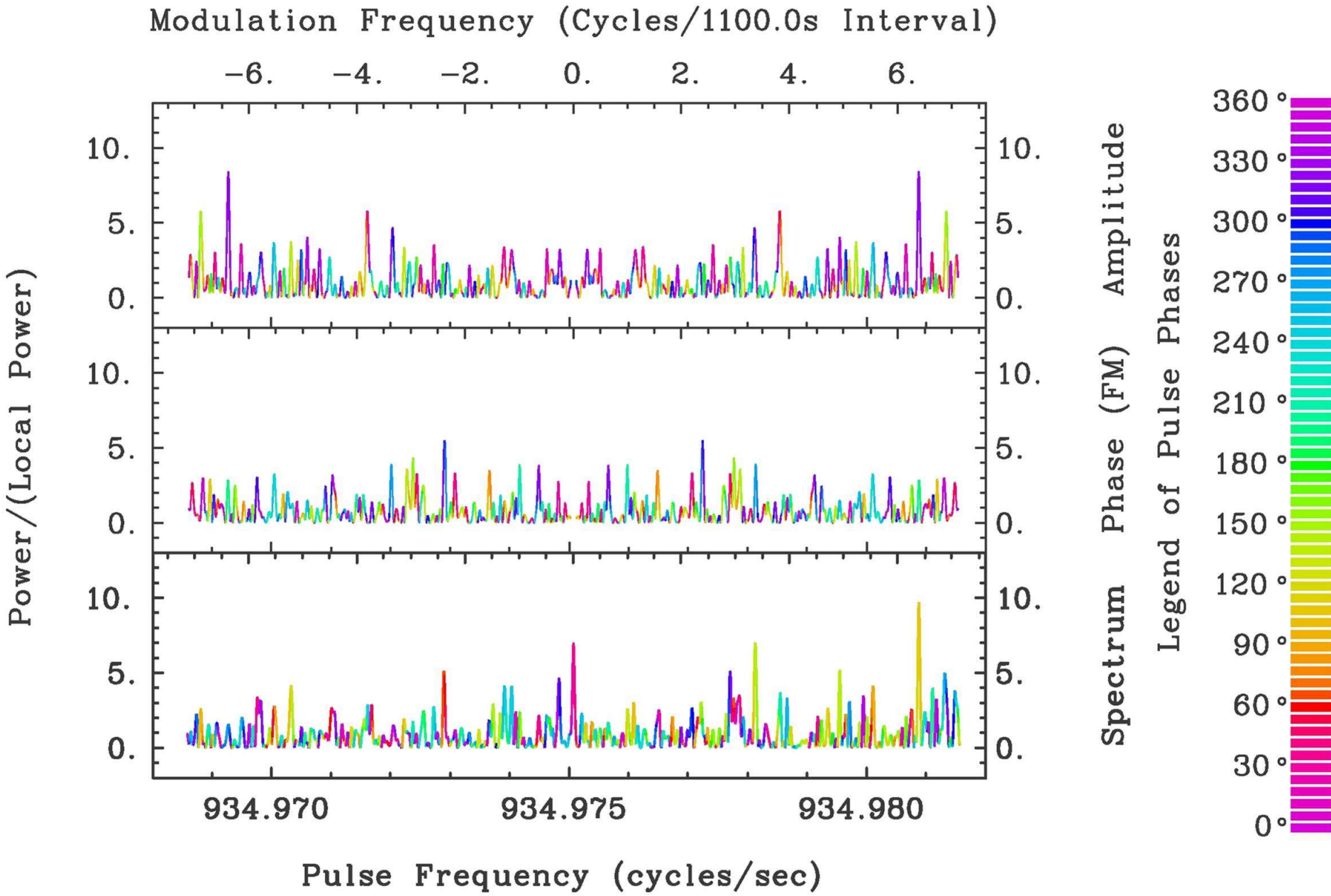
Modulation Frequency (Cycles/1100.0s Interval)
−6.
−4.
−2.
0.
2.
4.
6.
10.
5.
0.
Power/(Local Power)
934.970
934.975
934.980
Pulse Frequency (cycles/sec)
Spectrum Phase (FM) Amplitude
Legend of Pulse Phases
360°
330°
300°
270°
240°
210°
180°
150°
120°
90°
60°
30°
0°

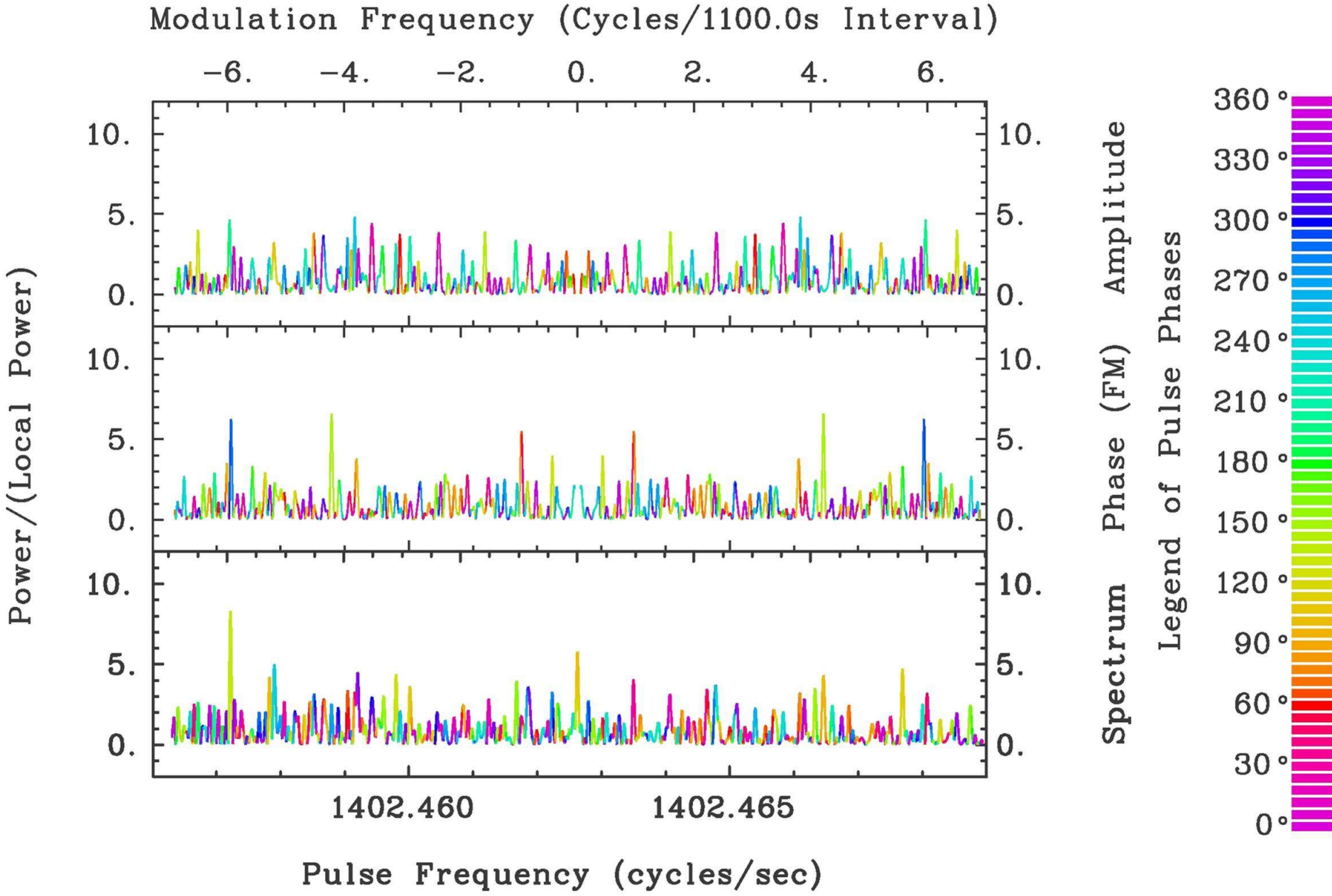
Modulation Frequency (Cycles/1100.0s Interval)
−6.
−4.
−2.
0.
2.
4.
6.
10.
5.
0.
Power/(Local Power)
1402.460
1402.465
Pulse Frequency (cycles/sec)
Spectrum Phase (FM) Amplitude
Legend of Pulse Phases
360°
330°
300°
270°
240°
210°
180°
150°
120°
90°
60°
30°
0°

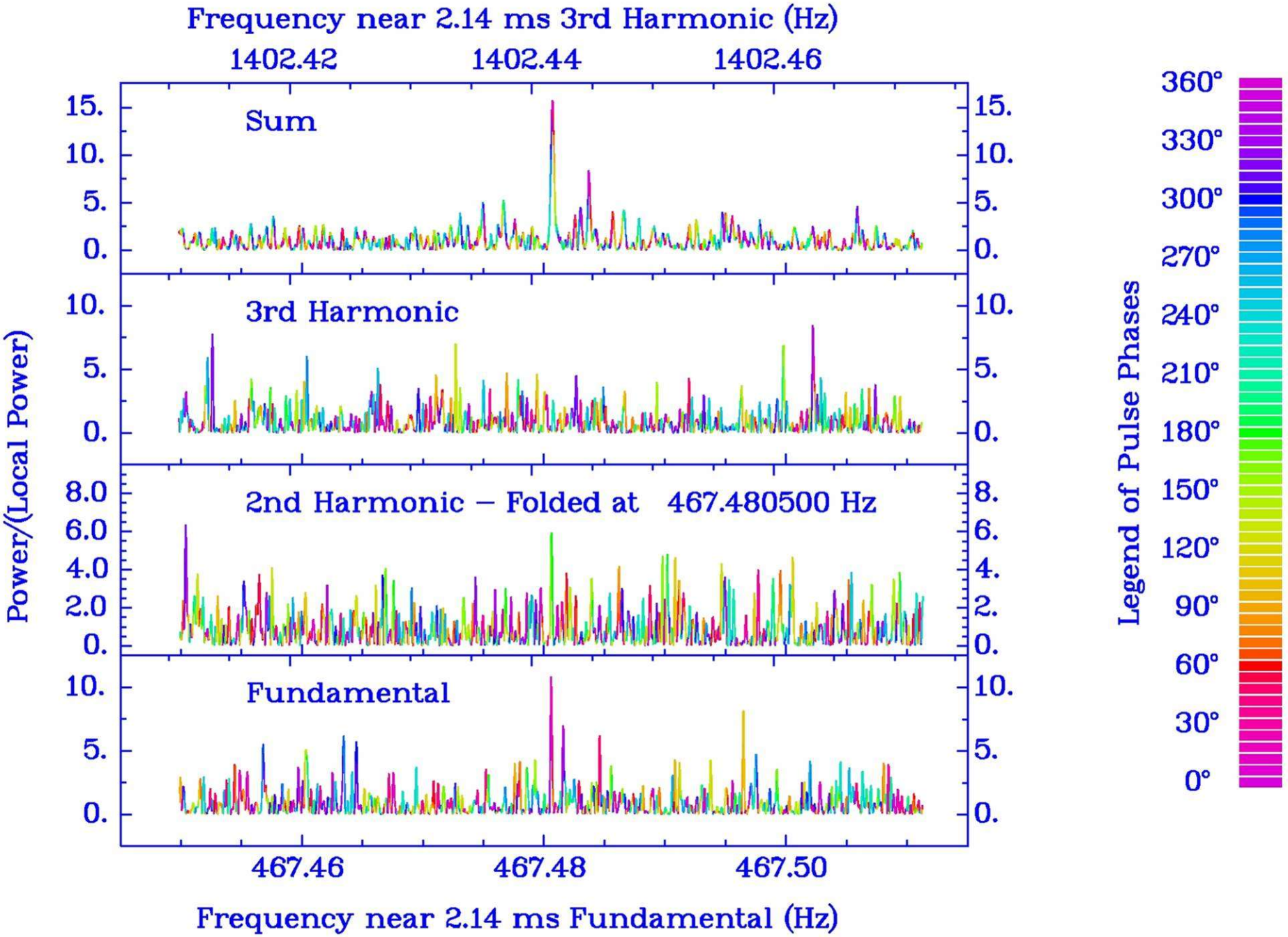
Frequency near 2.14 ms 3rd Harmonic (Hz)
1402.42
1402.44
1402.46
Sum
3rd Harmonic
2nd Harmonic – Folded at 467.480500 Hz
Fundamental
Power/(Local Power)
467.46
467.48
467.50
Frequency near 2.14 ms Fundamental (Hz)
Legend of Pulse Phases
360°
330°
300°
270°
240°
210°
180°
150°
120°
90°
60°
30°
0°

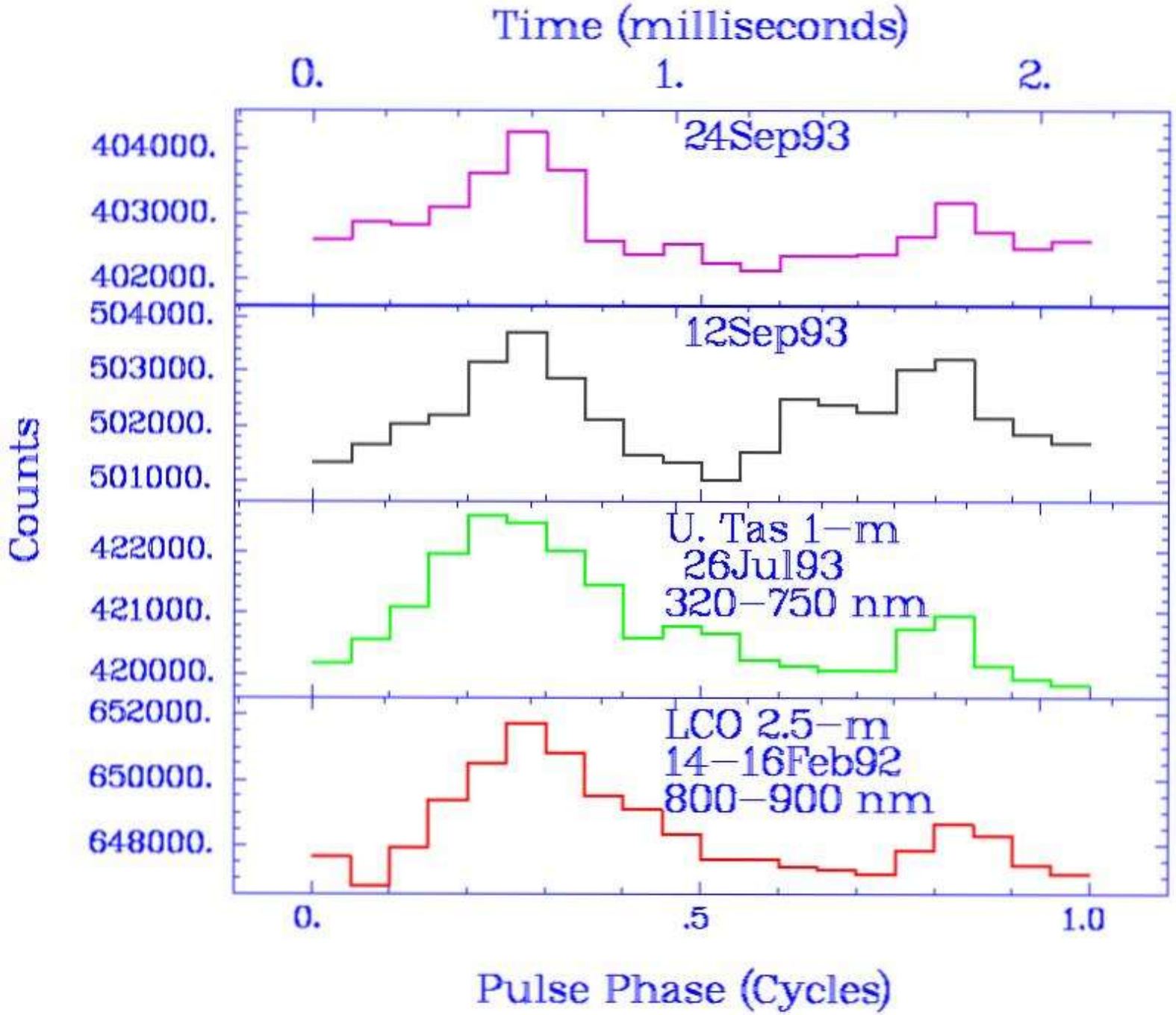
Time (milliseconds)
0.
1.
2.
Counts
404000.
403000.
402000.
24Sep93
504000.
503000.
502000.
501000.
12Sep93
422000.
421000.
420000.
U. Tas 1-m
26Jul93
320-750 nm
652000.
650000.
648000.
LCO 2.5-m
14-16Feb92
800-900 nm
0.
.5
1.0
Pulse Phase (Cycles)

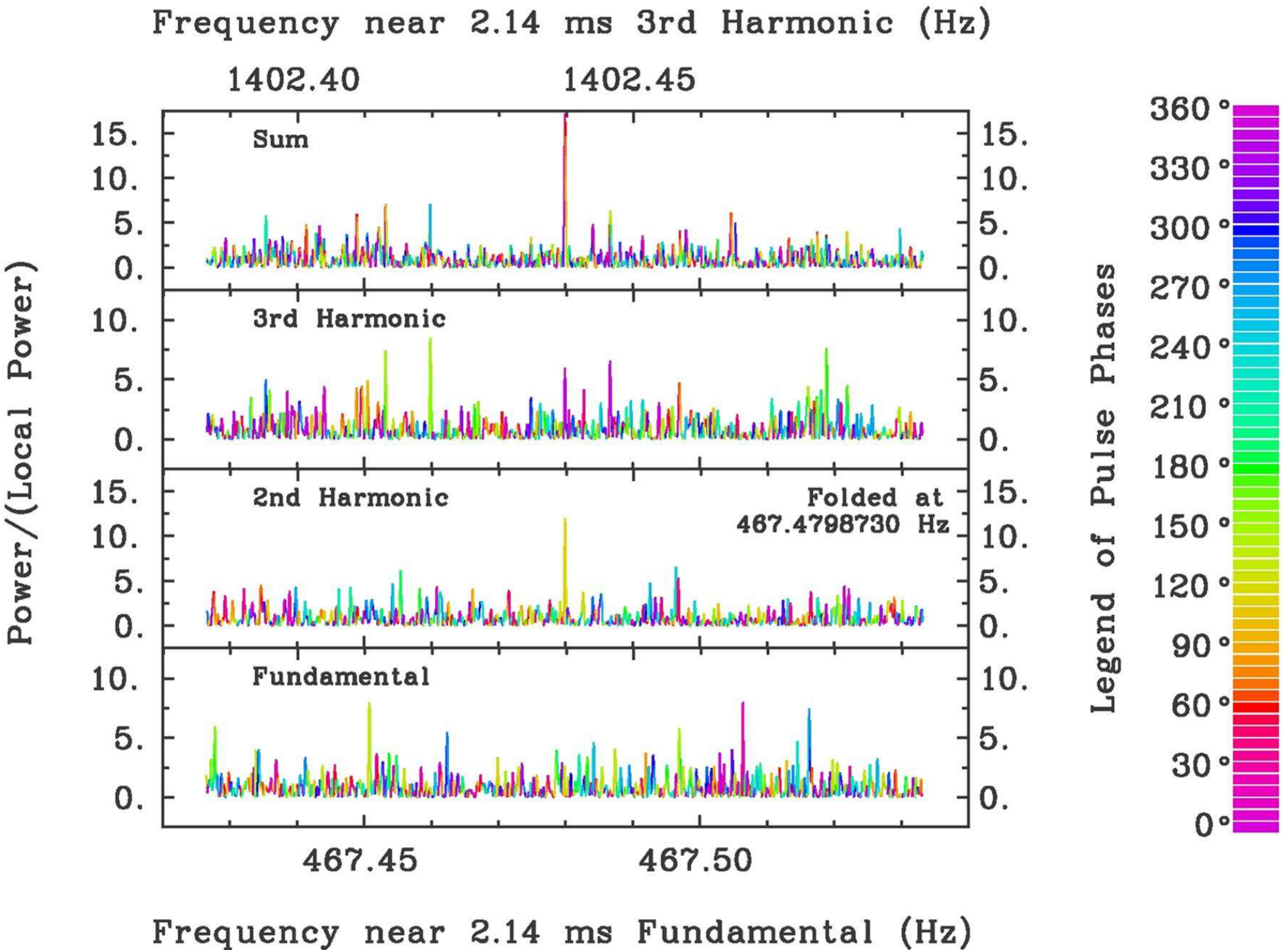
Frequency near 2.14 ms 3rd Harmonic (Hz)
1402.40
1402.45
Sum
3rd Harmonic
2nd Harmonic
Folded at
467.4798730 Hz
Fundamental
15.
10.
5.
0.
Power/(Local Power)
467.45
467.50
Frequency near 2.14 ms Fundamental (Hz)
Legend of Pulse Phases
360 °
330 °
300 °
270 °
240 °
210 °
180 °
150 °
120 °
90 °
60 °
30 °
0 °

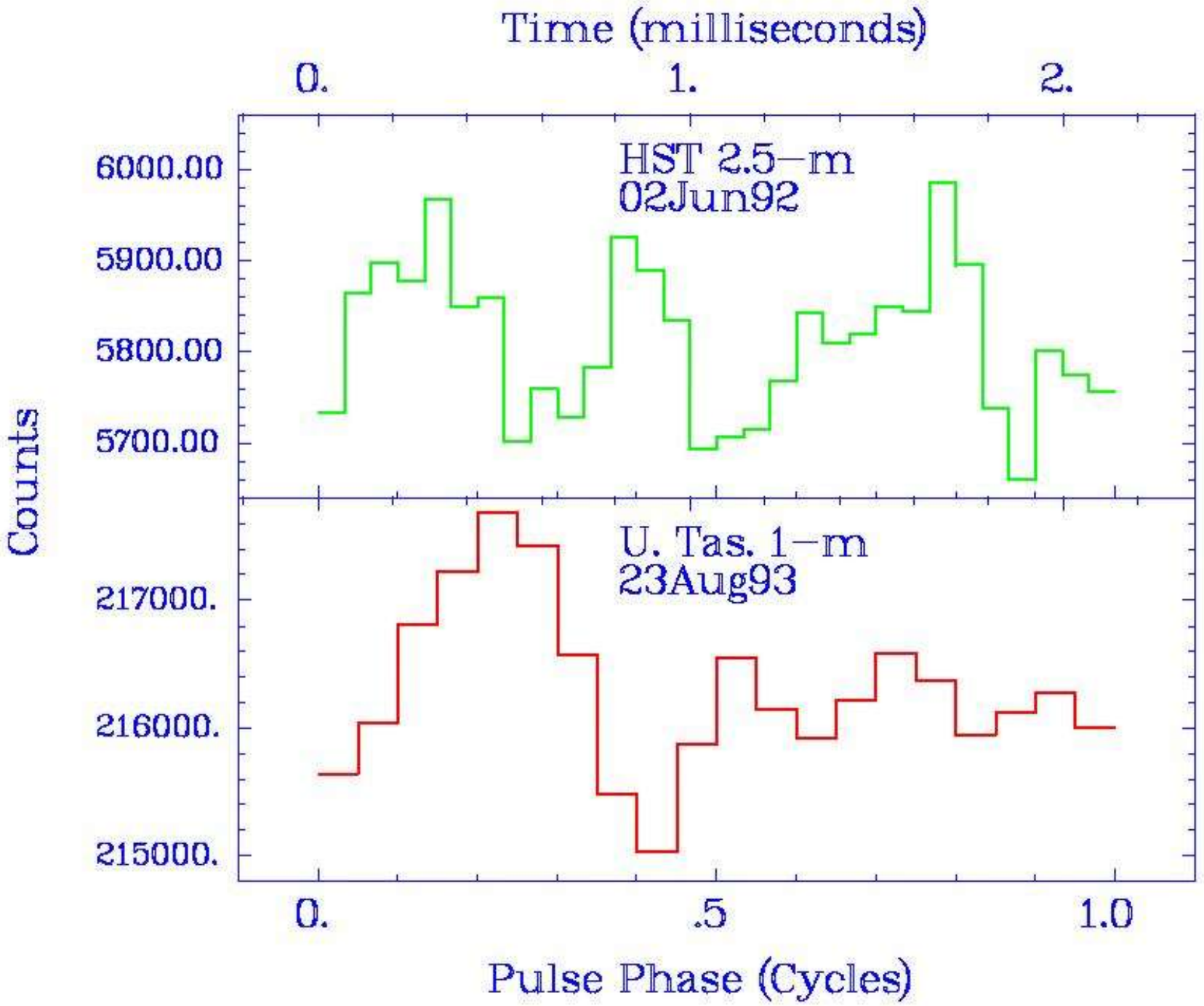
Time (milliseconds)
0.
1.
2.
HST 2.5−m
02Jun92
6000.00
5900.00
5800.00
5700.00
Counts
U. Tas. 1−m
23Aug93
217000.
216000.
215000.
0.
.5
1.0
Pulse Phase (Cycles)

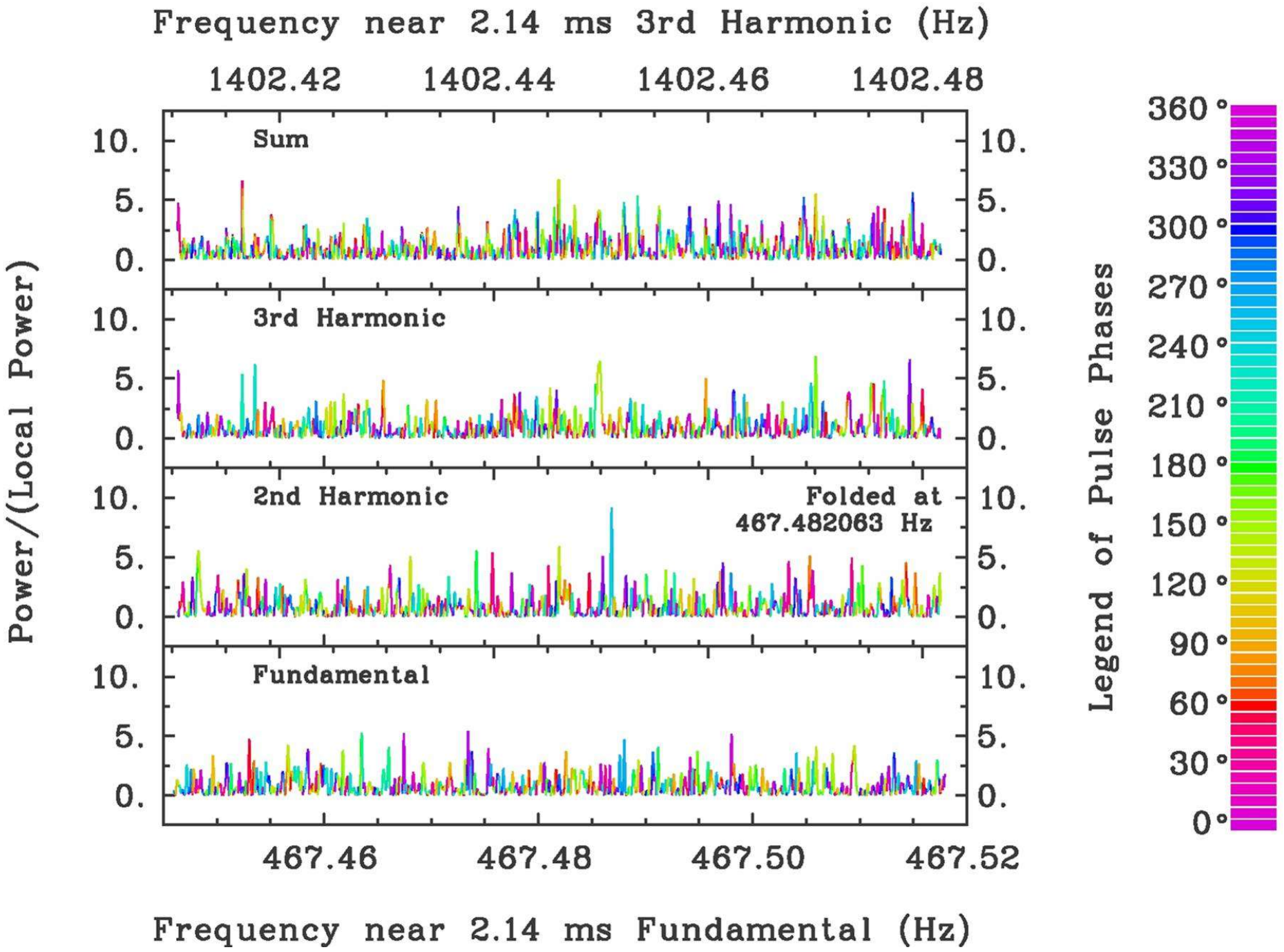
Frequency near 2.14 ms 3rd Harmonic (Hz)
1402.42
1402.44
1402.46
1402.48
Sum
3rd Harmonic
2nd Harmonic
Folded at
467.482063 Hz
Fundamental
10.
5.
0.
Power/(Local Power)
467.46
467.48
467.50
467.52
Frequency near 2.14 ms Fundamental (Hz)
Legend of Pulse Phases
360 °
330 °
300 °
270 °
240 °
210 °
180 °
150 °
120 °
90 °
60 °
30 °
0 °

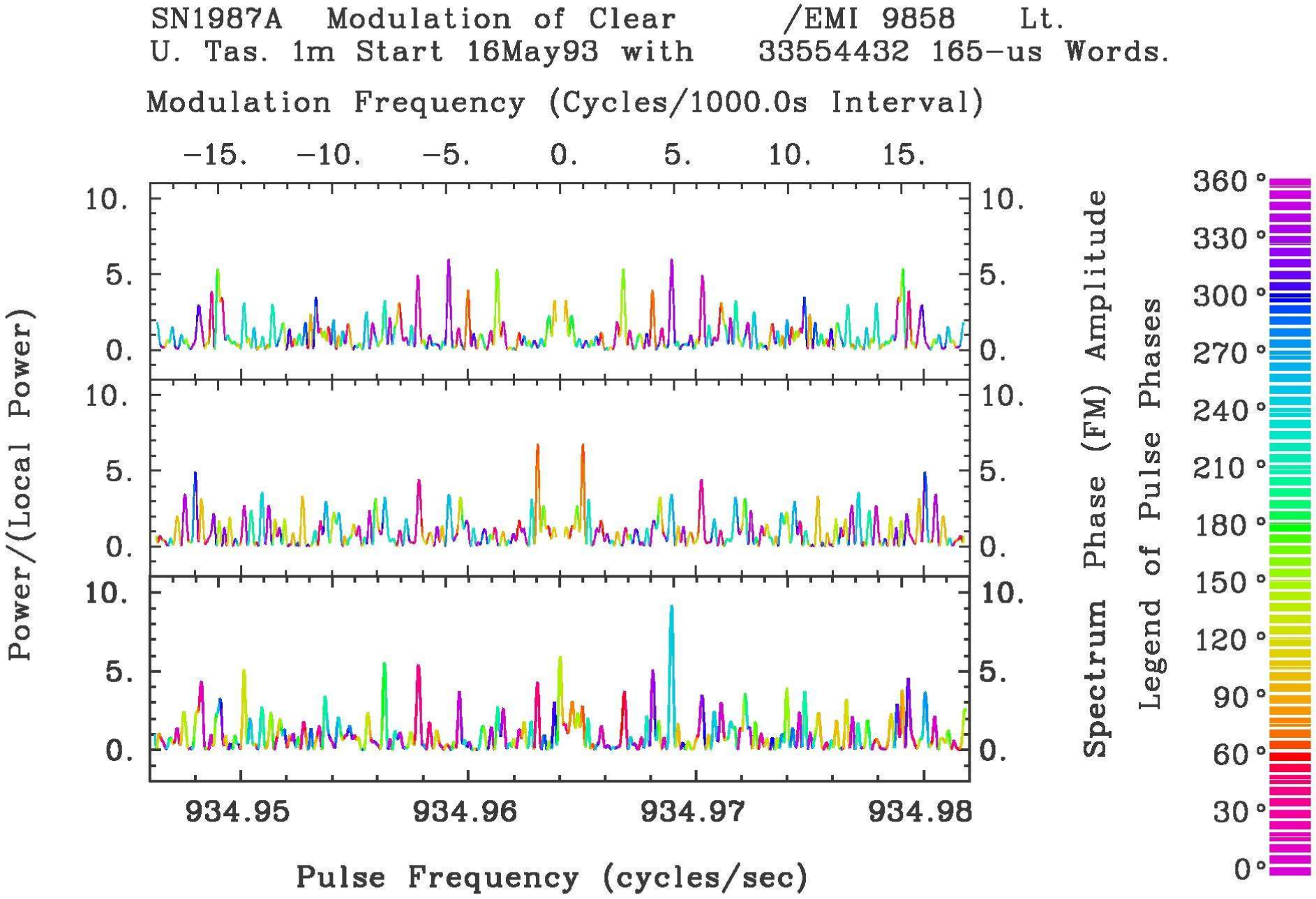
SN1987A Modulation of Clear /EMI 9858 Lt.
U. Tas. 1m Start 16May93 with 33554432 165-us Words.
Modulation Frequency (Cycles/1000.0s Interval)
-15.
-10.
-5.
0.
5.
10.
15.
Power/(Local Power)
10.
5.
0.
934.95
934.96
934.97
934.98
Pulse Frequency (cycles/sec)
Spectrum Phase (FM) Amplitude
Legend of Pulse Phases
360°
330°
300°
270°
240°
210°
180°
150°
120°
90°
60°
30°
0°

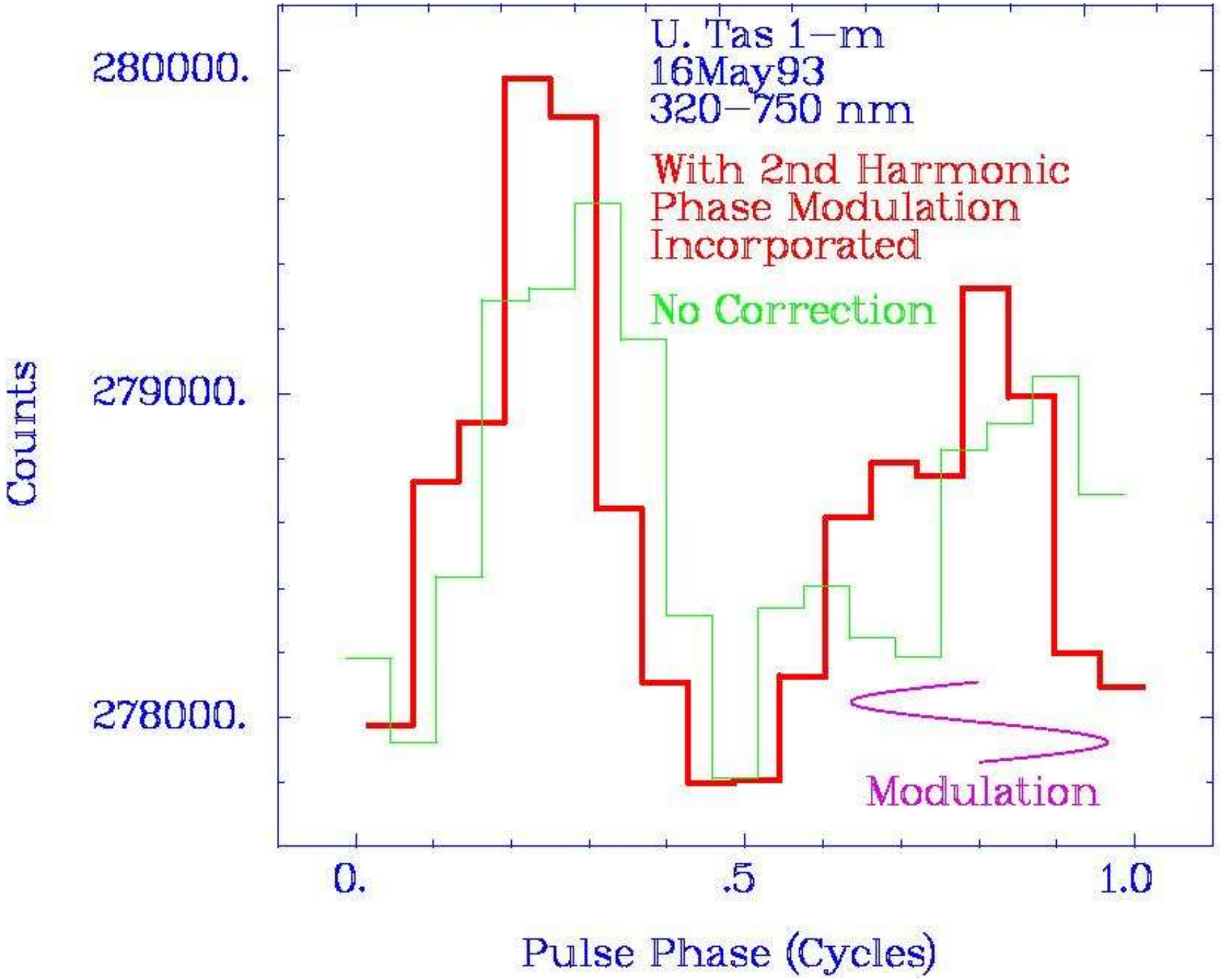
U. Tas 1-m
16May93
320-750 nm
With 2nd Harmonic
Phase Modulation
Incorporated
No Correction
Modulation
280000.
279000.
278000.
Counts
0.
.5
1.0
Pulse Phase (Cycles)

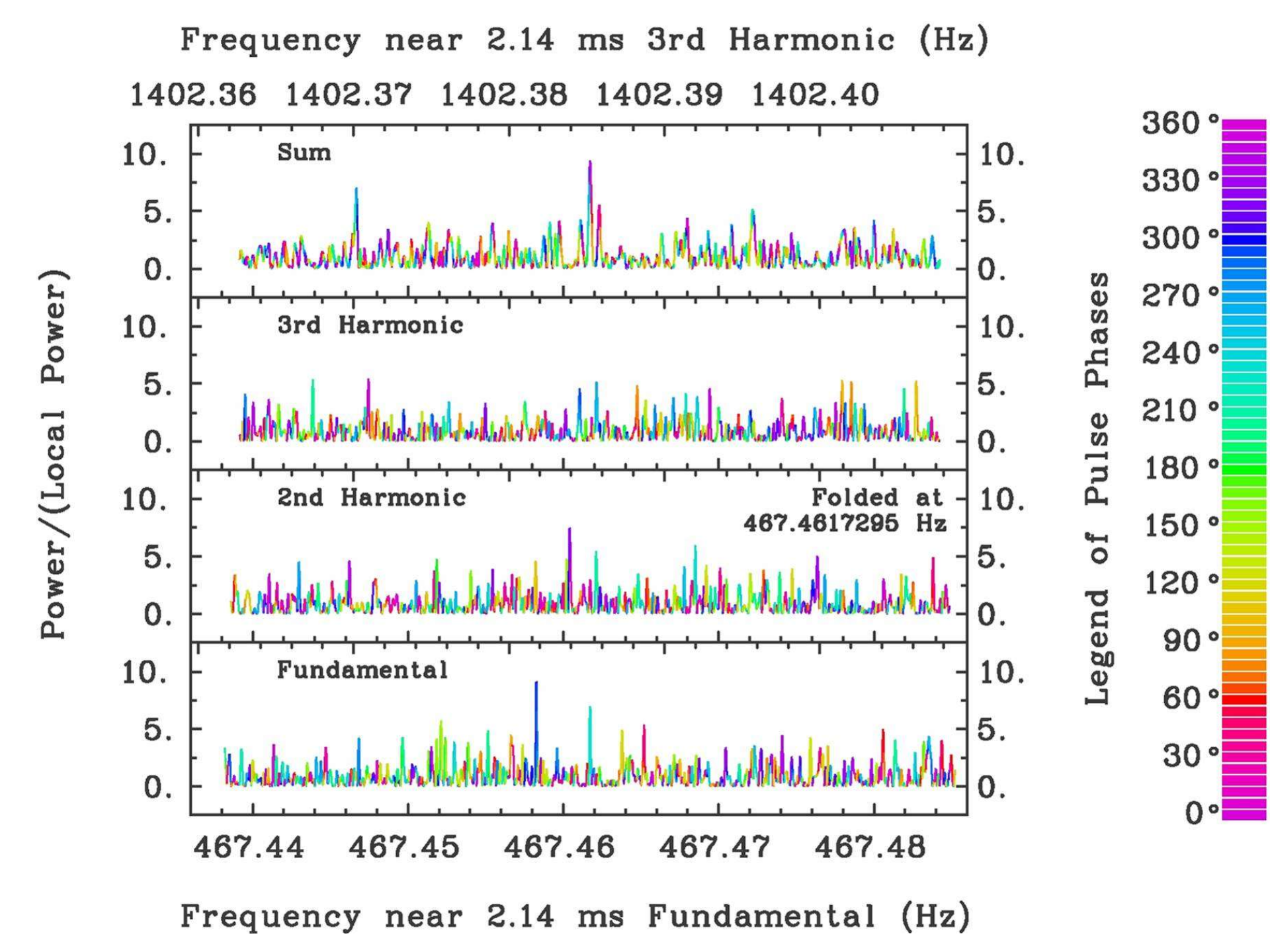
Frequency near 2.14 ms 3rd Harmonic (Hz)
1402.36
1402.37
1402.38
1402.39
1402.40
Power/(Local Power)
Sum
3rd Harmonic
2nd Harmonic
Folded at
467.4617295 Hz
Fundamental
10.
5.
0.
467.44
467.45
467.46
467.47
467.48
Frequency near 2.14 ms Fundamental (Hz)
Legend of Pulse Phases
360 °
330 °
300 °
270 °
240 °
210 °
180 °
150 °
120 °
90 °
60 °
30 °
0 °

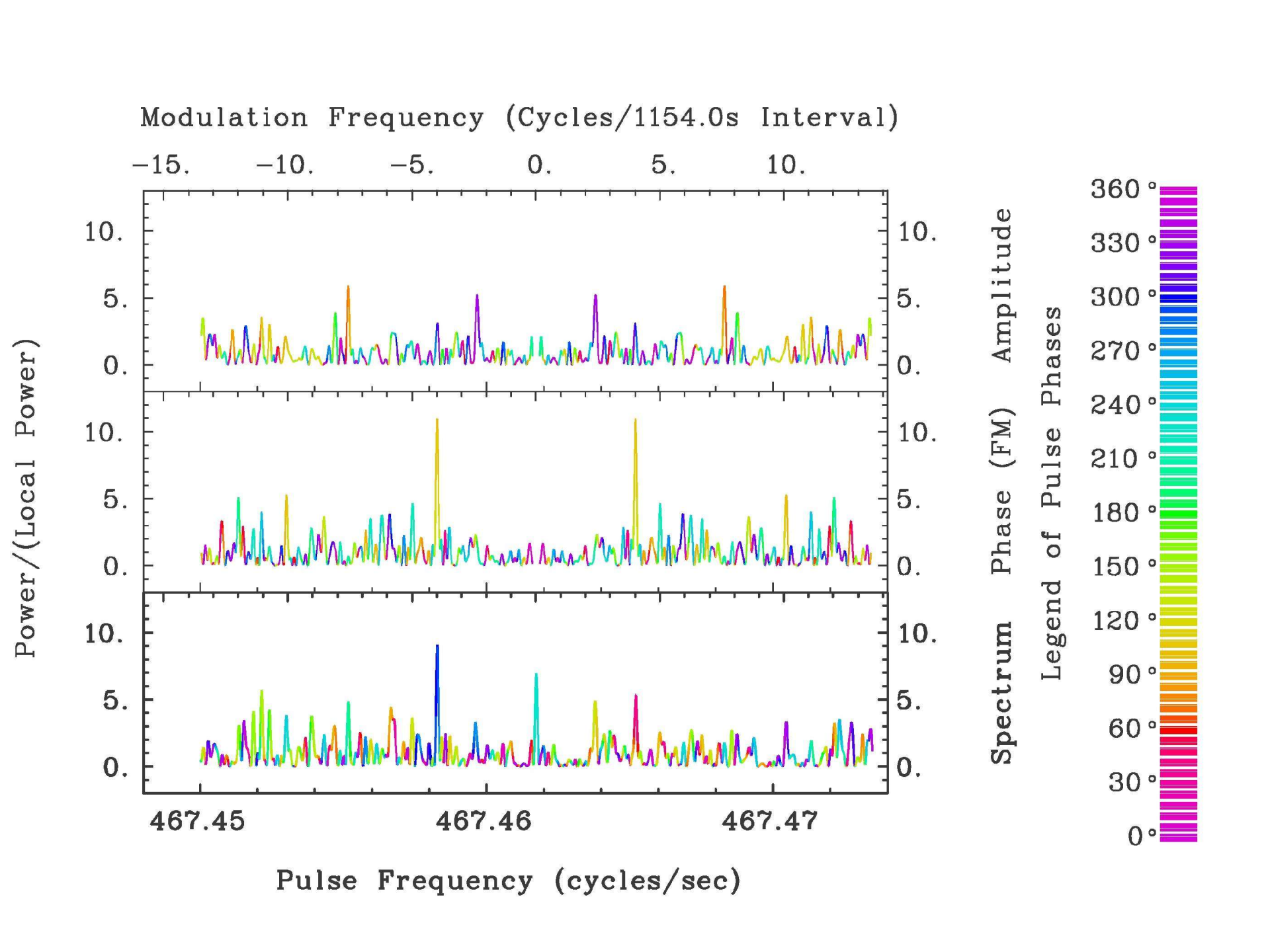
Modulation Frequency (Cycles/1154.0s Interval)
−15.
−10.
−5.
0.
5.
10.
Power/(Local Power)
10.
5.
0.
467.45
467.46
467.47
Pulse Frequency (cycles/sec)
Spectrum Phase (FM) Amplitude
Legend of Pulse Phases
360°
330°
300°
270°
240°
210°
180°
150°
120°
90°
60°
30°
0°

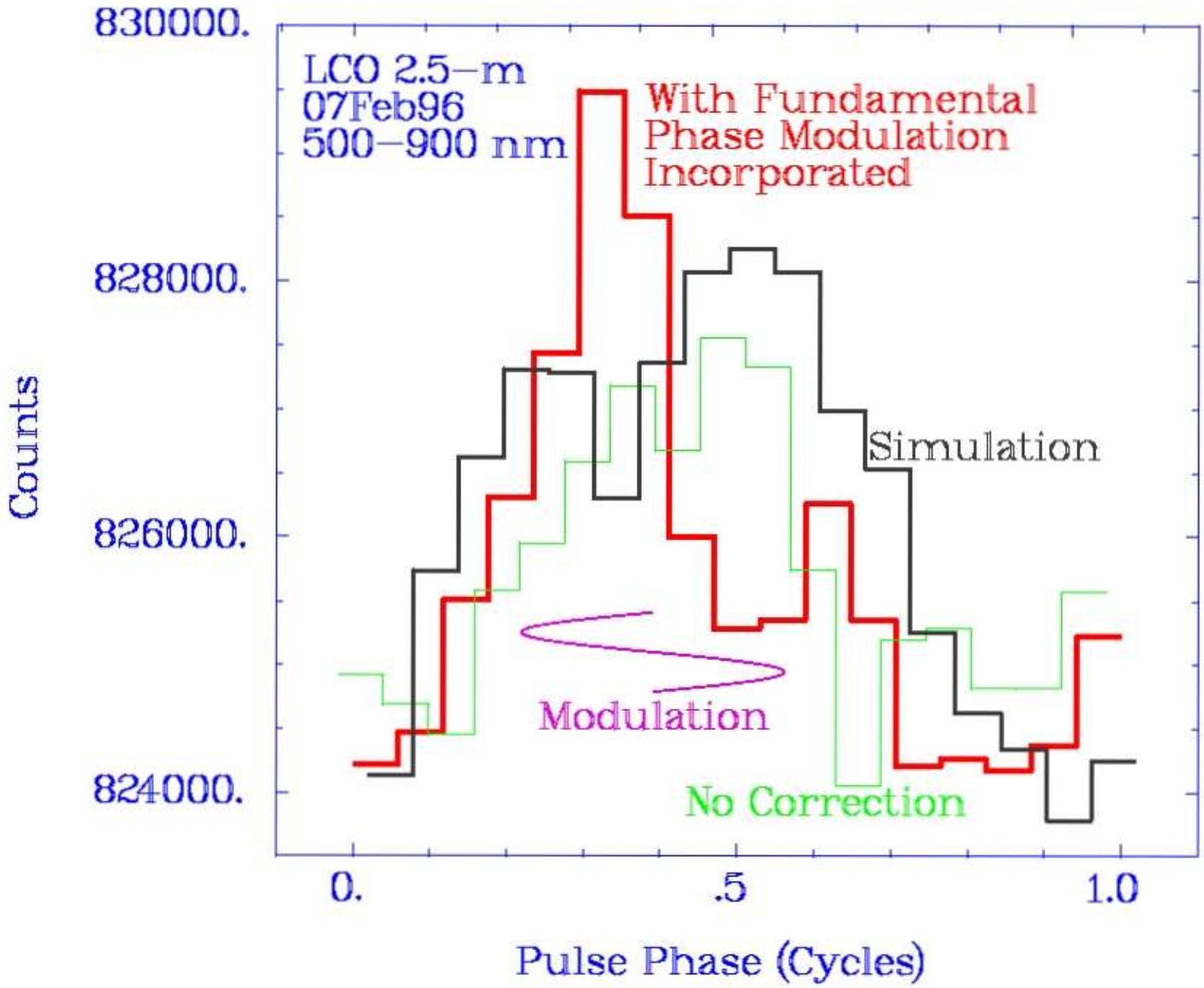
830000.
828000.
826000.
824000.
Counts
LCO 2.5-m
07Feb96
500-900 nm
With Fundamental
Phase Modulation
Incorporated
Simulation
Modulation
No Correction
0.
.5
1.0
Pulse Phase (Cycles)

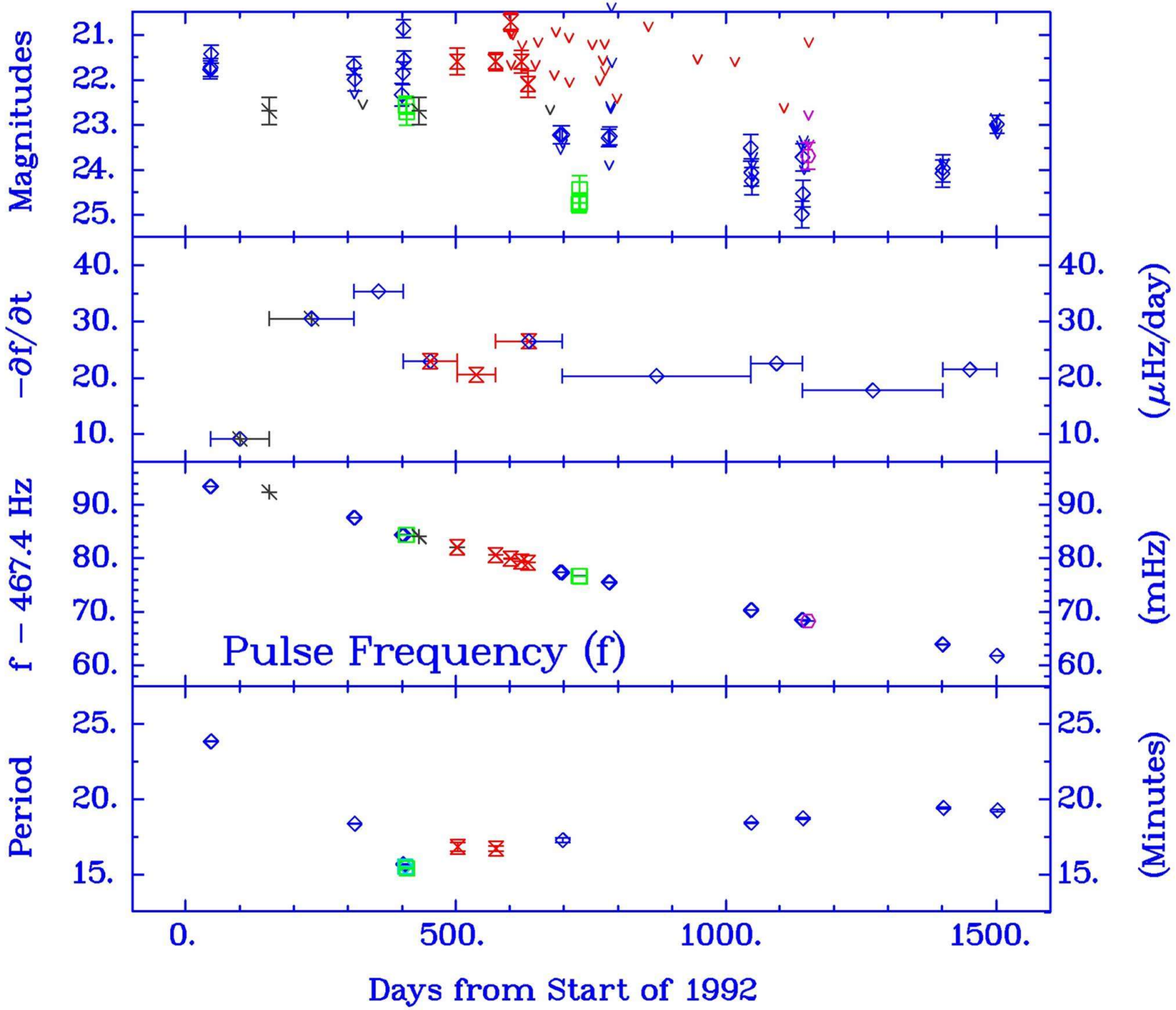
Magnitudes
21.
22.
23.
24.
25.
−∂f/∂t
40.
30.
20.
10.
(μHz/day)
f − 467.4 Hz
90.
80.
70.
60.
(mHz)
Pulse Frequency (f)
Period
25.
20.
15.
(Minutes)
0.
500.
1000.
1500.
Days from Start of 1992

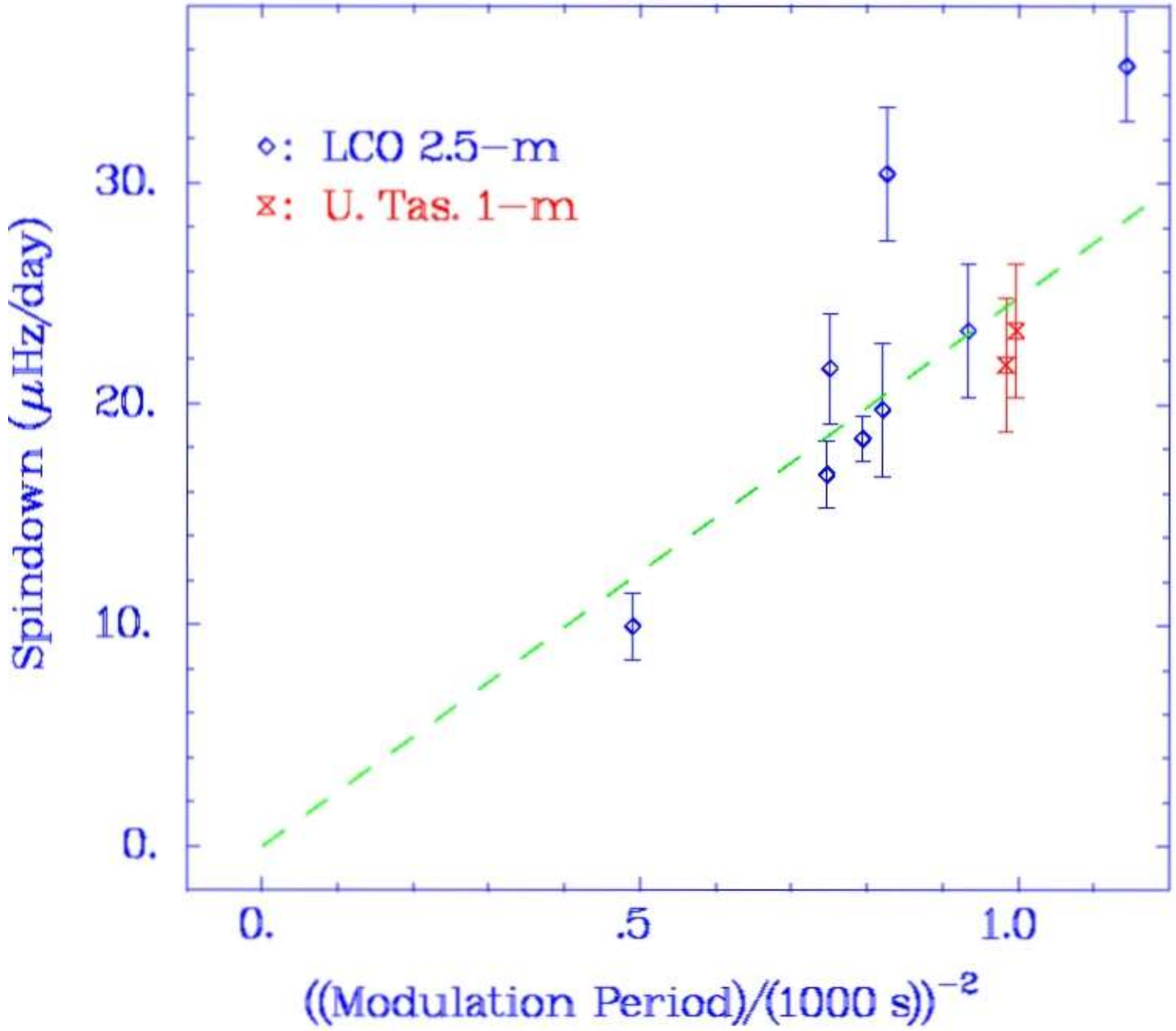
◇: LCO 2.5−m
x: U. Tas. 1−m
Spindown (μHz/day)
30.
20.
10.
0.
0.
.5
1.0
((Modulation Period)/(1000 s))^-2

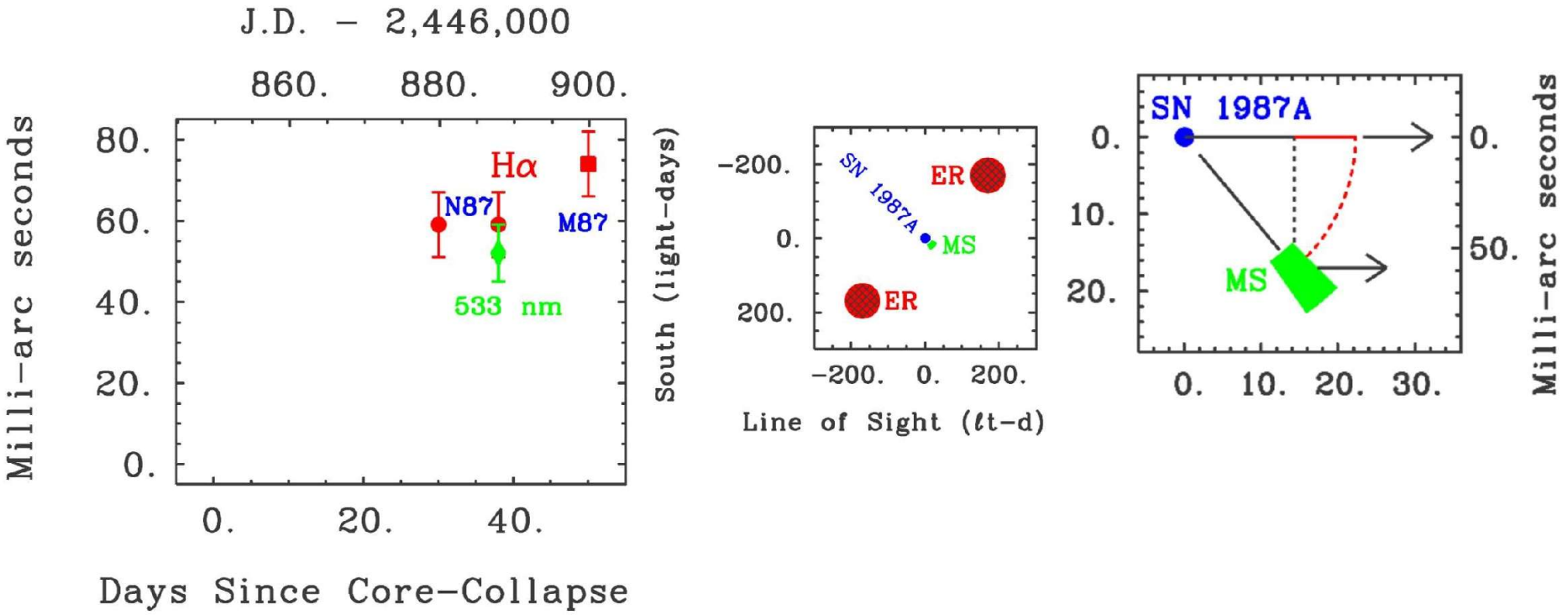

FIGURE 1. (Left) The distance of the MS from 87A at Hα and 533 nm vs time, from [13, 14] (M87/N87). (Center) The MS geometry and cross-sections of the equatorial ring (ER). (Right) The lines of sight from 87A to the Earth directly/through the MS (which takes an extra 8 days).

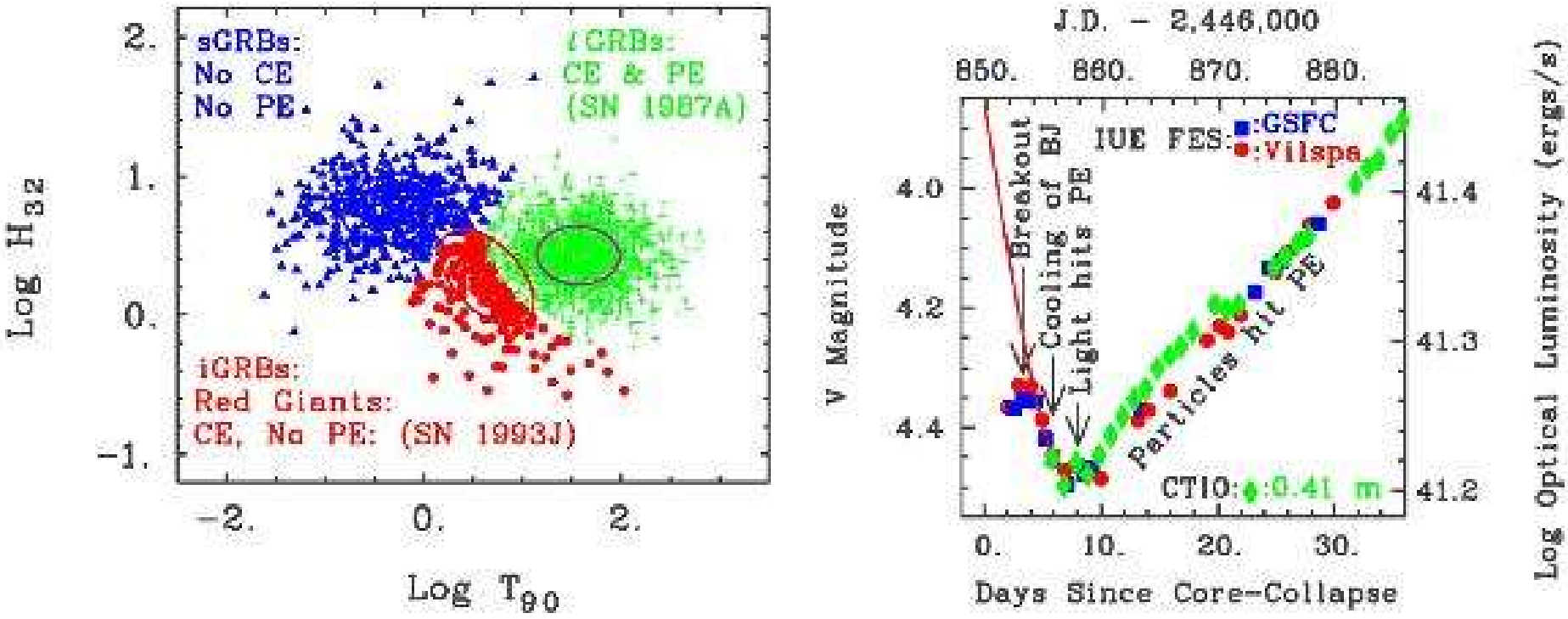

FIGURE 2. (Left) After [15] the GRBs from the BATSE Catalogue [16] scattered in duration (T_{90})-hardness (H_{32}) space. (Right) After [19] (Vilspa), with data from Sonneborne & Kirshner added (GSFC), the very early light curve of 87A from the IUE FES, together with data from the CTIO 16-inch telescope [20] (the centers of the two V bands are 5,100 Å & 5,500 Å respectively).

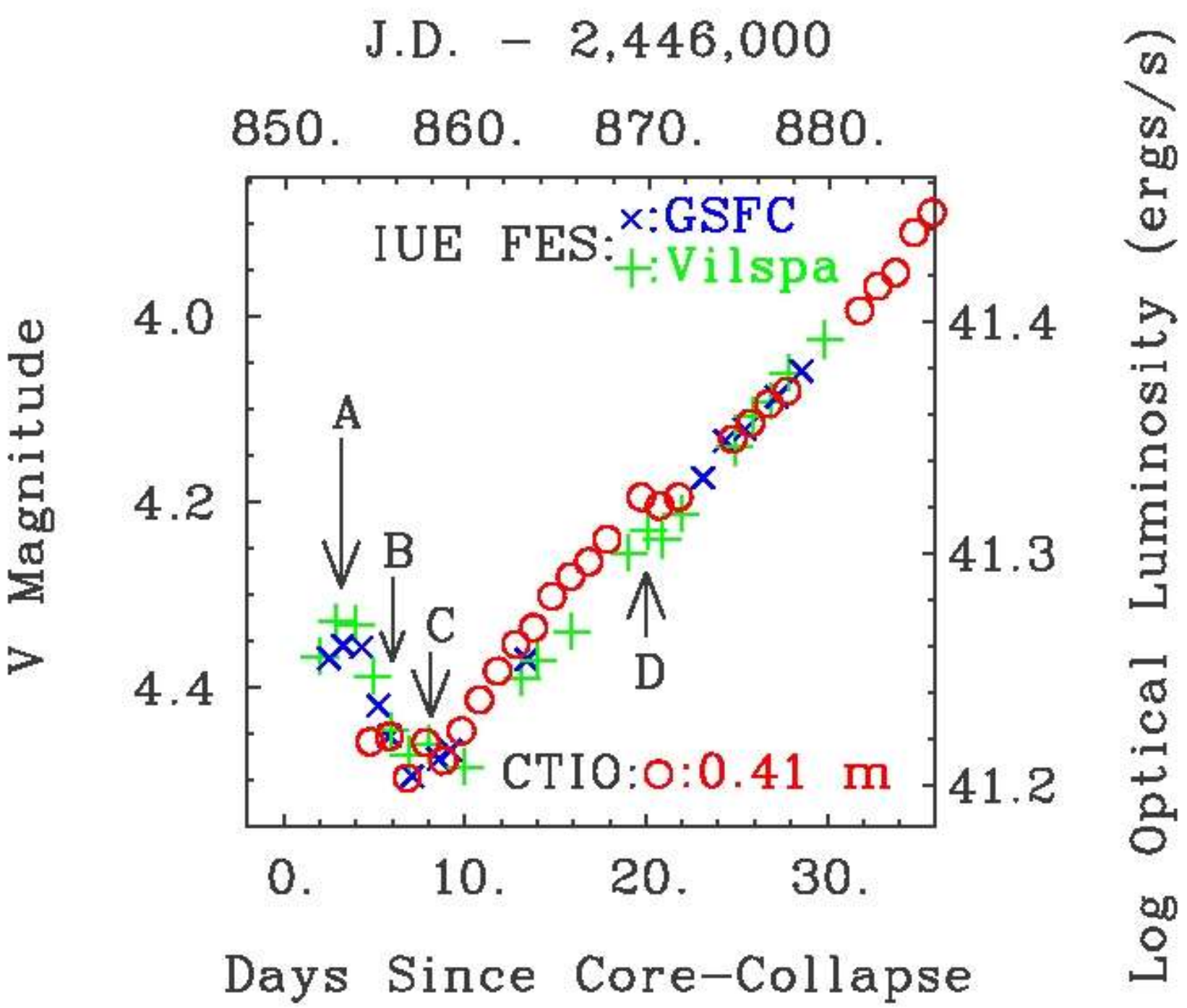
J.D. − 2,446,000
850.
860.
870.
880.
IUE FES: ×:GSFC
+:Vilspa
A
B
C
D
CTIO: o: 0.41 m
4.0
4.2
4.4
V Magnitude
41.4
41.3
41.2
Log Optical Luminosity (ergs/s)
0.
10.
20.
30.
Days Since Core-Collapse

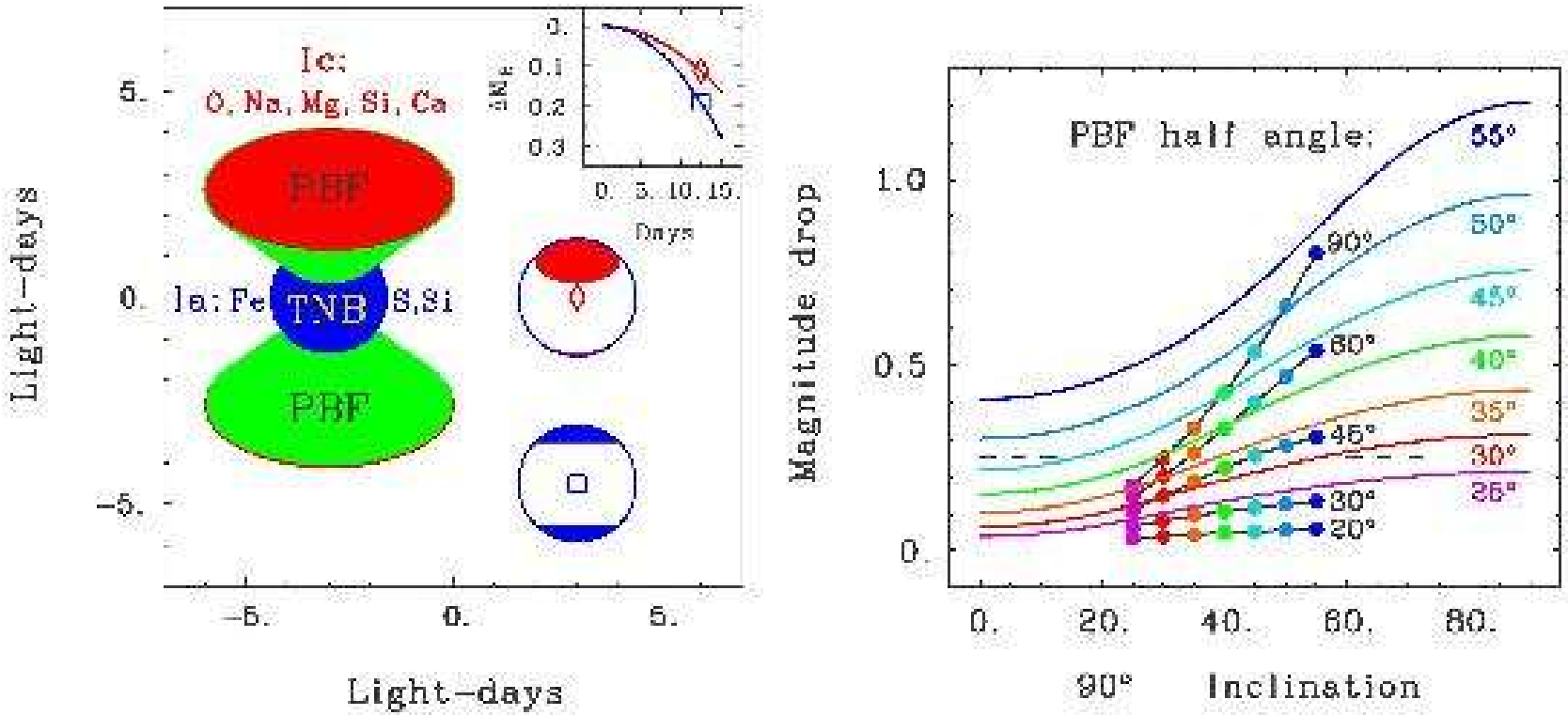

FIGURE 3. (Left) The geometry for type Ia/c SNe, as viewed 30° off the merger equator, with PBFs sketched as cones of half-angle 45°. The two circles at the right/lower right show the maximum PBF footprints on the much brighter TNBs, which can be exposed as the PBFs quickly depart, for merger co-inclinations (co-i's) of 0° (square) and 30° (diamond). These effects are compounded with a parabolic $\Delta M_{B,5}$ of 0.5 m in 15 days (inset). (Right) The maximum drop in magnitude from exposure of PBF footprints on the TNB as a function of co-i for PBF half angles of 25°-55° in 5° steps (curves without dots), and the excess drops over 0° for co-i's of 20°, 30°, 45°, 60°, and 90° (curves with dots), plotted at the abscissa values equal to their PBF half angles.

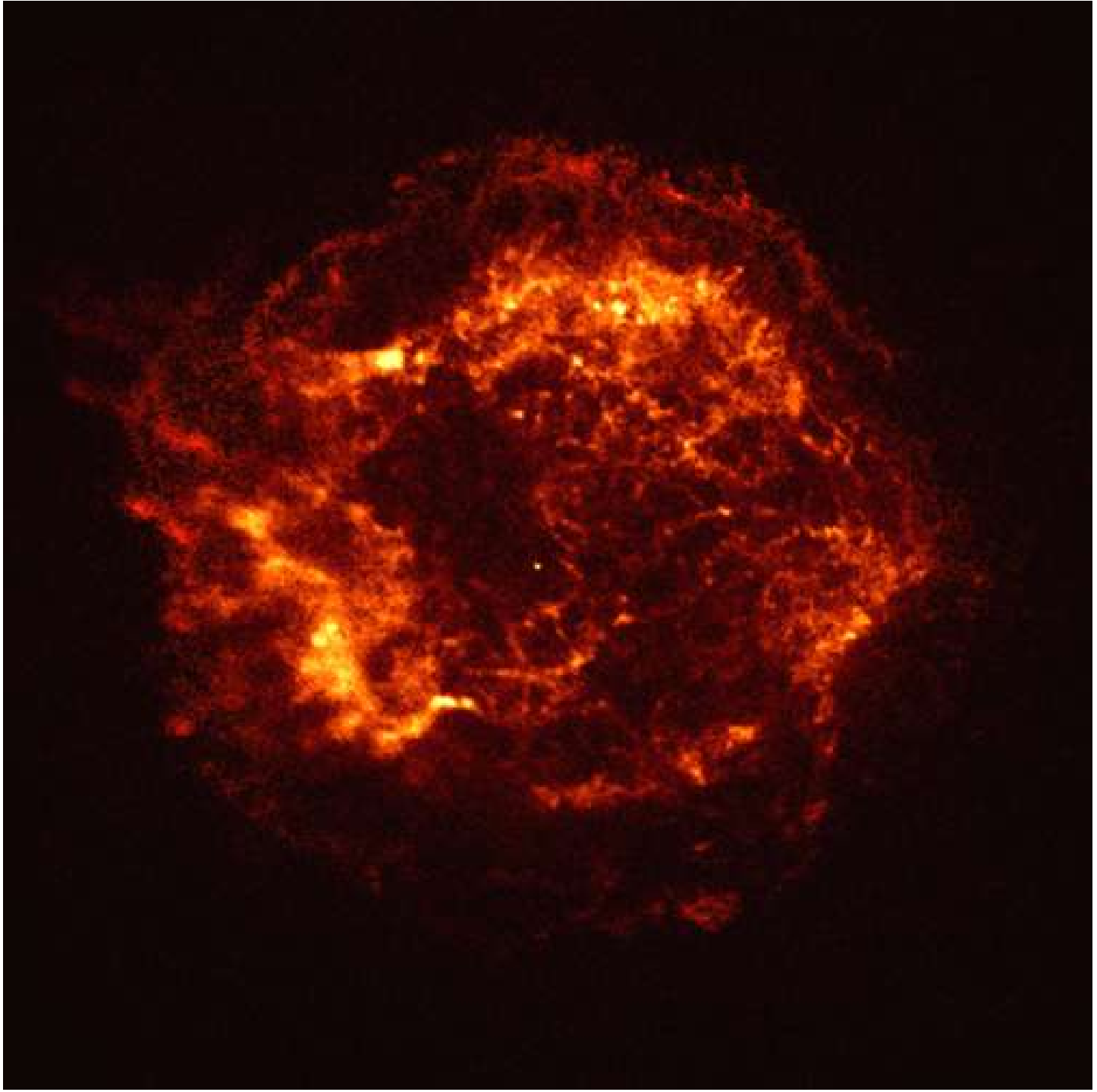

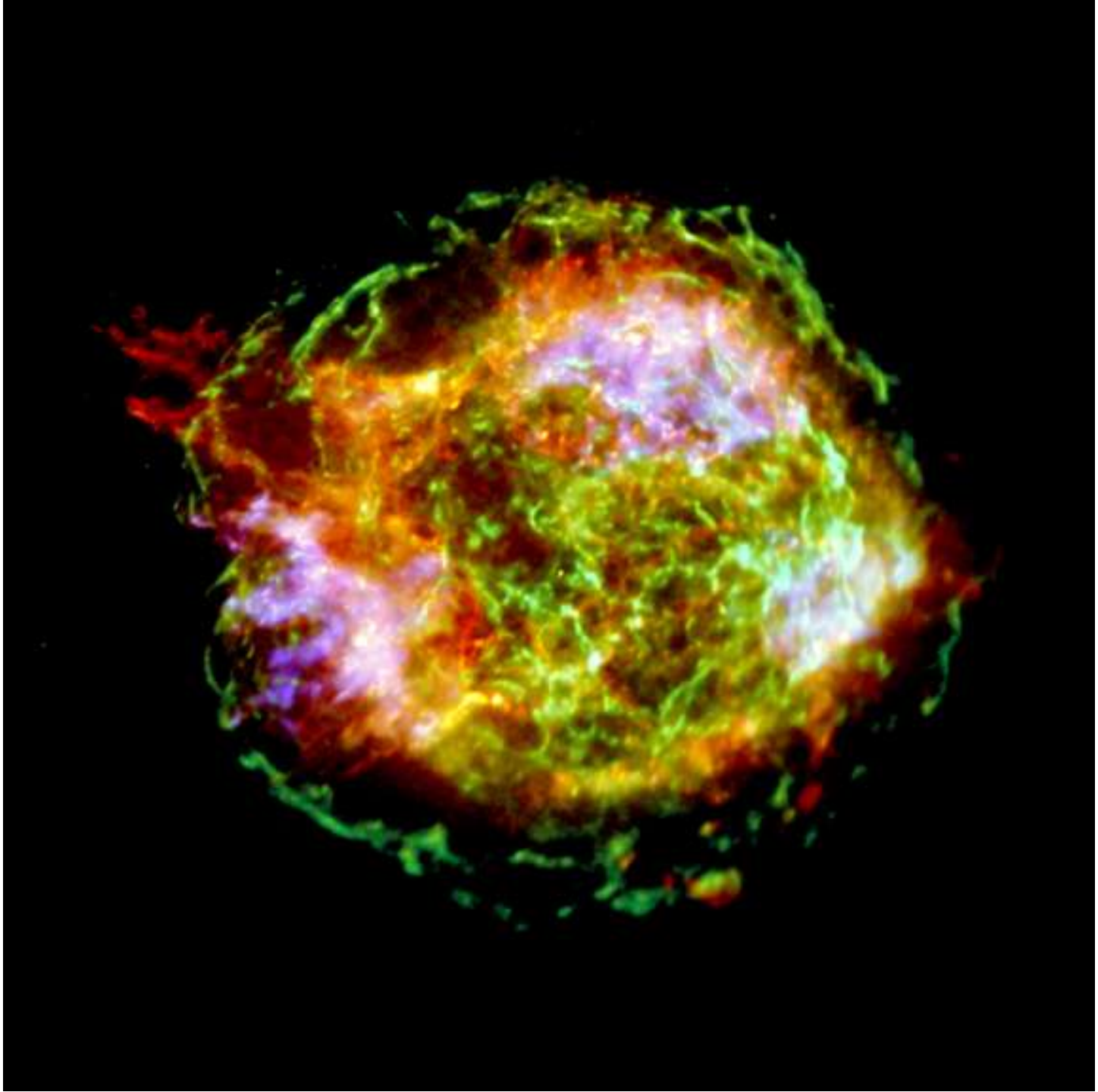

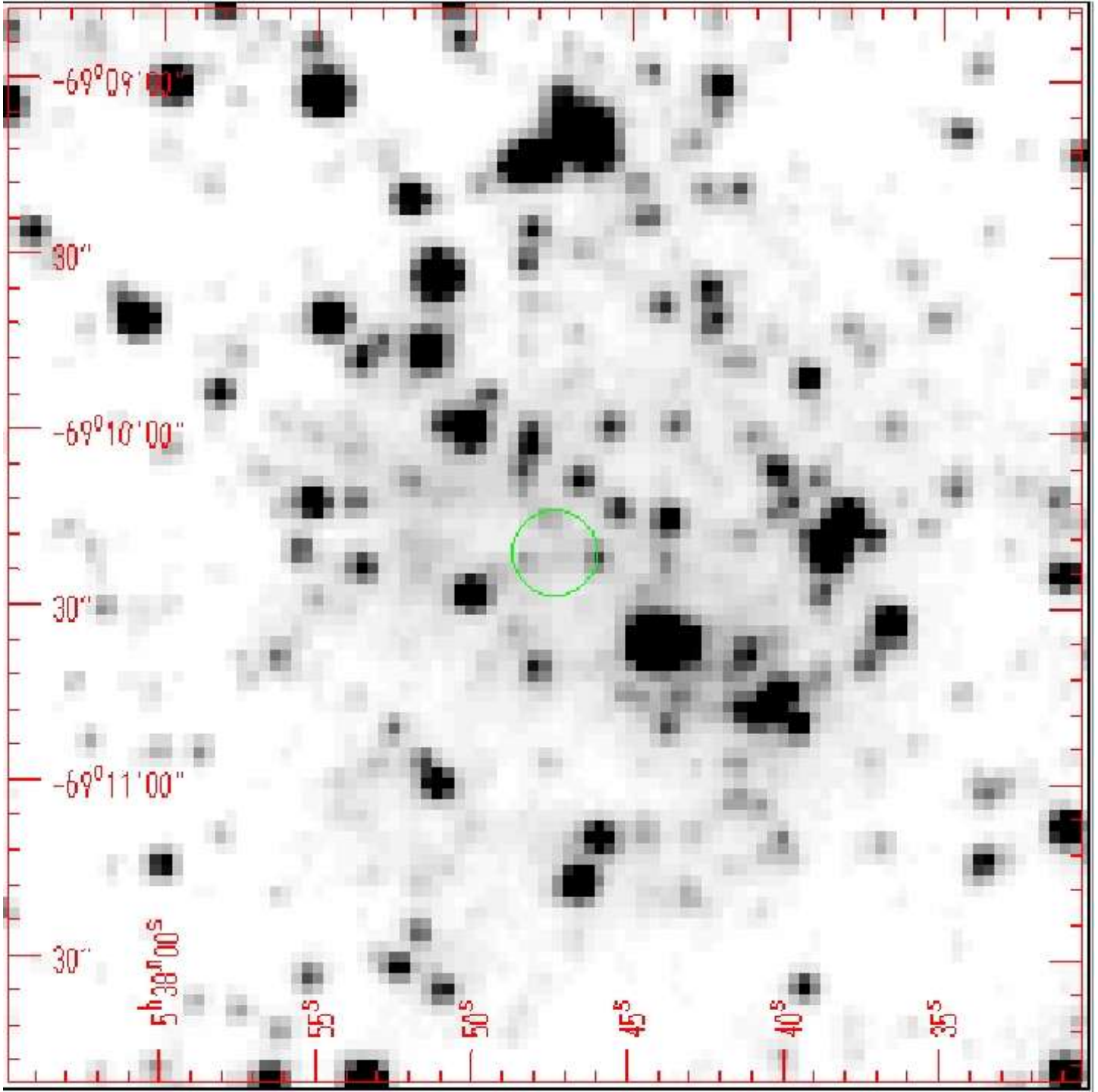
-69°09'00"
30"
-69°10'00"
30"
-69°11'00"
30"
5h38m00s
55s
50s
45s
40s
35s

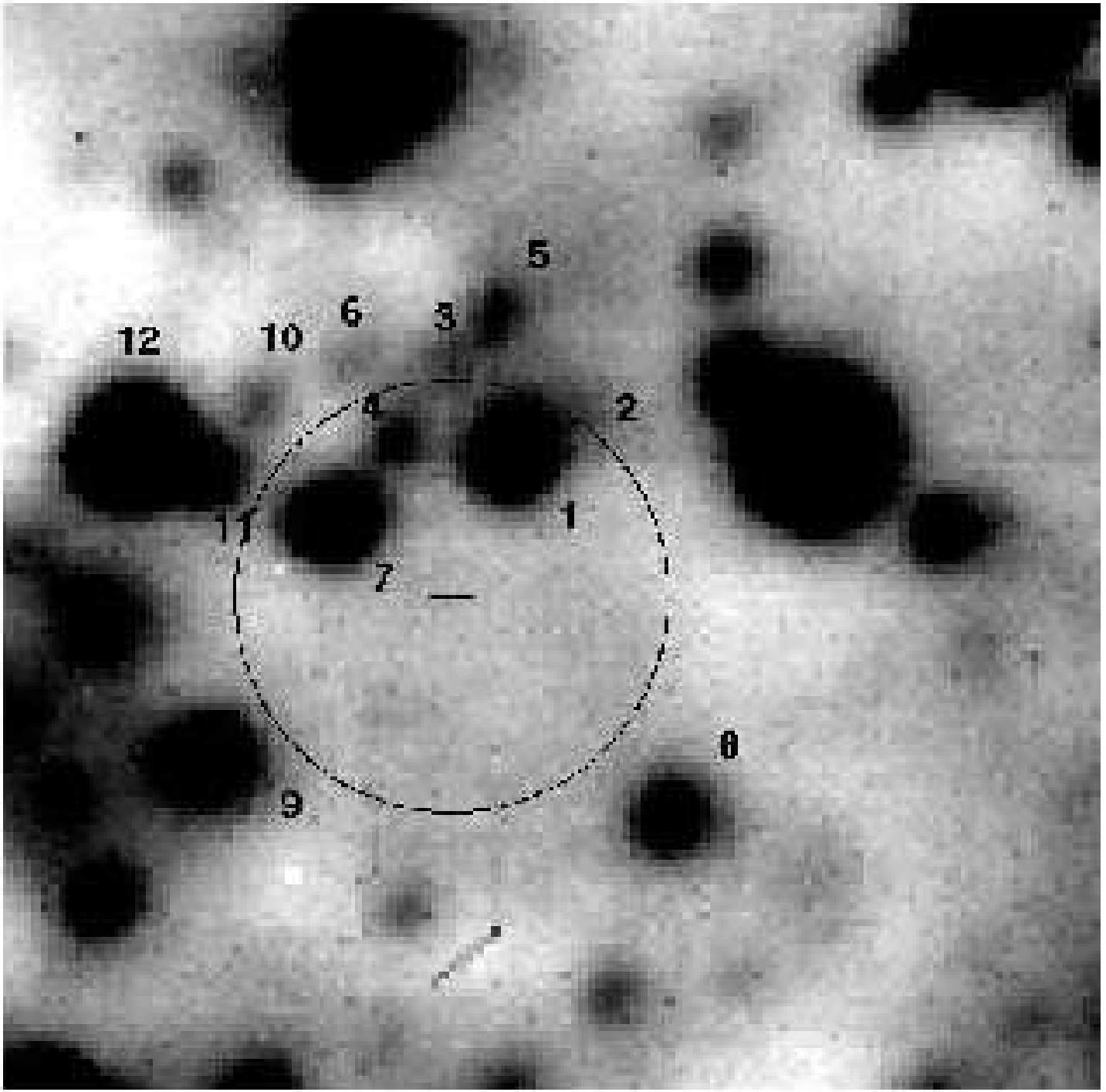
12
10
6
3
5
4
2
11
1
7
8
9

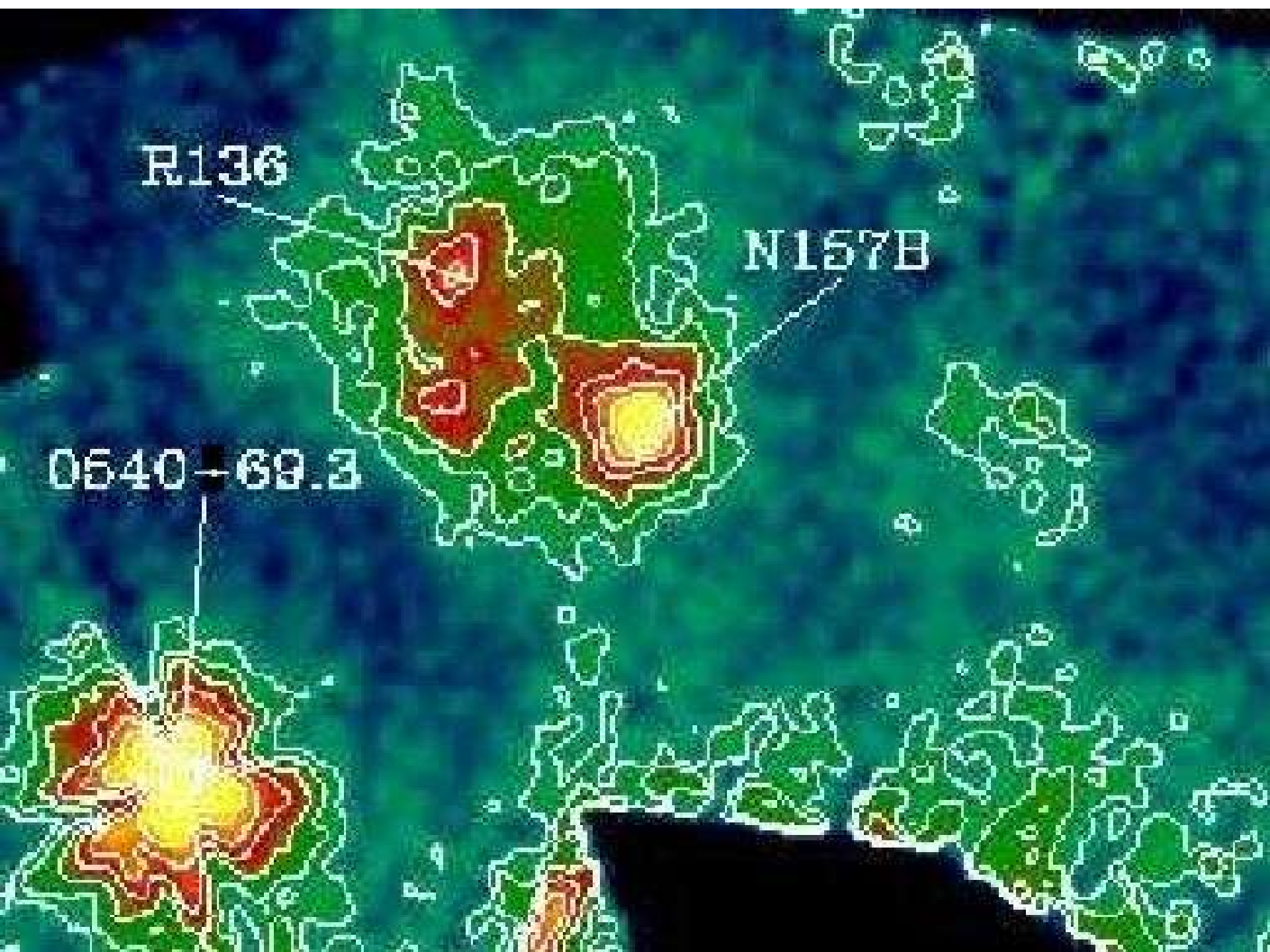
R136
N157B
0540-69.3

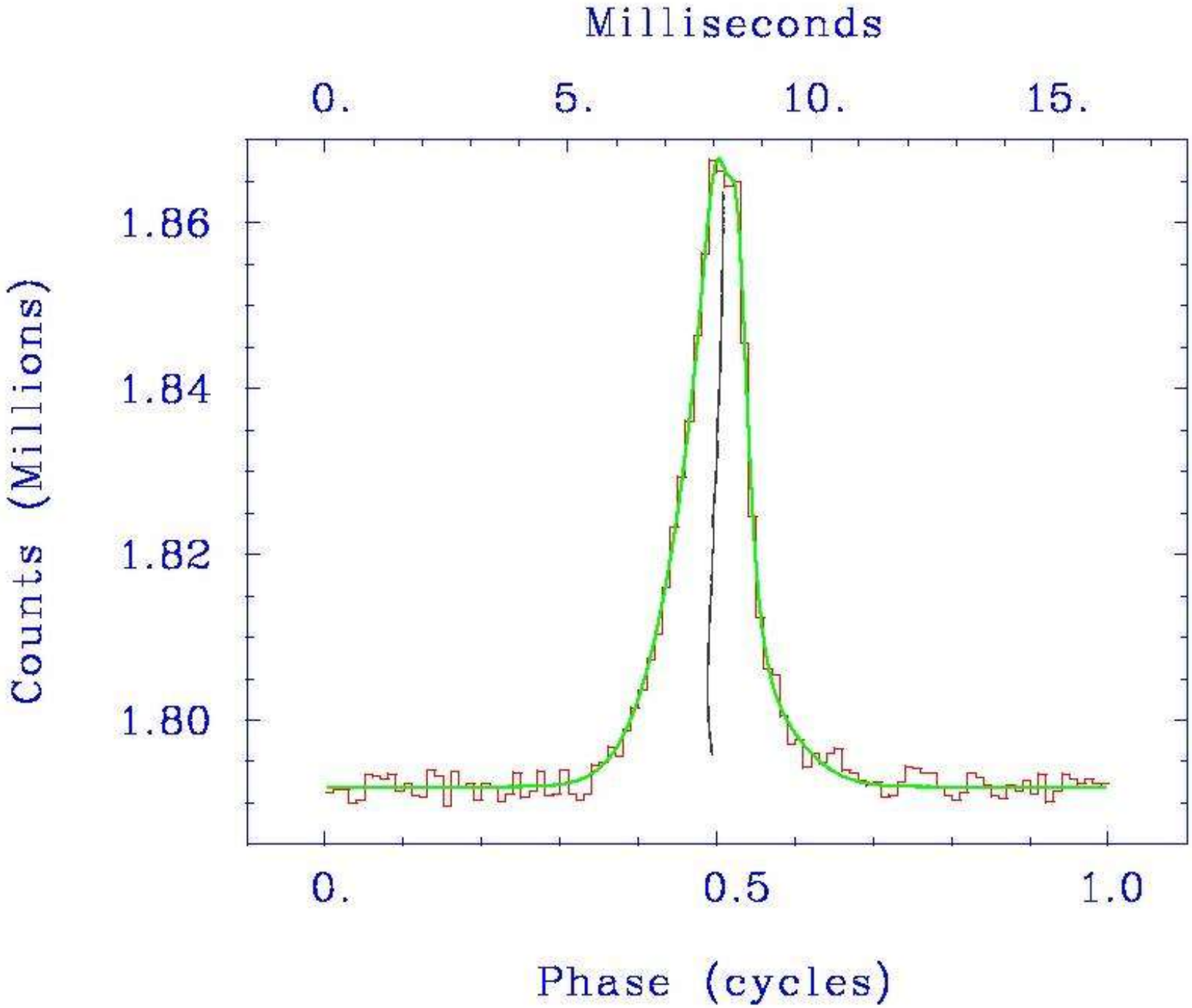
Milliseconds
0.
5.
10.
15.
1.86
1.84
1.82
1.80
Counts (Millions)
0.
0.5
1.0
Phase (cycles)

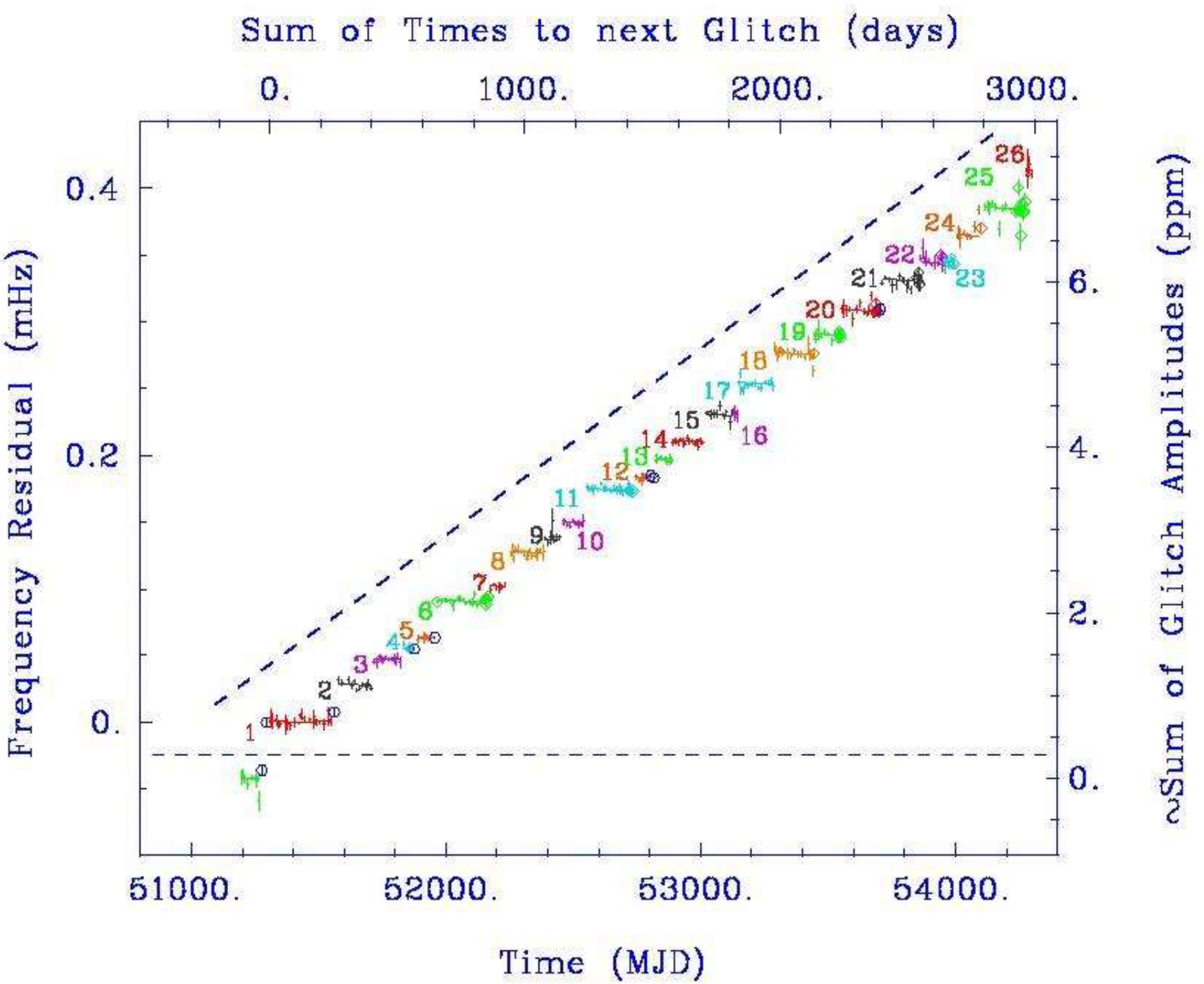
Sum of Times to next Glitch (days)
0.
1000.
2000.
3000.
Frequency Residual (mHz)
0.4
0.2
0.
Σ Sum of Glitch Amplitudes (ppm)
6.
4.
2.
0.
51000.
52000.
53000.
54000.
Time (MJD)
1
2
3
4
5
6
7
8
9
10
11
12
13
14
15
16
17
18
19
20
21
22
23
24
25
26

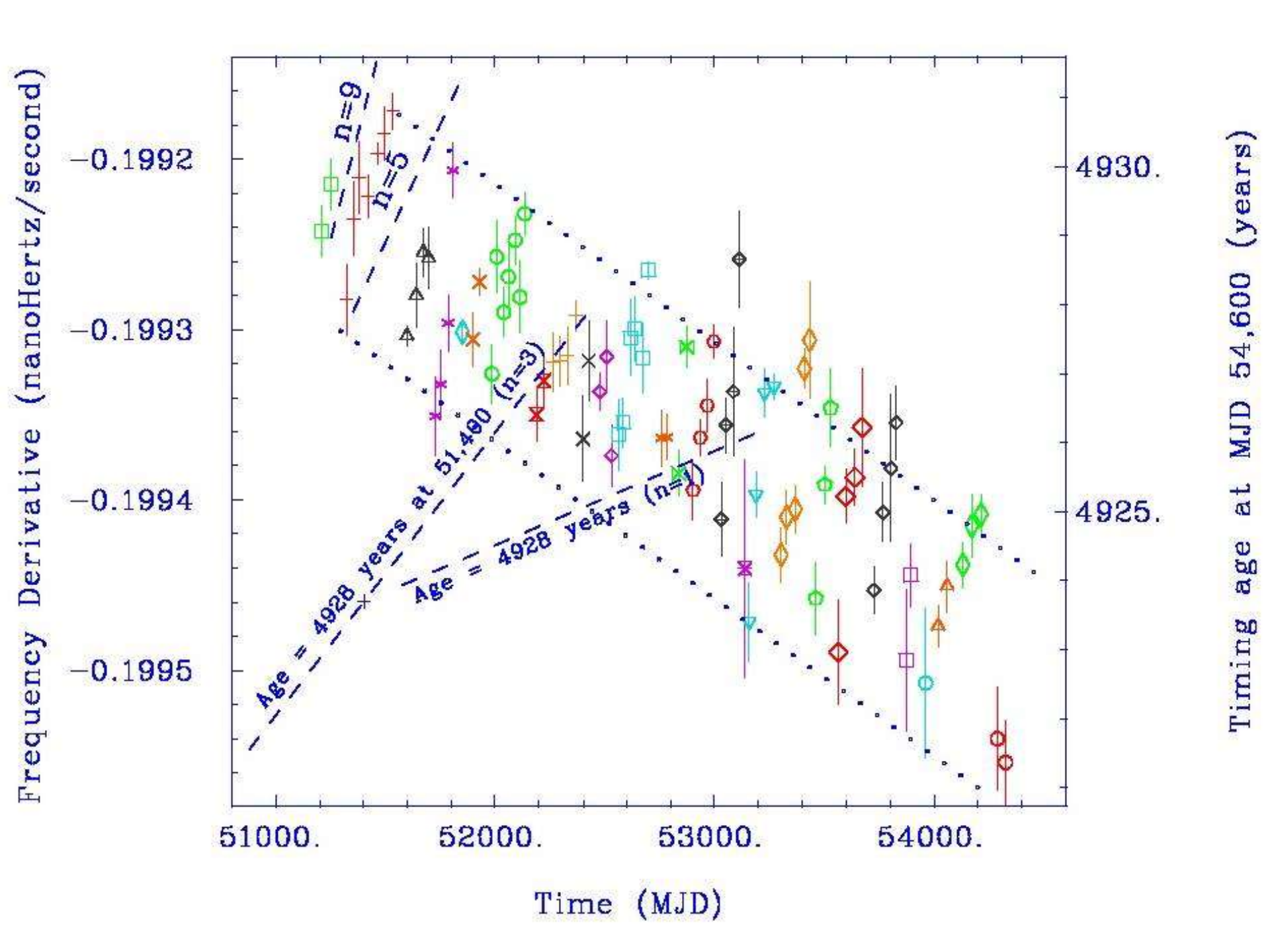
Frequency Derivative (nanoHertz/second)
−0.1992
−0.1993
−0.1994
−0.1995
Timing age at MJD 54,600 (years)
4930.
4925.
51000.
52000.
53000.
54000.
Time (MJD)
n=9
n=5
Age = 4928 years at 51,490 (n=3)
Age = 4928 years (n=1)

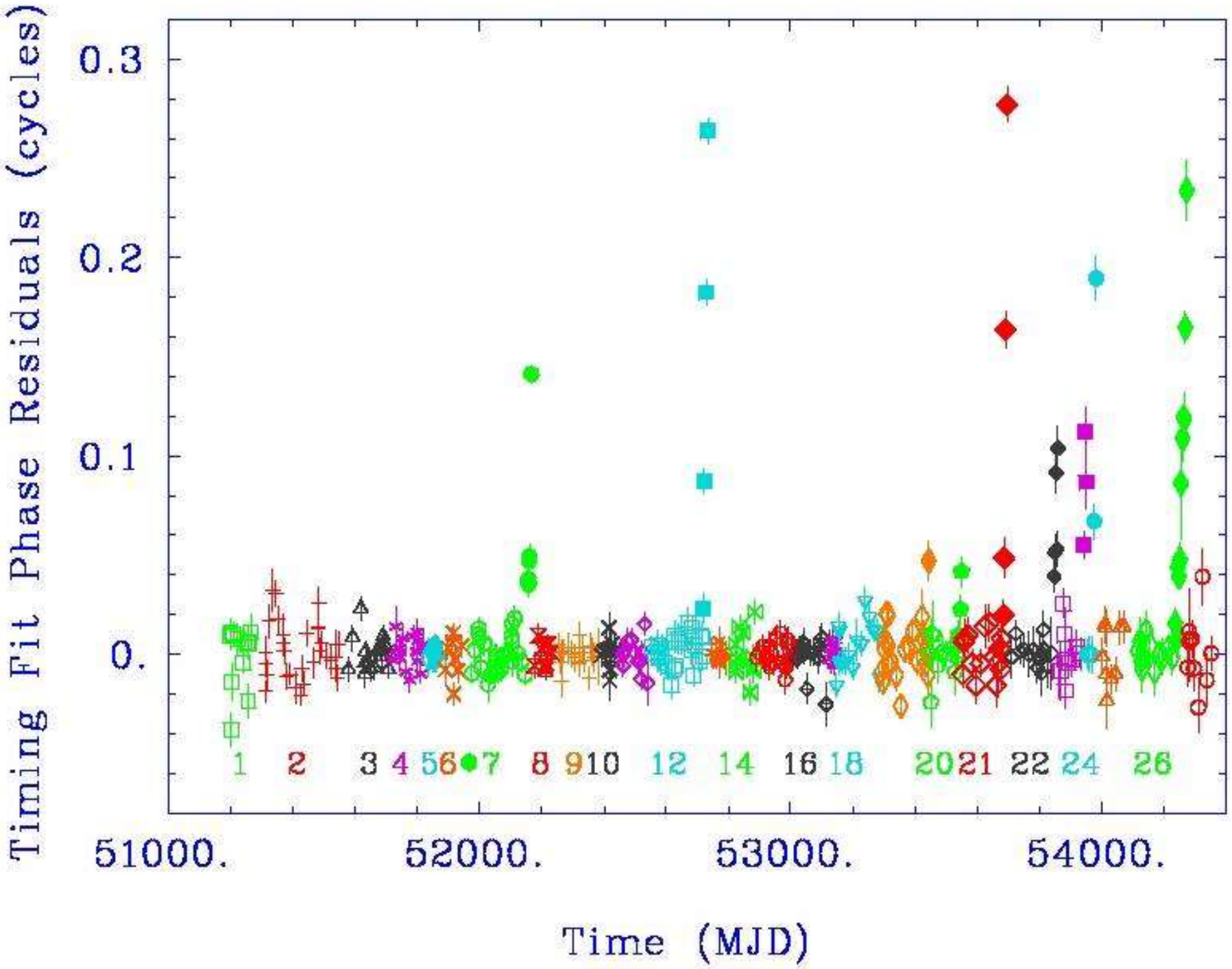
Timing Fit Phase Residuals (cycles)
0.3
0.2
0.1
0.
1 2 3 4 5 6 7 8 9 10 12 14 16 18 20 21 22 24 26
51000.
52000.
53000.
54000.
Time (MJD)

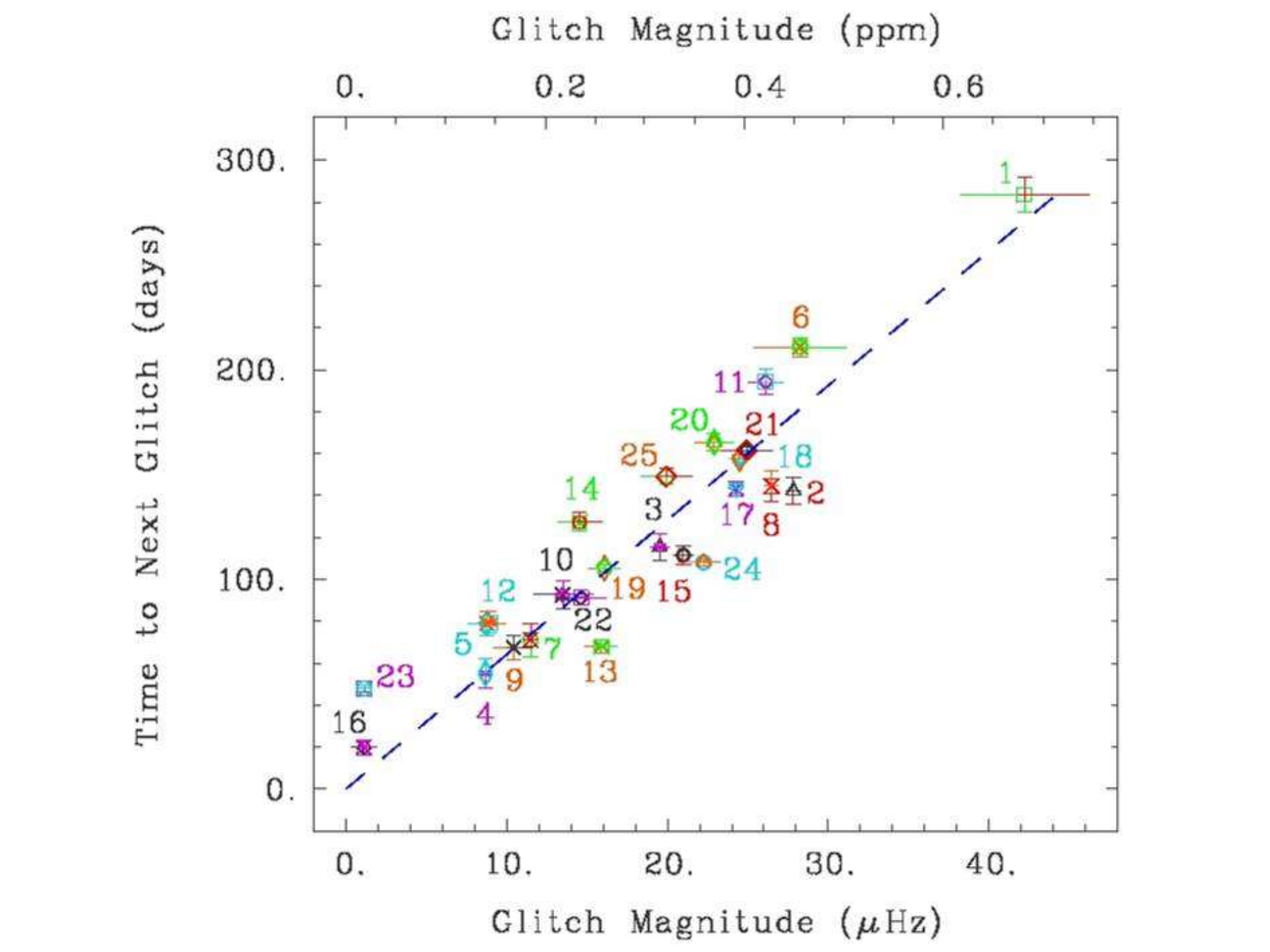
Glitch Magnitude (ppm)
0.
0.2
0.4
0.6
Time to Next Glitch (days)
300.
200.
100.
0.
0.
10.
20.
30.
40.
Glitch Magnitude (μHz)
1
6
11
20
21
25
18
14
3
2
17
8
10
24
12
19
15
22
5
7
13
23
9
4
16

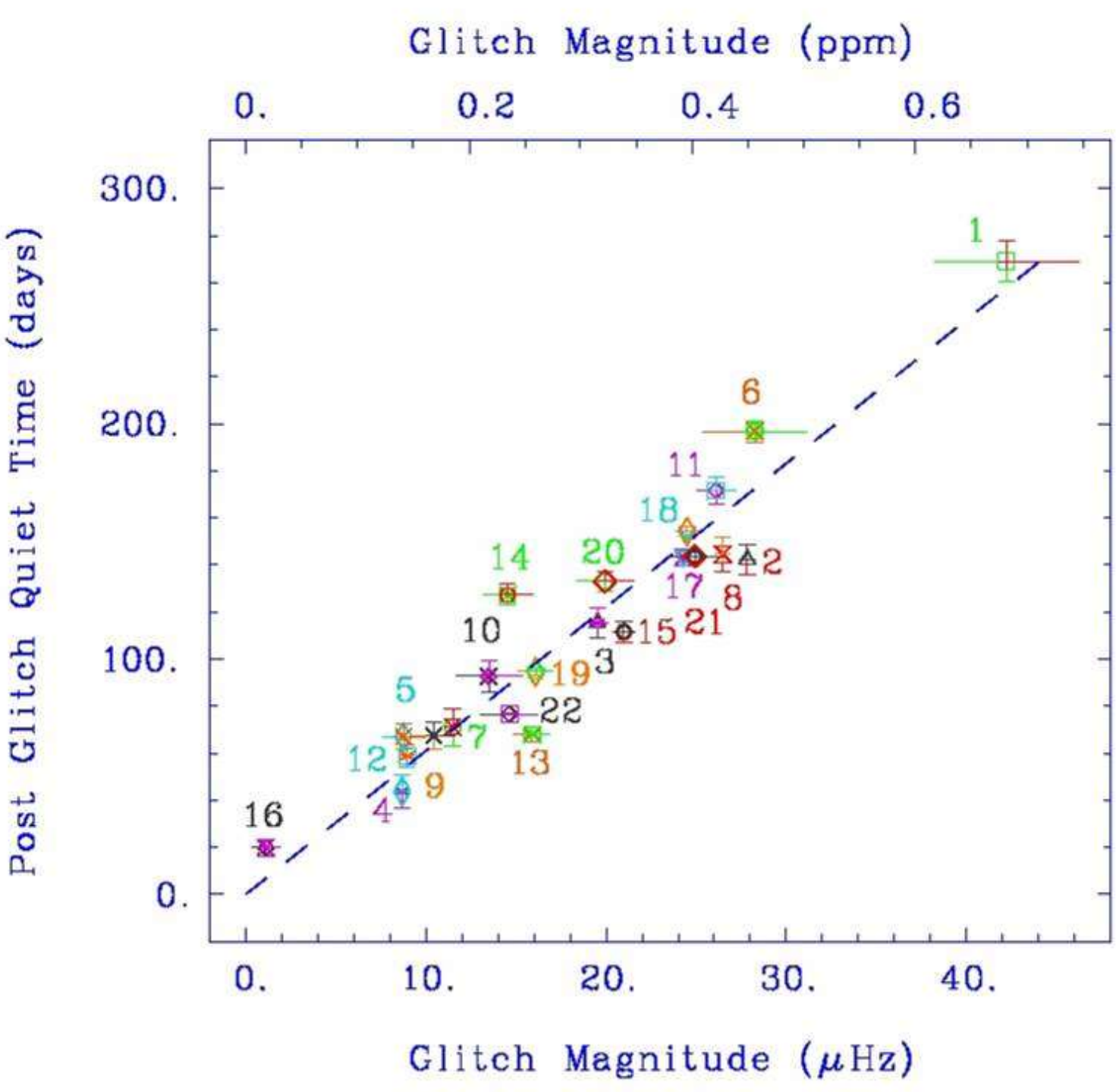
Glitch Magnitude (ppm)
0.
0.2
0.4
0.6
300.
200.
100.
0.
Post Glitch Quiet Time (days)
0.
10.
20.
30.
40.
Glitch Magnitude (μHz)
1
6
11
18
14
20
2
17
8
21
10
15
3
19
5
22
7
12
13
9
4
16

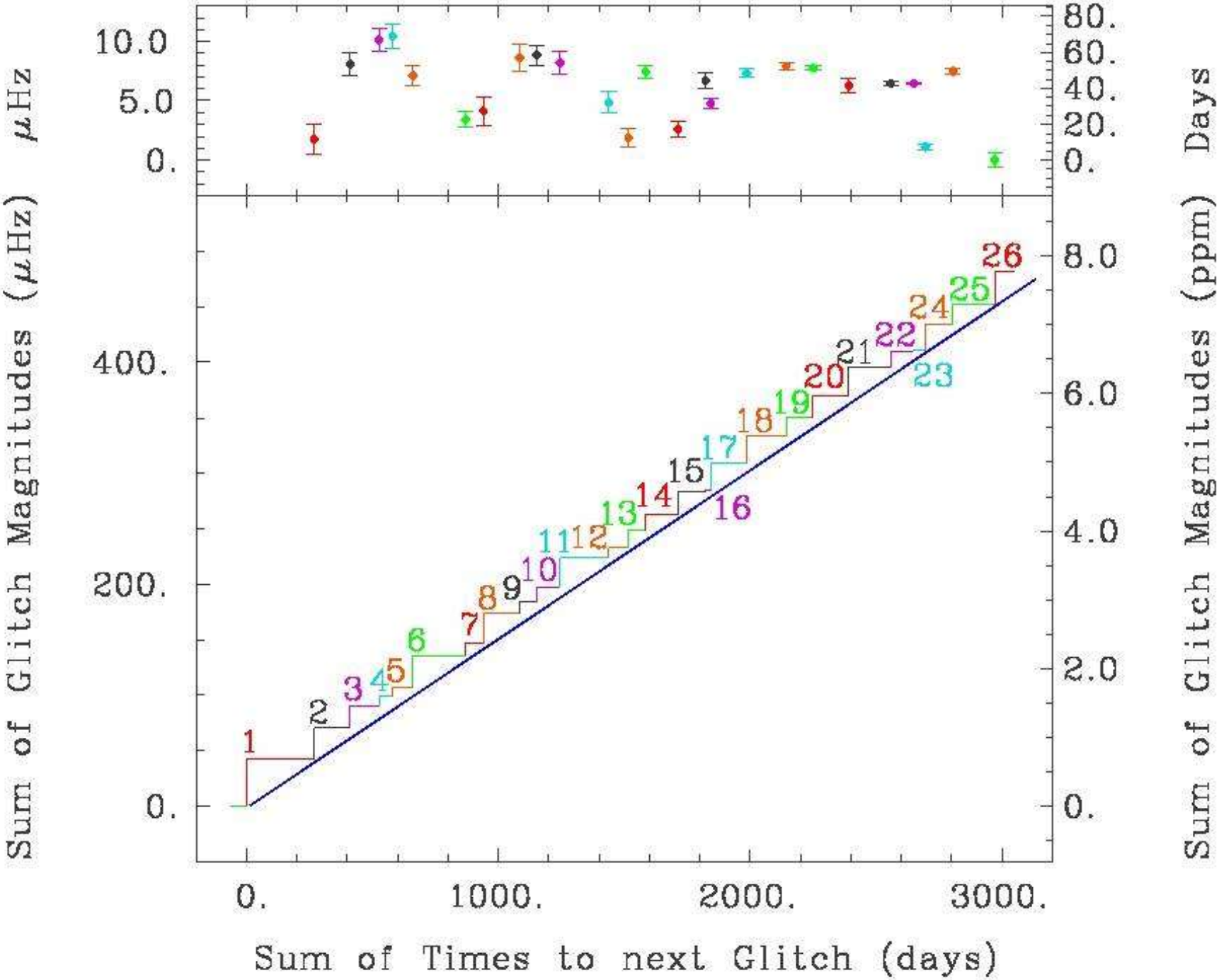
10.0
5.0
0.
80.
60.
40.
20.
0.
μHz
Days
400.
200.
0.
8.0
6.0
4.0
2.0
0.
1
2
3
4
5
6
7
8
9
10
11
12
13
14
15
16
17
18
19
20
21
22
23
24
25
26
0.
1000.
2000.
3000.
Sum of Glitch Magnitudes (μHz)
Sum of Glitch Magnitudes (ppm)
Sum of Times to next Glitch (days)

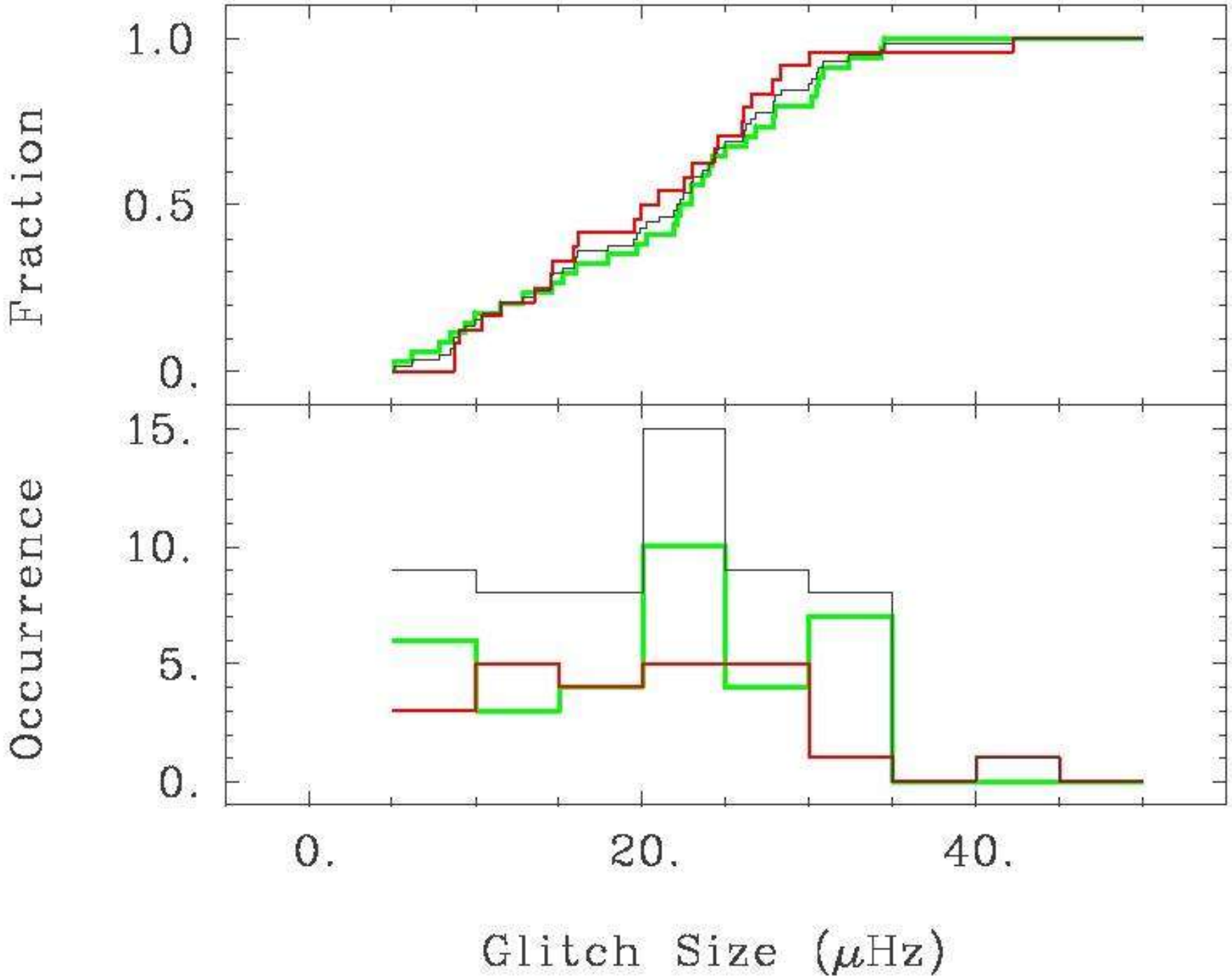
Fraction
1.0
0.5
0.
Occurrence
15.
10.
5.
0.
0.
20.
40.
Glitch Size (μHz)

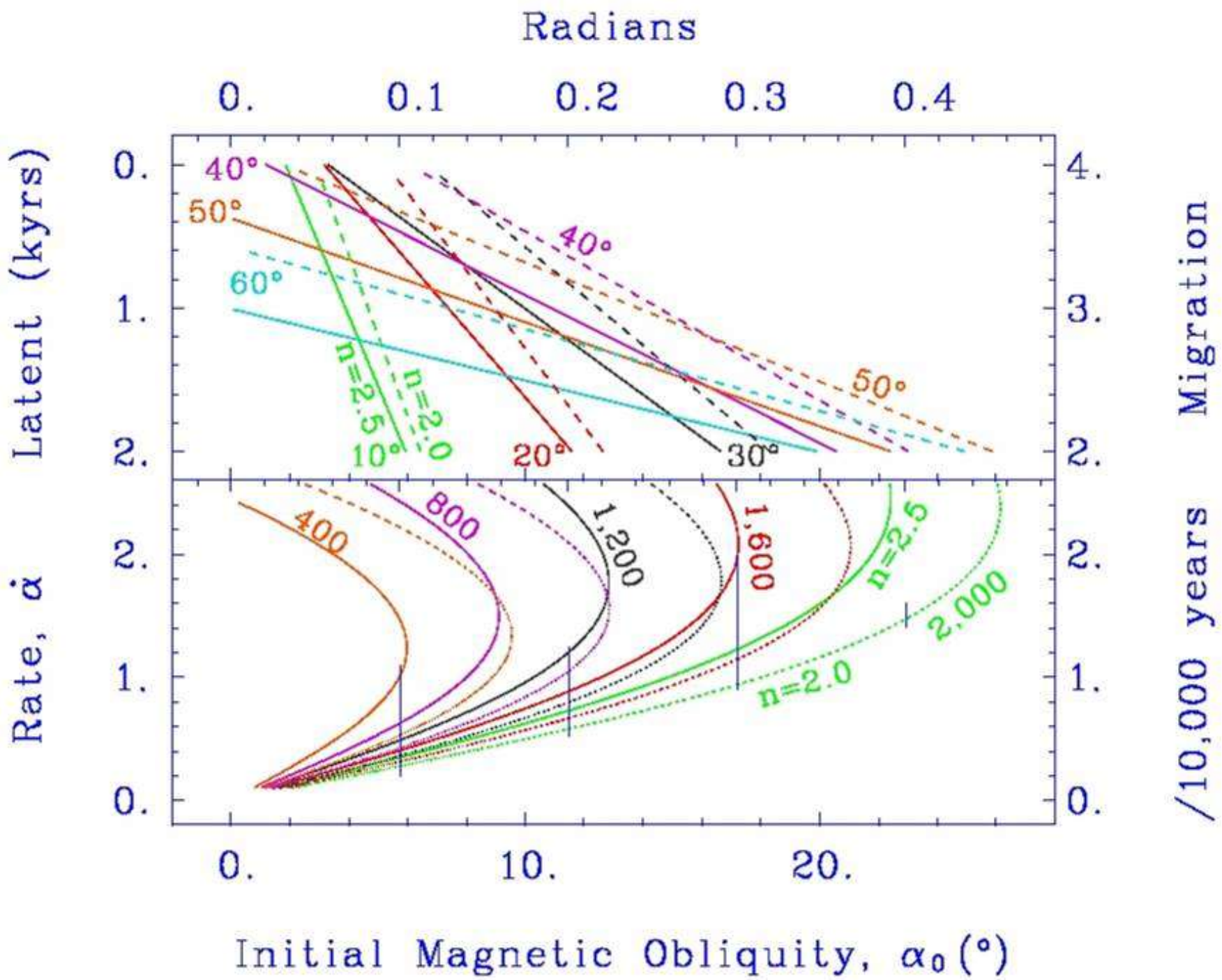
Radians
0.
0.1
0.2
0.3
0.4
Rate, $\dot{\alpha}$ Latent (kyrs)
/10,000 years Migration
0.
1.
2.
4.
3.
40°
50°
60°
n=2.5
n=2.0
10°
20°
30°
40°
50°
400
800
1,200
1,600
n=2.5
2,000
n=2.0
0.
10.
20.
Initial Magnetic Obliquity, α_0 (°)

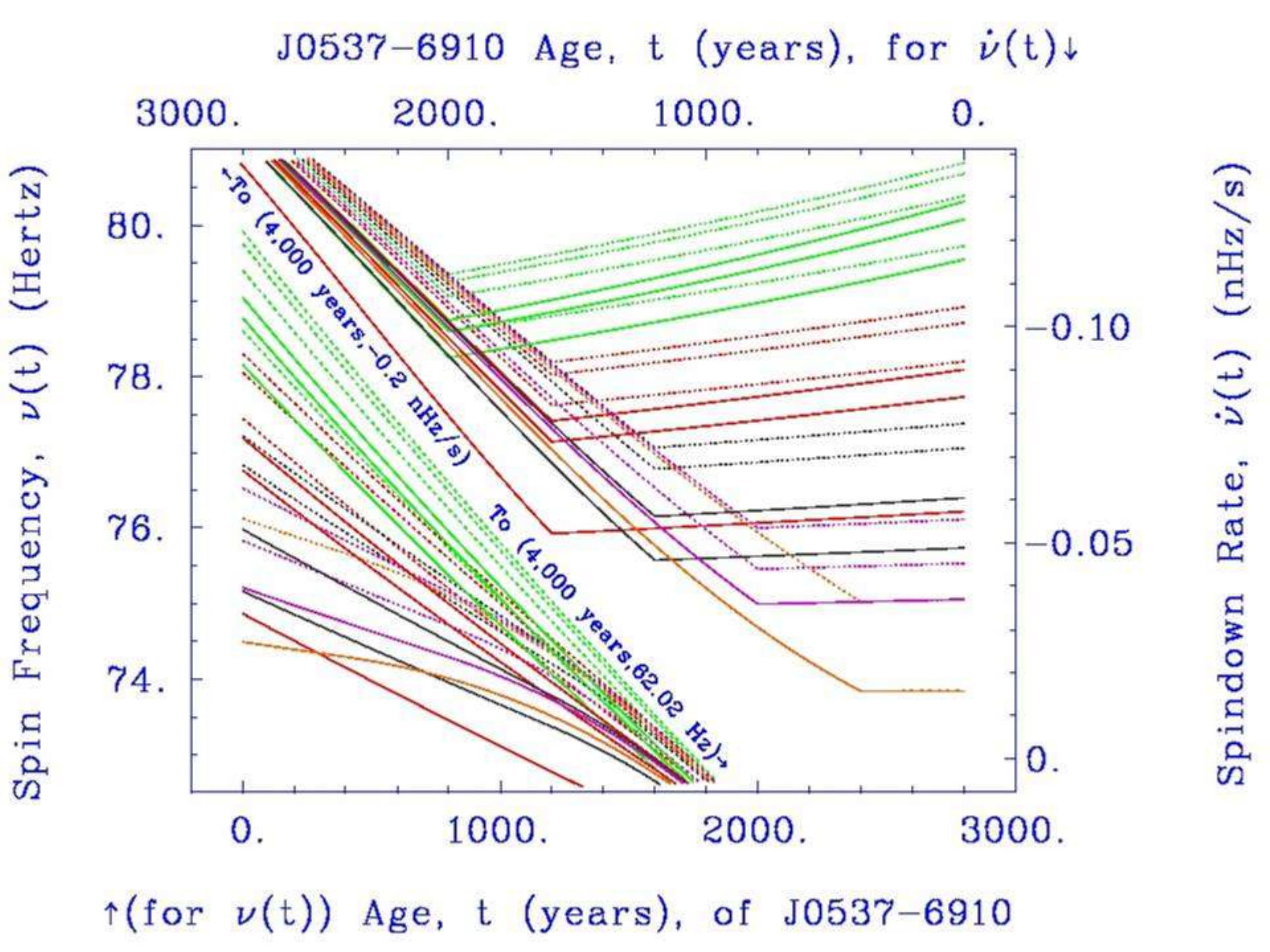
J0537−6910 Age, t (years), for $\dot{\nu}$(t)↓
3000.
2000.
1000.
0.
Spin Frequency, ν(t) (Hertz)
80.
78.
76.
74.
Spindown Rate, $\dot{\nu}$(t) (nHz/s)
−0.10
−0.05
0.
To (4,000 years,−0.2 nHz/s)
To (4,000 years,62.02 Hz)→
0.
1000.
2000.
3000.
↑(for ν(t)) Age, t (years), of J0537−6910

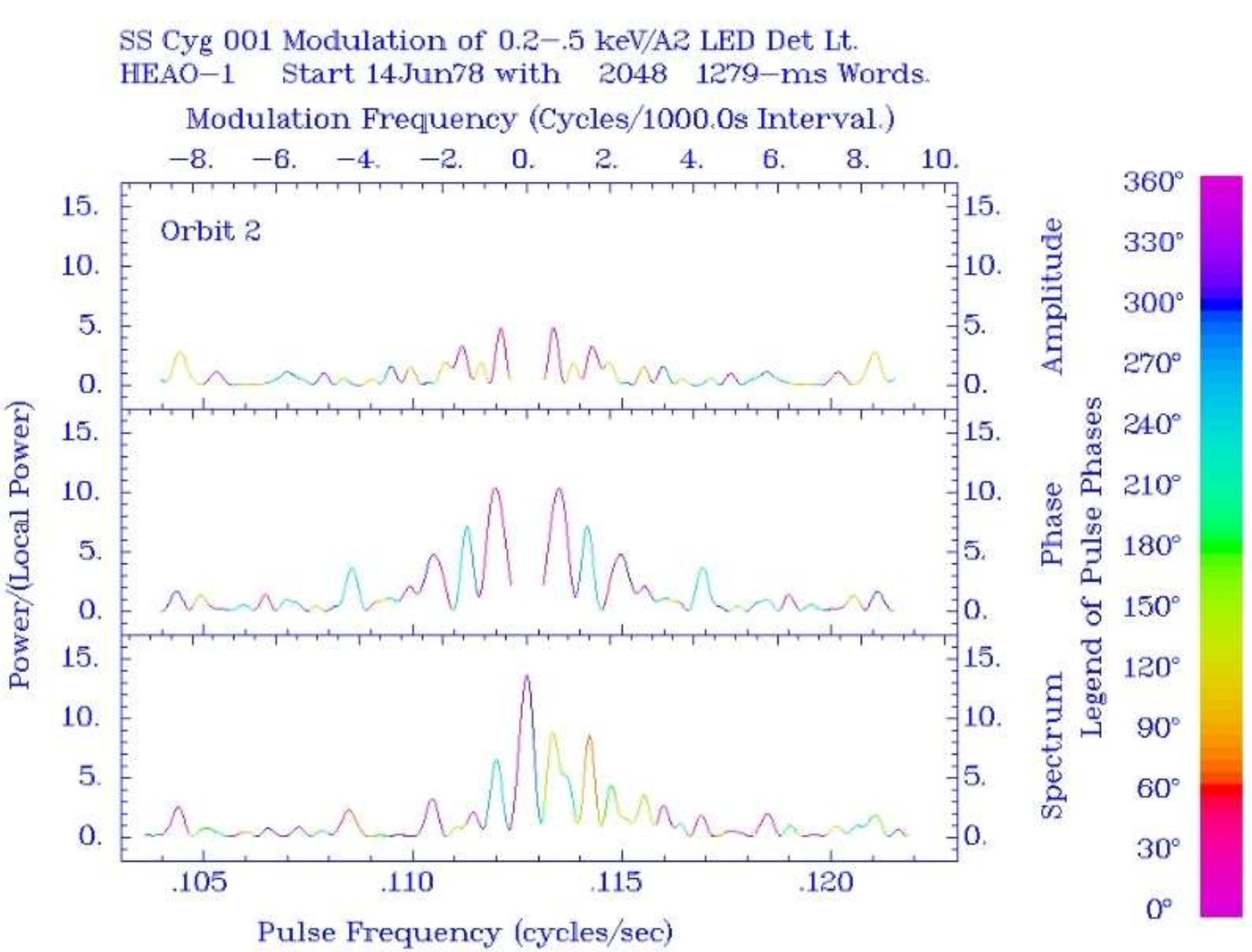
SS Cyg 001 Modulation of 0.2–.5 keV/A2 LED Det Lt.
HEAO–1 Start 14Jun78 with 2048 1279–ms Words.
Modulation Frequency (Cycles/1000.0s Interval.)
−8. −6. −4. −2. 0. 2. 4. 6. 8. 10.
Orbit 2
Power/(Local Power)
15.
10.
5.
0.
.105 .110 .115 .120
Pulse Frequency (cycles/sec)
Amplitude
Phase
Spectrum
Legend of Pulse Phases
360°
330°
300°
270°
240°
210°
180°
150°
120°
90°
60°
30°
0°

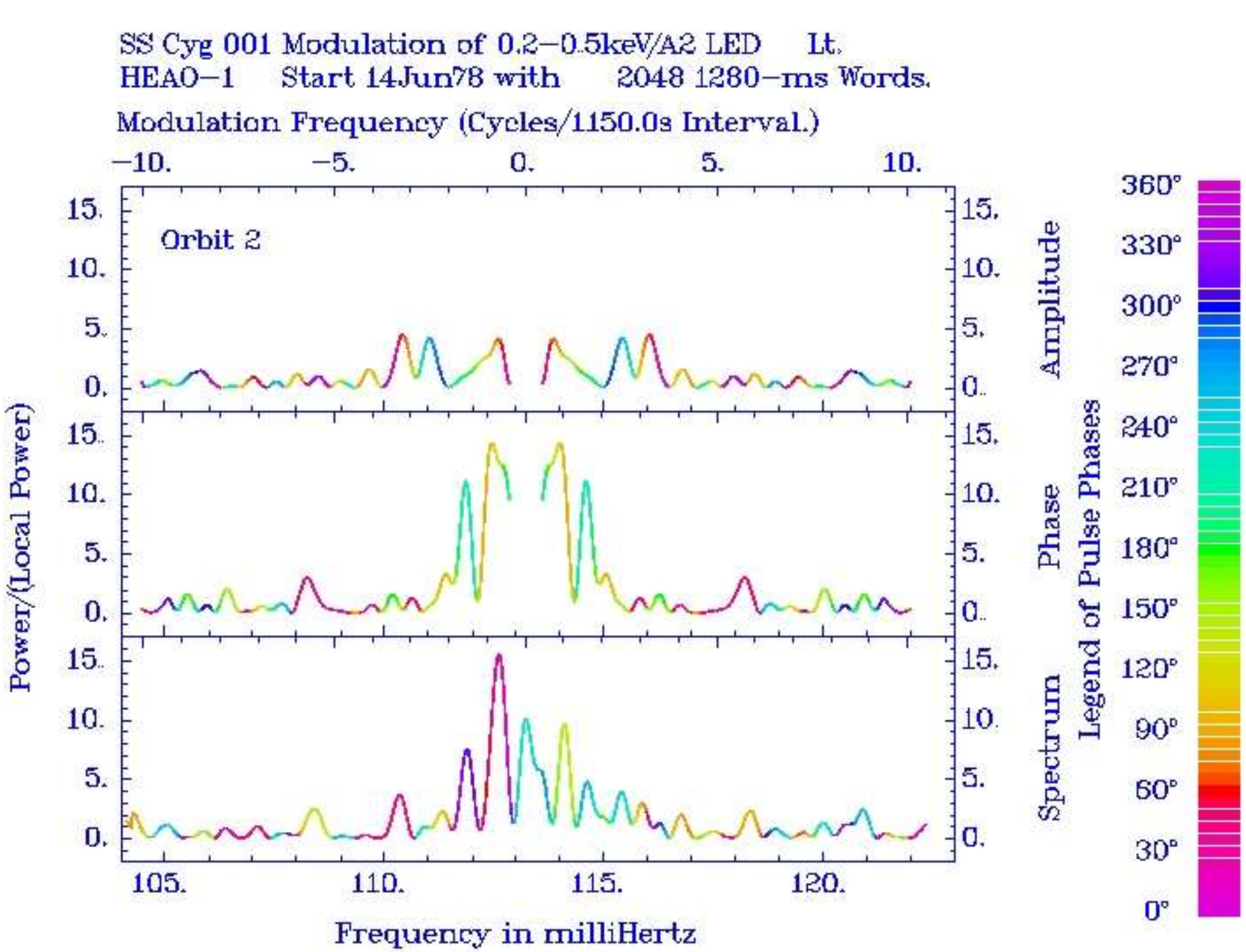
SS Cyg 001 Modulation of 0.2−0.5keV/A2 LED Lt.
HEAO−1 Start 14Jun78 with 2048 1280−ms Words.
Modulation Frequency (Cycles/1150.0s Interval.)
−10.
−5.
0.
5.
10.
Orbit 2
15.
10.
5.
0.
Power/(Local Power)
105.
110.
115.
120.
Frequency in milliHertz
Amplitude
Phase
Spectrum
Legend of Pulse Phases
360°
330°
300°
270°
240°
210°
180°
150°
120°
90°
60°
30°
0°

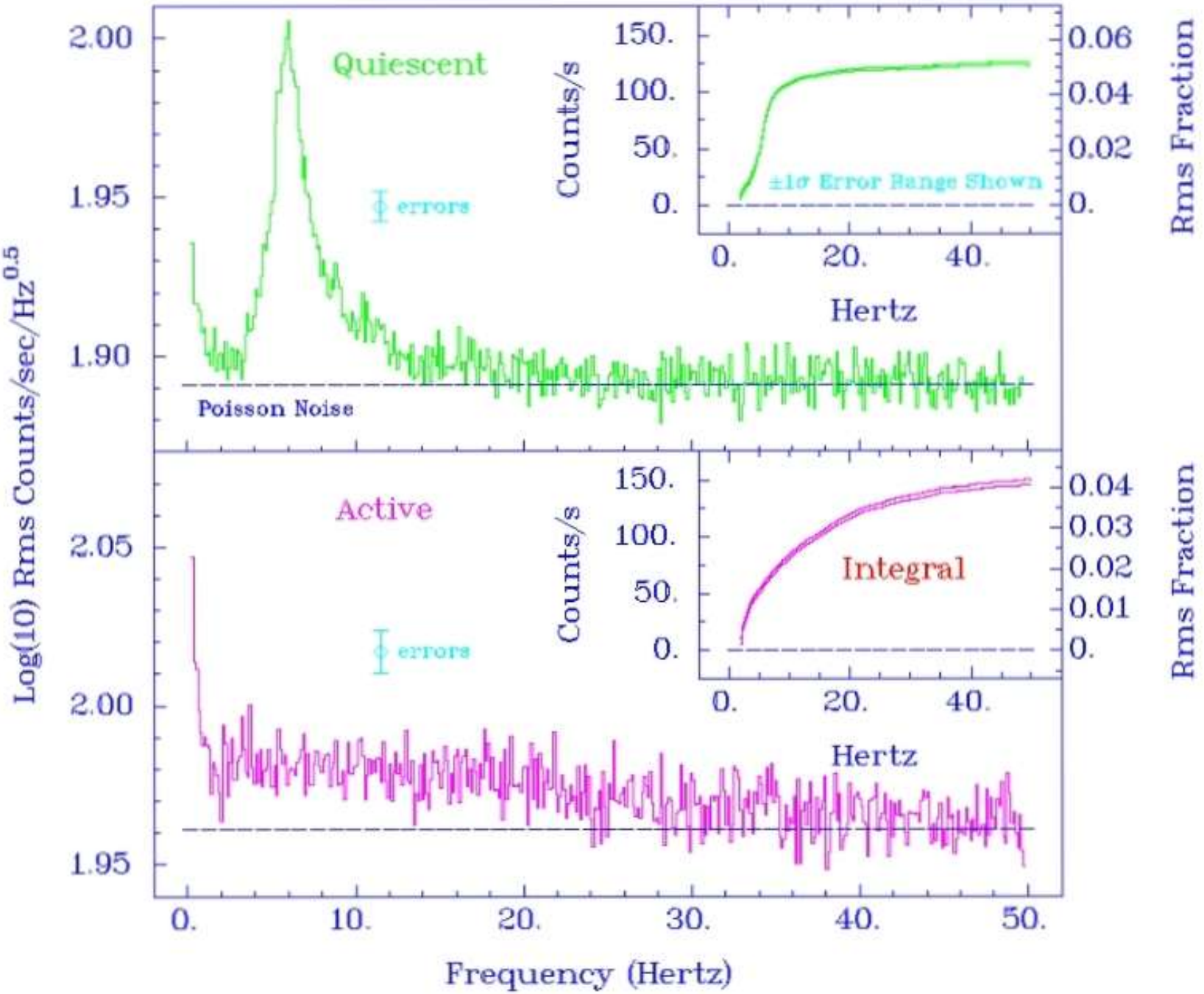
Quiescent
errors
Poisson Noise
Counts/s
150.
100.
50.
0.
±1σ Error Range Shown
0.
20.
40.
Hertz
Rms Fraction
0.06
0.04
0.02
0.
Active
errors
Integral
0.04
0.03
0.02
0.01
2.05
2.00
1.95
0.
10.
30.
50.
Log(10) Rms Counts/sec/Hz$^{0.5}$
Frequency (Hertz)

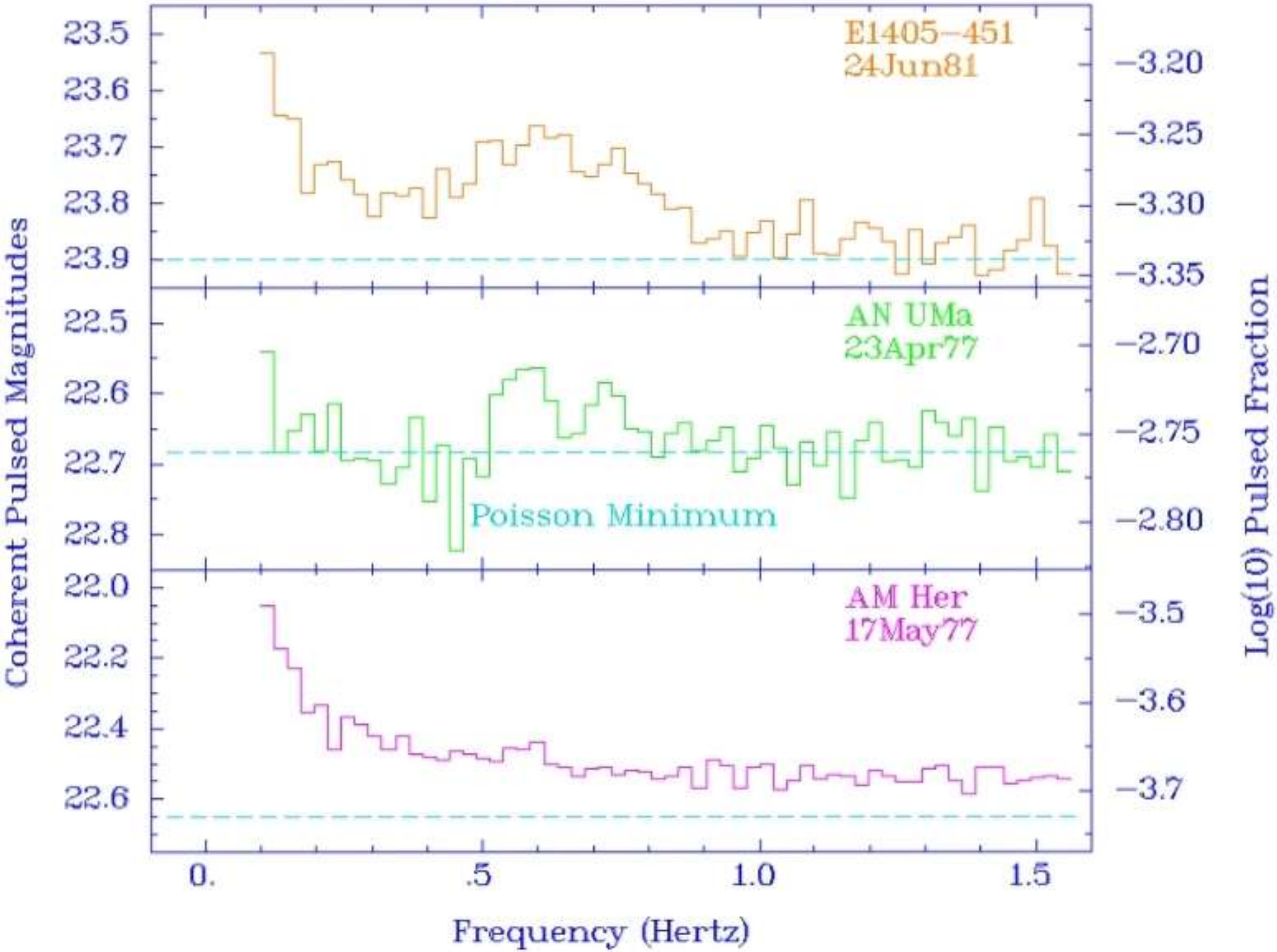
E1405−451
24Jun81
AN UMa
23Apr77
Poisson Minimum
AM Her
17May77
23.5
23.6
23.7
23.8
23.9
22.5
22.6
22.7
22.8
22.0
22.2
22.4
22.6
−3.20
−3.25
−3.30
−3.35
−2.70
−2.75
−2.80
−3.5
−3.6
−3.7
0.
.5
1.0
1.5
Coherent Pulsed Magnitudes
Log(10) Pulsed Fraction
Frequency (Hertz)

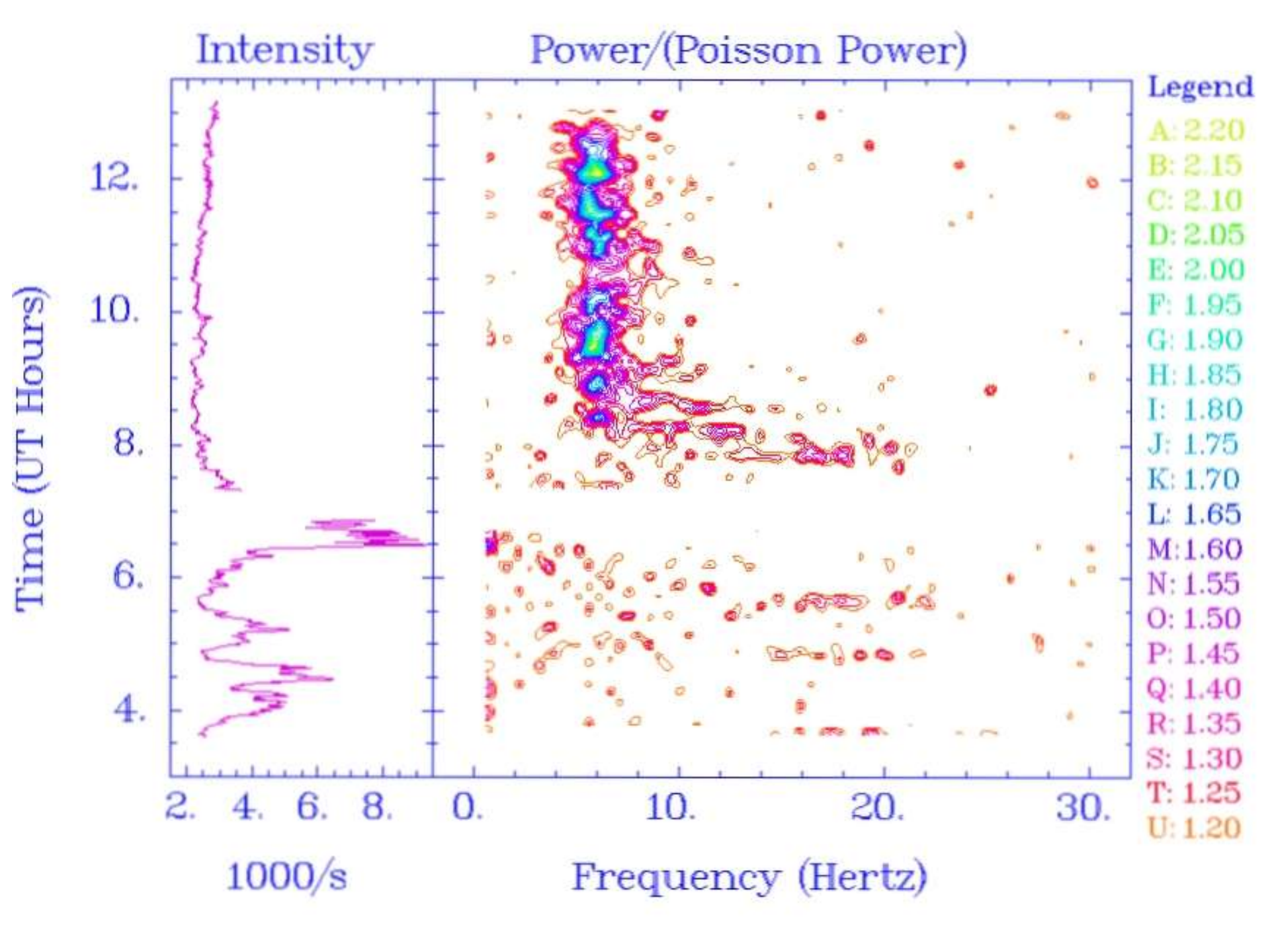
Intensity
Power/(Poisson Power)
Time (UT Hours)
12.
10.
8.
6.
4.
2.
4.
6.
8.
1000/s
0.
10.
20.
30.
Frequency (Hertz)
Legend
A: 2.20
B: 2.15
C: 2.10
D: 2.05
E: 2.00
F: 1.95
G: 1.90
H: 1.85
I: 1.80
J: 1.75
K: 1.70
L: 1.65
M: 1.60
N: 1.55
O: 1.50
P: 1.45
Q: 1.40
R: 1.35
S: 1.30
T: 1.25
U: 1.20

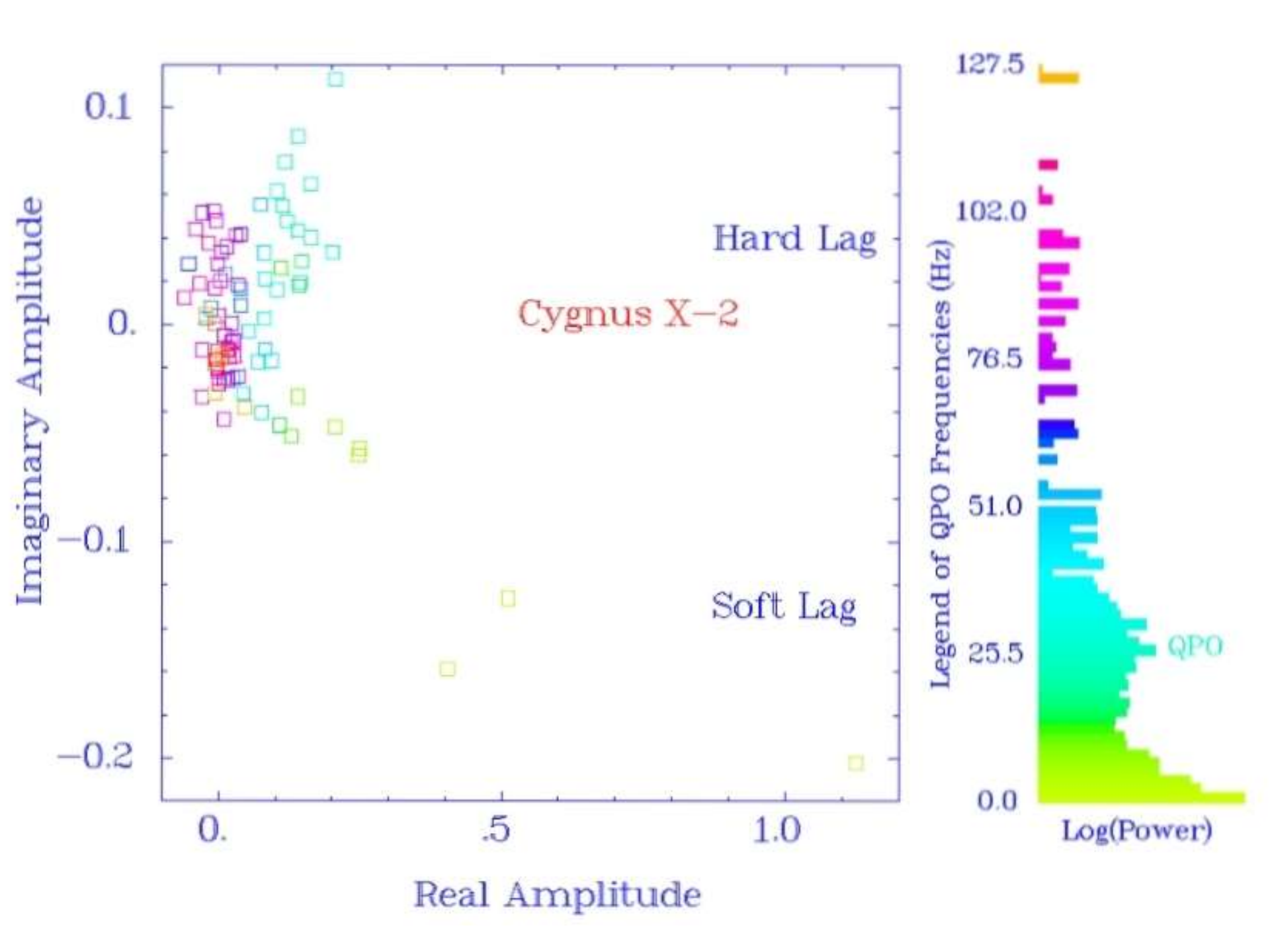
Hard Lag
Cygnus X−2
Soft Lag
Imaginary Amplitude
Real Amplitude
0.1
0.
−0.1
−0.2
0.
.5
1.0
Legend of QPO Frequencies (Hz)
127.5
102.0
76.5
51.0
25.5
0.0
QPO
Log(Power)